

Climate Science Inquiry and Research Projects for Students: Earth's Radiative Balance

Version 2.0, January 2014

David R. Brooks, PhD

Institute for Earth Science Research and Education

© 2013, 2014



“Blue marble” image from http://apod.nasa.gov/apod/image/0304/bluemarble2k_big.jpg

Support for the preparation of this work comes from the National Aeronautics and Space Administration, through Award NNX10AT76A. The author is solely responsible for its contents. The contents of this work have not been reviewed by NASA, nor do its contents necessarily reflect the views of NASA.

This work may be copied and distributed freely for any educational or non-profit use, but it may not be reproduced for sale or used for any commercial purpose without the express written consent of the author. If you reference this work, please provide a citation, including a link to

<http://www.instesre.org/ClimateResearchProjectsForStudents.pdf>.

The *Institute for Earth Science Research and Education* does not have any financial interest in or organizational connection with any manufacturer or distributor of the commercial products mentioned in this work. Descriptions of these products and their possible use in research projects do not imply endorsement by sponsoring agencies or organizations, or by the *Institute for Earth Science Research and Education* to the exclusion of comparable products.

Contents

1. Introduction	1
Resources	6
2. Earth's Radiative Balance – A Starting Point for Climate Research	7
2.1 It Starts With the Sun	7
2.2 Earth and Its Atmosphere: A System in Radiative Balance	8
2.3 Research Question	15
2.4 Resources	15
3. Recording Data from Sun and Atmosphere Monitoring Instruments	17
3.1 Data Loggers for Student Research	17
3.2 Organizing Your Data	21
4. Insolation: Total Solar Radiation at Earth's Surface	23
4.1 Background	23
4.2 Clear-Sky Insolation Models	24
4.3 Measuring Insolation	25
4.4 Measuring Solar Radiation for Other Purposes	26
4.5 Insolation and Clouds	27
4.6 Quantifying the Effects of Clouds and Tree Canopies on Insolation	30
4.7 Inquiry and Research Questions	33
4.8 Resources	34
5. Surface Reflectance	37
5.1 Background	37
5.2 Setting Up an Experiment	38
5.3 Reflectance Data	40
5.4 Indices for Monitoring the Health of Vegetation (and Snow?)	42
5.5 Inquiry and Research Questions	44
5.6 Resources	48
6. Surface and Sky Thermal Radiation	51
6.1 Background	51
6.2 Continuously Monitoring Surface Radiating Temperature	51
6.3 Comparing Radiating Temperature of Surfaces	54
6.4 Infrared Radiation from the Nighttime Sky	55
6.5 Monitoring the Daytime Sky	57
6.6 Converting Temperature to Radiated Power	58
6.7 Inquiry and Research Questions	60
6.8 Resources	61

7. Sky Photography	63
7.1 Background	63
7.2 Sky Brightness Measured from the Horizon	64
7.3 Horizontal Visibility	65
7.4 Photographing the Solar Aureole	66
7.5 Cloud Observations and Photography	71
7.6 Inquiry and Research Questions	73
7.7 Resources	75
8. Atmospheric Water Vapor	77
8.1 Background	77
8.2 Measuring Atmospheric Water Vapor	78
8.3 Inquiry and Research Questions	81
8.4 Resources	82
9. Climate Trends	85
9.1 Background	85
9.2 30-Year Climate Normals	85
9.3 The U.S. Historical Climatology Network	90
9.4 The U.S. Climate Reference Network	95
9.5 Inquiry and Research Questions	100
9.6 Resources	103
Appendix A: Student Research Project Template	105
Appendix B: Sources for Figure s	109

1. Introduction

The purpose of this document is to provide some background and specific ideas for authentic climate-related research by students. The intended audience is middle school and older students working with their teachers and other mentors.

In 2011, the *Institute for Earth Science Research and Education* (IESRE) started a three-year project, Climate Science Research for Educators and Students (CSRES): Understanding Sun/Earth/Atmosphere Interactions project. [IESREa, 2013]. Funding for CSRES has been provided by NASA's Innovations in Climate Education (NICE) Program, formerly Global Climate Change Education (GCCE). [NASA]. Its primary audience has been older middle school and secondary school students and their teachers. CSRES' goals include:

- Developing a comprehensive approach to improving teachers' and students' understanding of sun/Earth/atmosphere interactions through student research, using hands-on activities that combine existing climate data with innovative and inexpensive instruments for ground-based measurements.
- Establishing an infrastructure, including mentoring, equipment, and experiment protocols, that enables schools and science teachers to support independent student climate science research projects that will be competitive in high-level national science competitions.

CSRES was designed around a specific science focus: Earth's radiative balance. This is a fundamental topic in climate science – a graphic showing basic inputs to and outputs from the Earth/atmosphere system appears in every Earth science text. This focus also takes advantage of IESRE's expertise in the development of inexpensive instrumentation for solar and atmosphere monitoring and its desire to promote authentic climate science research by students. In 2010, IESRE organized a workshop on student climate research, sponsored by the National Science Foundation and the National Oceanic and Atmospheric Administration [Brooks, 2011].

The lack of an infrastructure to support student climate science research comparable to the kind of support available in other areas of student research (biosciences, for example) helps to explain why it is rare to find climate research represented in high-level science fairs. Even if answers to the “big picture” questions of Earth's present and future climate are beyond the capabilities of students, there are nonetheless many interesting research projects that can be undertaken with the proper support.

Focusing on Earth's radiative balance will help students make the connection between what they can observe and measure locally and the global picture of Earth's radiative balance. But hands-on research requiring data collection can be prohibitively expensive for students.

Consider this basic research question: How does the reflectance of a natural surface such as grass differ from a manmade surface such as concrete or asphalt? This question translates easily to global considerations of planetary albedo and changing land use patterns caused by human encroachment or climate-induced changes such as more extensive and longer droughts. The question is conceptually within the grasp of middle school students and it is easy to outline an experiment: Measure simultaneously the incoming and reflected solar radiation at two different sites and calculate the ratio of reflected to incoming radiation for each surface.

At a basic inquiry level, this is an experiment that does not even have to extend across seasons to produce interesting data. However, it does require a minimum of four radiometers and two data loggers to record the data at each of at least two sites. Commercial equipment, which will have to be dedicated to this project potentially for many months, will cost well over \$1000. Hence, this undertaking is expensive even for well-funded schools and almost certainly too expensive for individual student researchers. As a result, this straightforward research project will almost certainly not be undertaken by students.

The CSRES project has provided a solution: develop inexpensive equipment where possible and provide it on loan for the duration of a student climate research project, which may extend over several seasons, in return for a written research plan which includes disseminating results. To facilitate such investigations, CSRES has developed a series of research project descriptions [IESREb, 2013]. Some of them make use of IESRE-developed instruments. (More information about solar and atmosphere monitoring instruments can be found in Brooks [2008].) Some use a combination of IESRE-developed and commercial equipment. Others make use of existing climate-related data, or may combine existing data with student-collected data.

If “authentic science” is defined as conducting research that produces previously unknown results, do all the CSRES projects qualify as authentic science? Not necessarily. CSRES originally focused on secondary school teachers and students who were already committed to high-level science fair projects. However, we soon found that the process of doing science research involving instrumentation and data collection was unclear to students *and* their teachers. As a result, earlier intervention was indicated, with projects that developed inquiry skills.

It is very important to be honest with students, especially older students, about whether they are doing “inquiry” or “research.” Too often, any student science activities beyond classroom assignments are called “research.” The 2010 Workshop on Student Climate Science [Brooks, 2011] was careful to distinguish between inquiry, which is a process, and research, which is inquiry plus new science content. It is possible to conduct inquiry without producing new science content, but authentic research cannot be done without the inquiry process. Hence, some of the projects described in this document can be conducted by younger students who first need to understand the inquiry process before moving on to projects that can fairly be called research.

The 1996 National Science Education Standards [National Research Council, 1996] gave this definition of inquiry:

“Inquiry is a multifaceted activity that involves

- Making observations;
- Posing questions;
- Examining books and other sources of information to see what is already known;
- Planning investigations;
- Reviewing what is already known in light of experimental evidence;
- Using tools to gather, analyze, and interpret data;
- Proposing answers, explanations, and predictions;
- Communicating the results.

Inquiry requires identification of assumptions, use of critical and logical thinking, and consideration of alternative explanations.”

A project comparing the reflectance of two different surfaces will not necessarily produce any new science, but a properly conducted experiment will definitely develop a thorough understanding of the inquiry process. During the CSRES project, my colleagues and I have been gratified to watch middle school or 9th grade students and their teachers start with simple inquiry-based projects and refine them over two or three years into more in-depth research.

Inquiry and research project ideas are suggested at the end of Chapter 2 and in all other chapters starting with Chapter 4. Inquiry projects involve data collection and analysis that can be undertaken even by younger middle school students. These projects will develop an understanding of the scientific inquiry process and will serve as the basis for authentic research projects. Converting inquiry to research may involve extending data collection times, paying more attention to instrument calibrations, changing the focus of the experiment, additional analysis of existing data, or building mathematical models to explain results. Research *always* includes a plan for presenting and disseminating results.

Taking a position on climate change... or not

It is important to note that student researchers and their teachers do not need to, and probably should not, take a position about the relative contributions of natural processes and anthropogenic activities as drivers of Earth’s climate. There is ample evidence that Earth’s climate is changing rapidly compared to the pace of past changes, but there is also some evidence that during the last decade or so, global warming has “taken a break” for reasons not yet understood. Some scientists believe that the ability of Earth’s climate to self-regulate even in the presence of increasing levels of greenhouse gases (by changing cloud distributions, for example) has been underestimated. Some scientists believe that significantly decreased solar

activity in the early 21st century is the culprit and some even believe that, as a result of this solar near-dormancy, Earth may cool in coming years. Whatever the facts or their causes, the previously popular “global warming” phrase is now often replaced by a more ambiguous and inclusive reference to “climate change.”

The inability of climate models to explain the details of all that is observed in past and present climates has led to much skepticism about the ability of climate scientists to predict the future of Earth’s climate, especially at the regional level. Even with the most sophisticated computer models, it is clear that the links between cause and effect as it pertains to natural causes and human activities have not been unambiguously determined. In the face of uncertainty, with huge economic and political stakes (over the continuing reliance on fossil fuels, for example), an ongoing battle still rages between climate change “believers” and “deniers” over what should be fundamentally scientific questions, the answers to which should not, but obviously do, depend on one’s politics. There is no reason for student researchers to be distracted by this endless debate!

The scientific and political controversies surrounding climate science (and some climate scientists) do not make student research about climate any less important. Fortunately, there is a lot of interesting hands-on work that can be done by students to characterize the current state of Earth’s climate at the local level. There is also a lot of existing climate data that has not been thoroughly explored. So, there are plenty of opportunities for students to engage in *doing* climate science, instead of just reading about it, and for making meaningful contributions toward meeting one of the most important science challenges facing humankind in the 21st century.

Getting help

Finally, a note about finding resources and getting help. Many of the references cited in this document are web links. Unless there is information on the site about when it has been posted or modified, these references are undated.¹ If you use such references, you should indicate the date on which you accessed sites or downloaded documents. Of course, I cannot guarantee that website links I have cited will always be available.

There are reasonable concerns about over-reliance on online sources. But, there is a huge amount of useful information about the topics discussed in this document available online and there is no reason not to take advantage of that fact. Unfortunately, in the area of climate science, it is not always easy to distinguish between online (or offline) fact and opinion. The mere fact that there exists a wide range of anthropogenic climate change “believers” and “deniers” should serve as a warning to anyone seeking information about this topic. Although there is rarely any reason to question the integrity of information about straightforward technical matters when it is obtained from sources such as U.S. government research

¹ When you create your own web pages, *please* include a date/time stamp which tells when the site was most recently modified. Insert this code following the <title>...</title> tag in your HTML document:

```
<script language="javascript" type="text/javascript">  
document.write("This document was last modified on "+document.lastModified); </script>
```

organizations such as NASA and NOAA and scientific or academic institutions, even then “facts” about climate and especially about its future are open to interpretation and possibly misinterpretation. There is, for example, a vigorous debate about whether the methodologies NOAA and others have used to interpret current temperature data and “correct” historical temperature records have created warming trends which do not actually exist. See, for example, NOAA (monthly updates); Watts, 2012; Wikipedia (undated). Much of the input to this debate, including the NOAA monthly climate updates and the Watts “study,” never undergoes a peer review process. In any case, with or without peer review, questions of interpretation and mathematical modeling are serious matters which demand close ongoing examination.

You need to be much more cautious about relying upon possibly biased, misleading, and inaccurate information from the many privately funded pseudo-scientific “institutes,” whose sources of financial support are deliberately obscure and whose political or economic agendas are hidden behind benign or official-sounding names and slickly-produced materials, often aimed at teacher and students. Information consumer, beware! In the final analysis, you are responsible for finding appropriate sources, separating fact from opinion, and cross-checking multiple sources.

Accessing articles in peer-reviewed journals can be a problem for student researchers, teachers, and other non-professionals. Although older articles are sometimes freely available online, some scientific journals *never* make their articles freely available and they are almost always very expensive to download. But, for serious research, access to peer-reviewed journal articles is a necessity. The best way to get this access is to enlist the support of a faculty member at a nearby college or university or a government research facility. Libraries at these institutions have subscriptions to important printed journals and they will also have subscriptions to services which provide online journal access.

It is often worthwhile contacting authors directly. They may have pre-publication versions of articles which they are able to share. They may also be able to point you to other relevant sources and they may even take an interest in your research. For any college-bound student, learning how to communicate effectively with college and university faculty is a skill that will pay huge dividends when you apply to colleges and, later, during your entire college experience.

Regardless of whether you are a student or a teacher who is mentoring students, I hope this document will help you get started with your own climate science research! More information is available on the CSRES project website [IESREa]. Please let me know what you are doing and how I can help. You can reach me at brooksdrr@InstESRE.org.

Resources

Brooks, David R. *Bringing the Sun Down to Earth: Designing Inexpensive Instruments for Monitoring the Atmosphere*. Springer, 2008. ISBN 978-1-4020-8693-9.

Brooks, David R. Workshop Report. Workshop to Define Collaborative Student Climate Research: Raising the Bar for Climate Science Education in the 21st Century, 2011. <http://www.instesre.org/NSFWorkshop/index.htm>

IESREa. Climate Science Research for Educators and Students: Understanding Sun/Earth/Atmosphere Interactions, 2013.
<http://www.instesre.org/GCCE/GCCEHome.htm>

IESREb. CSRES Activities and project descriptions, 2013.
<http://www.instesre.org/GCCE/ProjectAbstracts.htm>

NASA, undated. <https://nice.larc.nasa.gov/>

National Research Council. *National Science Education Standards*. Washington, DC: National Academy Press, 1996.
http://www.nap.edu/openbook.php?record_id=4962

NOAA, National Climatic Data Center. State of the Climate. (monthly updates)
<http://www.ncdc.noaa.gov/sotc/>

Watts, Anthony: New study shows half of the global warming in the USA is artificial. <http://wattsupwiththat.com/2012/07/29/press-release-2/>

Wikipedia. Instrumental temperature record.
http://en.wikipedia.org/wiki/Instrumental_temperature_record

2. Earth's Radiative Balance: A Starting Point for Climate Science Research

The study of any planet's climate starts with the fundamental concept that in the presence of constant energy input, an object attain radiative balance with that input. Earth is no exception. As viewed from space, our home planet and its atmosphere as viewed from space must, on average, be in radiative balance with the energy it receives from the sun. That is, any solar energy absorbed by the Earth/atmosphere system must eventually be re-radiated back to space in order to maintain the balance.

What happens in Earth's atmosphere and on its surface is another matter. The surface radiative balance may be altered by changing conditions at the surface and in the atmosphere. Understanding the flow of energy to and from space, the atmosphere, and the surface underlies all climate science and the concept of climate change.

2.1 It Starts With the Sun

The sun radiates energy approximately like a blackbody whose behavior is described by the Stefan-Boltzmann law.² The power radiated by a blackbody is proportional to the 4th power of its absolute temperature in units of kelvins (K):

$$(1) \quad \text{radiated power} = \epsilon\sigma T^4 \text{ W/m}^2$$

where the emissivity $\epsilon = 1$ (dimensionless) and $\sigma = 5.67 \times 10^{-8} \text{ (W/m}^2\text{)/K}^4$ is the Stefan-Boltzmann constant. Figure 2.1 shows the distribution of solar power at the top of Earth's atmosphere, compared to a blackbody at 5780K.

The average Earth-sun distance is about 150,000,000 km. As shown in Table 2, our sun is a type G star, unremarkable in energy output and size.³ It generates about $3.9 \times 10^{26} \text{ W}$. Its radius is about $6.96 \times 10^5 \text{ km}$, roughly 100 times Earth's radius (6380

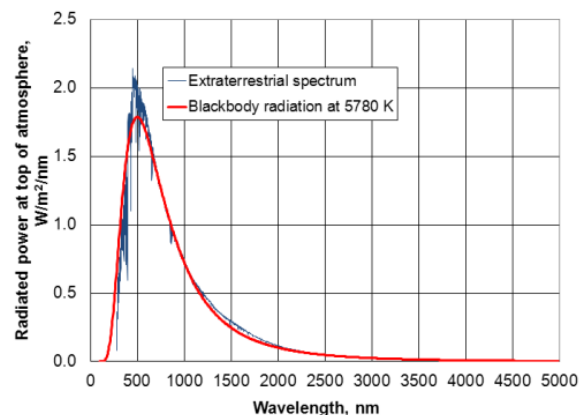


Figure 2.1. The sun as a blackbody.

Table 2.1. Stellar designations.

Spectral Letter	Temperature Range (K)	Stellar Color
O	>33,000	Blue
B	10,000 – 33,000	Blue
A	7,500 – 10,000	Blue-white
F	6,000 – 7,500	White
G	5,200 – 6,000	Yellow-white
K	3,700 – 5,200	Orange
M	<3,700	Red

² An online search will yield a great deal of information about blackbodies and the Stefan-Boltzmann law.

³ See the Harvard spectral classification here, for example: http://en.wikipedia.org/wiki/Stellar_classification

km). The power available at the average Earth orbital radius (the “extraterrestrial solar constant,” S_0) is about 1360 W/m^2 .⁴

2.2 Earth and Its Atmosphere: A System in Radiative Balance

The average Earth/sun distance is about 150,000,000 km. The Earth/atmosphere system, viewed as a disk with radius R_E intercepts an average power of $S_0 \pi R_E^2$ (Figure 2.1(a)). We will use a value of 1360 W/m^2 for S_0 . The average reflectivity of the Earth/atmosphere system (the planetary albedo α) is about 29%. So, the Earth/atmosphere system absorbs about 71% of the incoming energy and reflects the rest back to space:

$$(2) \quad \text{absorbed power} = S_0(1 - \alpha)(\pi R_E^2) W$$

As shown in Figure 2.1(b), the Earth/atmosphere system, like the sun, behaves like a spherical blackbody, radiating power from its surface area ($4\pi R_E^2$) equally in all directions (on average) at a rate proportional to the 4th power of its absolute temperature T_e (which is, of course, *much* less than the temperature of the sun):

$$(3) \quad \text{emitted power} = (4\pi R_E^2)\sigma T_e^4 W$$

Because of the wavelength differences, it is easy to separate incoming solar radiation from outgoing (emitted) thermal radiation, as shown in Figure 2.2.

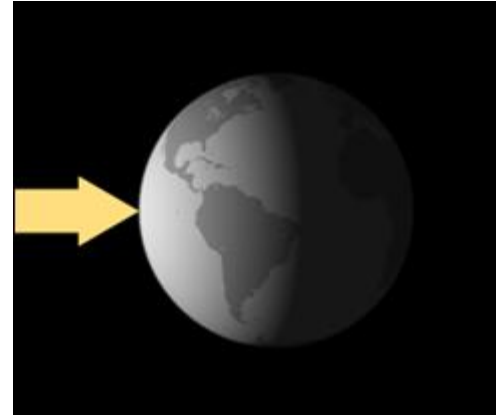


Figure 2.1(a). Incoming solar radiation.

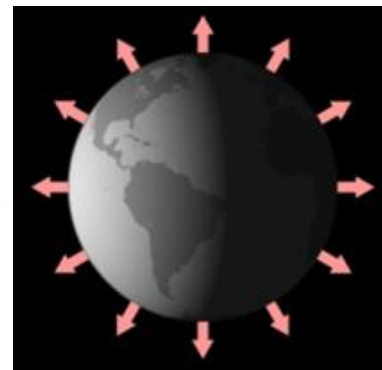


Figure 2.1(b). Outgoing thermal radiation.

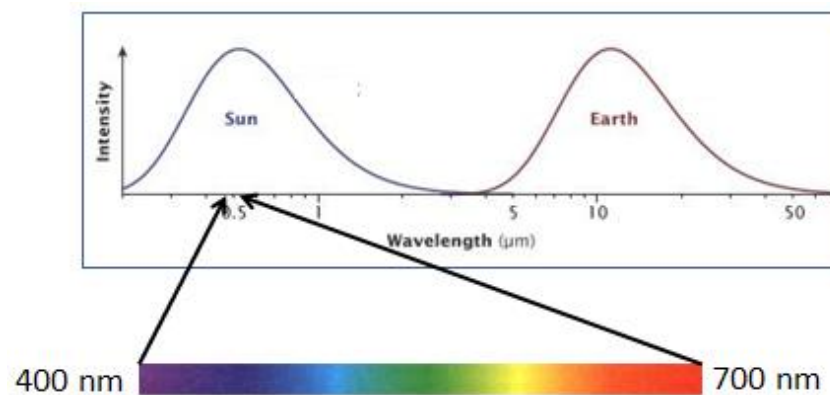


Figure 2.2. Wavelength distribution for incoming and outgoing radiation

⁴ S_0 is measured from spacecraft. Various sources use values in the $1360\text{-}1370 \text{ W/m}^2$ range.

on Earth.

For the Earth/atmosphere system to be in radiative balance, incoming solar radiation must be balanced on average by the outgoing thermal radiation, regardless of conditions on Earth's surface:

$$(4) \quad \text{absorbed} = \text{emitted} \\ S_0(1 - \alpha)/4 \text{ W} = \sigma T_e^4 \text{ W}$$

Solving for T:

$$(5) \quad T_e = [(340 \cdot 0.71)/5.67 \times 10^{-8}]^{1/4} = 255.4\text{K} \approx -18^\circ\text{C}$$

But, the actual average global surface temperature on Earth is around $+15^\circ\text{C}$. The greenhouse effect in the atmosphere, in which certain gases absorb and re-emit radiation, explains the difference of about 33°C .

Our solar system contains three potentially habitable planets (Figure 2.3). But, the Earth/atmosphere temperature as viewed from space places it a little outside the "Goldilocks zone" where a planet can support liquid water – a prerequisite for advanced life as we understand it. So, it is fortunate that Earth's atmosphere provides a "just right" greenhouse effect which warms the surface. Mars' thin atmosphere provides very little greenhouse effect, while Venus' thick CO_2 atmosphere has resulted in a huge "runaway" greenhouse effect that produces surface temperatures more than twice as hot as the melting point of common 60/40 tin/lead solder.

The previous discussion describes the behavior only of the total Earth/atmosphere system as seen by an observer from space. Is it possible to construct a simple model that accounts for how the greenhouse effect modifies temperatures at Earth's surface? Assume:

1. Earth is surrounded by a single-layer atmosphere at constant temperature (an isotropic atmosphere).
2. Solar (shortwave) radiation passes through the atmosphere without interacting with it.
3. The greenhouse effect is taken into account by assuming the atmosphere has an emissivity significantly less than 1. This means that the atmosphere will absorb (and then re-emit) some of the thermal radiation coming from Earth's surface.



Figure 2.3. Atmospheric greenhouse gas effects at potentially habitable planets in our solar system.

4. Don't worry about the physical mechanisms which transfer energy back and forth between the surface and the atmosphere.

Figure 2.4(a) shows the first step. Solar radiation passes through the atmosphere and 29% of it is reflected back through the atmosphere – as if the atmosphere weren't there at all. Then Earth's surface re-radiates the absorbed solar energy as thermal energy at temperature T_s , according to the Stefan-Boltzmann equation (Figure 2.4(b)).

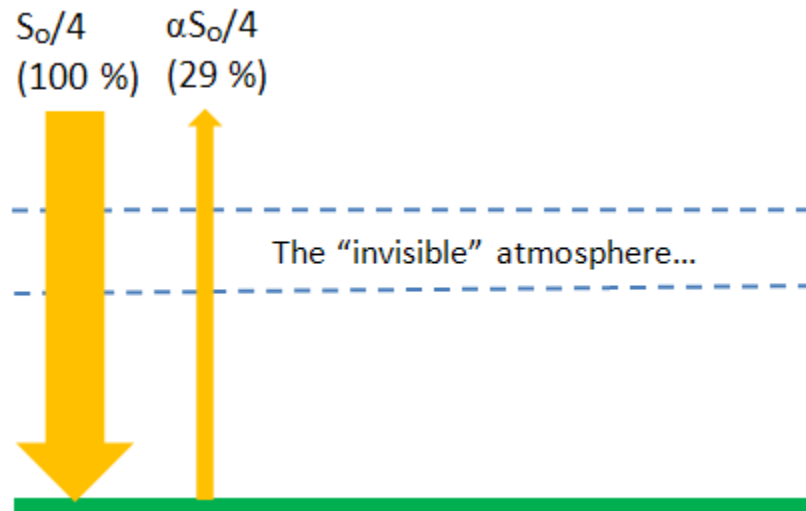


Figure 2.4(a). Incoming solar radiation passes through a transparent atmosphere.

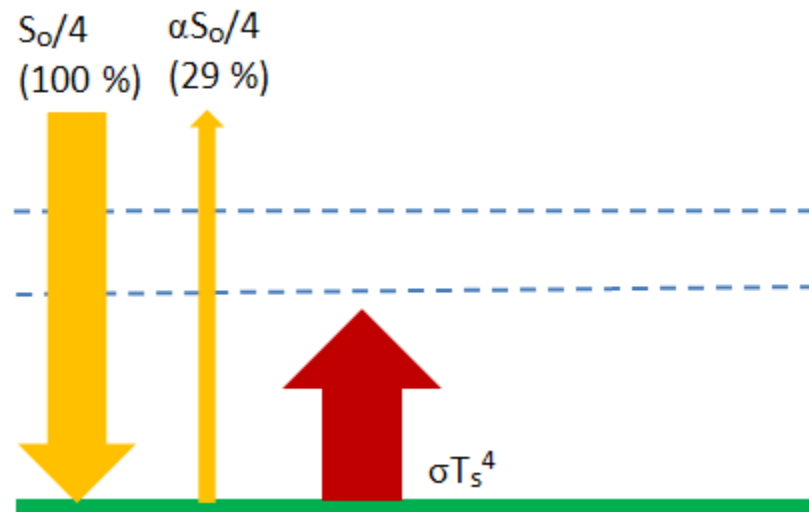


Figure 2.4(b). Earth's surface emits thermal radiation.

Because of the greenhouse effect, the atmosphere is not transparent to thermal radiation. The atmosphere acts like a "graybody" with an emissivity less than 1 so that $(1 - \epsilon)$ of the thermal radiation from the surface passes through the

atmosphere and the rest is absorbed by greenhouse gases, primarily water vapor (Figure 2.4(c)). This absorbed radiation is then re-emitted at the temperature of the atmosphere, half back to space and half down toward Earth's surface (Figure 2.4(d)).

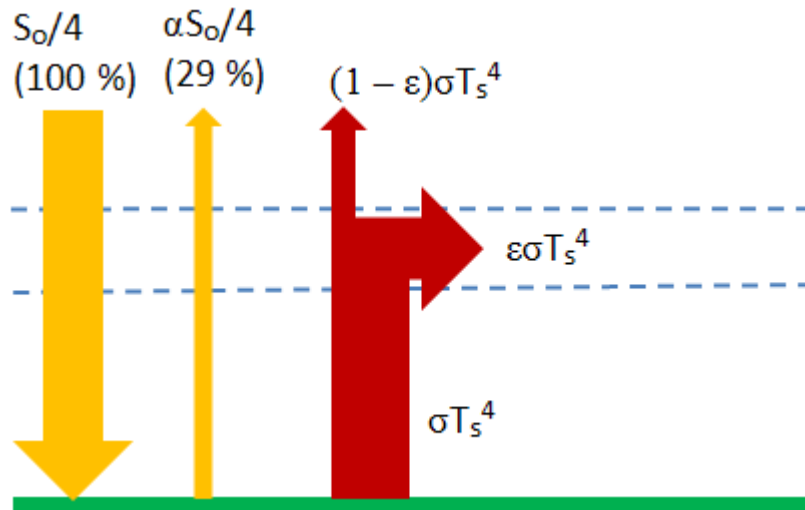


Figure 2.4(c). Most thermal radiation is absorbed by the atmosphere.

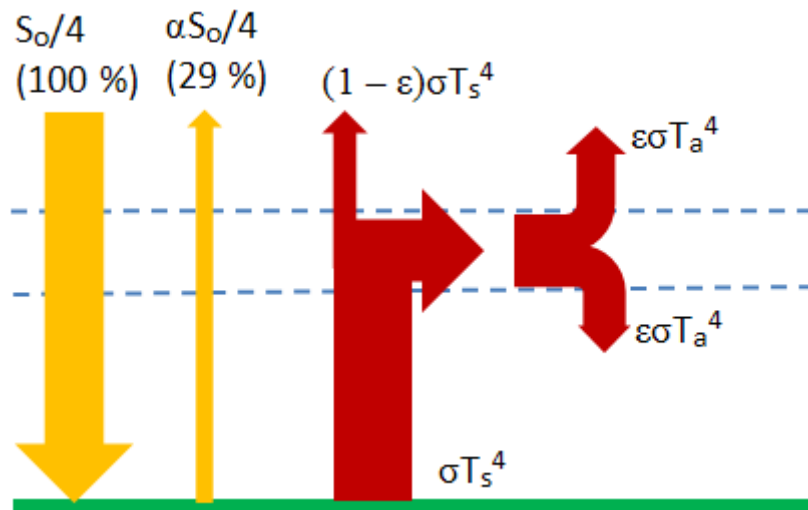


Figure 2.4(d). The atmosphere re-radiates the absorbed radiation.

The top of the atmosphere – the Earth/atmosphere system as viewed from space – must remain in radiative balance, so the absorbed portion of the incoming solar radiation must be balanced by the total outgoing thermal radiation from Earth's surface and the atmosphere (Figure 2.4(e)).

Finally, in order for Earth's surface to be in radiative balance, the absorbed solar radiation plus the thermal radiation from the surface must be balanced by the outgoing thermal radiation from the surface (Figure 2.4(f)).

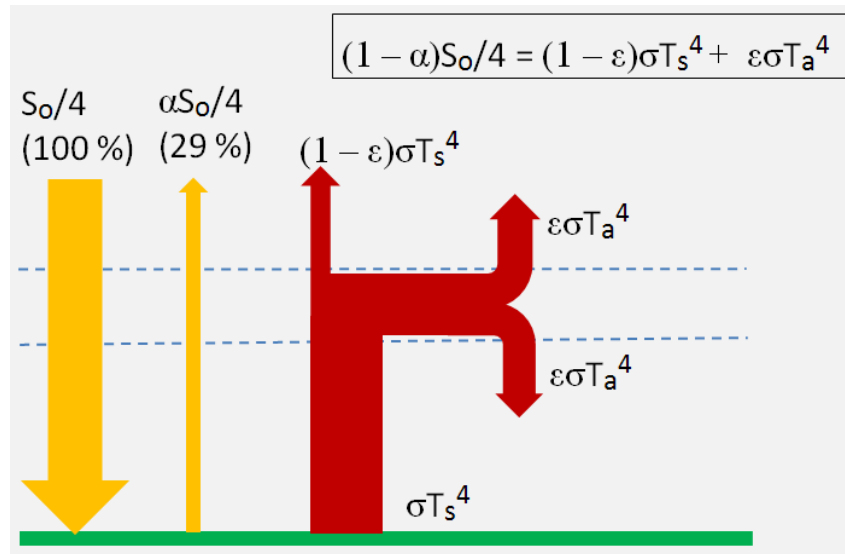


Figure 2.4(e). The top of the atmosphere is in radiative balance.

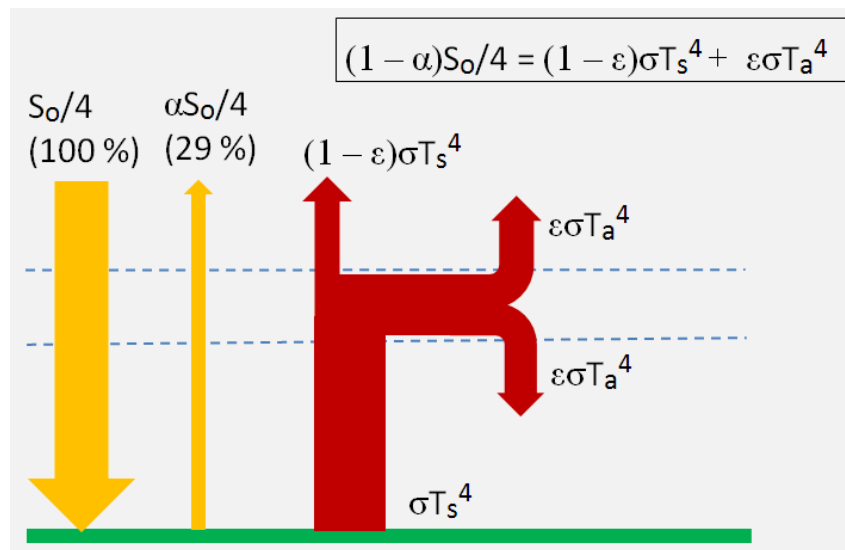


Figure 2.4(f). Earth's surface is in radiative balance.

Using these two radiation balance equations:

(6) $(1 - \alpha)S_0/4 = (1 - \epsilon)\sigma T_s^4 + \epsilon\sigma T_a^4$ (at the top of the atmosphere)

(7) $(1 - \alpha)S_0/4 + \epsilon\sigma T_a^4 = \sigma T_s^4$ (at the surface)

Eliminate $(1 - \alpha)S_0/4$ and solve for T_a in terms of T_s :

(8) $T_a = T_s/2^{1/4} = 0.841T_s$

Use (6) or (7) to solve for T_s :

$$(9) \quad T_s = [(1 - \alpha)S_0 / (4\sigma)(1 - \epsilon/2)]^{1/4}$$

In terms of the temperature of the Earth/atmosphere system as viewed from space,

$$(10) \quad T_s = T_e / (1 - \epsilon/2)^{1/4}$$

Thus, the three temperatures T_a , T_e , and T_s , are all related through the emissivity of the atmosphere. Use (10) to solve for emissivity:

$$(11) \quad \epsilon = 1 - (T_e / T_s)^4$$

For $T_e = -18^\circ\text{C} = 255.15\text{K}$ and $T_s = +15^\circ\text{C} = 288.15\text{K}$, $\epsilon = 0.77$. (Remember that the temperatures in these equations must always be expressed in units of kelvins.) That is, about 23% of the thermal radiation from Earth's surface escapes through the atmosphere and 77% is absorbed and re-emitted to space and back to the surface. From (8), the temperature of the atmosphere corresponding to a surface temperature of 15°C is -30.8°C . Not surprisingly, the temperature of the Earth/atmosphere system as viewed from space is somewhere in between the temperature of the surface and this single-layer atmosphere.

There are many unrealistic assumptions in this model! The atmosphere is obviously not a single layer with a constant temperature – temperature varies dramatically with altitude and the atmosphere doesn't act like a graybody because its absorption and emission of radiation is strongly wavelength dependent. It is not true that incoming and reflected solar radiation do not interact at all with the atmosphere. This simple model considers clouds basically as white features painted on Earth's surface whose only effect is to modify the planetary albedo. In reality, some solar radiation is absorbed by clouds and by the atmosphere. Changing cloud amounts must also affect water vapor, a potent greenhouse gas, which will in turn affect the emissivity of the atmosphere. Finally, the premise that Earth's climate is changing means that, by definition, there are radiative imbalances between Earth's surface and its atmosphere. Nonetheless, this simple model helps to understand how the greenhouse effect works.

Globally, the components that keep the Earth/atmosphere system in radiative balance are shown beautifully in NASA graphics derived from satellite data (Figure 2.5). These images reinforce the realization that understanding a global system which must be in radiative balance on average is an extremely challenging task! More information about Earth's radiative balance and these graphics, including how to interpret the colors, can be found online [NASAa, b, c].

The point of this exercise with a single-layer atmosphere model is to provide a context for designing your own research projects using ground-based measurements and existing data. These projects are interesting in their own right, but you will have a better “story” if your research connects local observations to the global view of radiative balance.



Figure 2.5(a). October 2013, average planetary albedo.

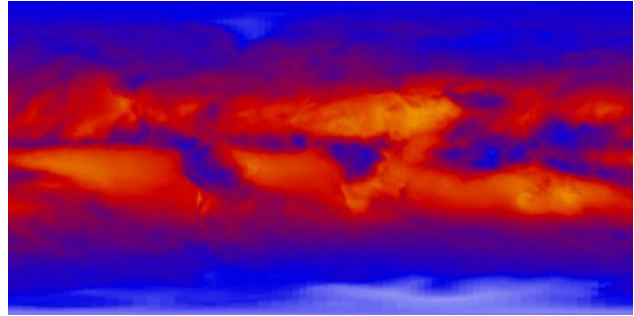


Figure 2.5(b). October 2013, average outgoing top-of-the-atmosphere LW radiation.

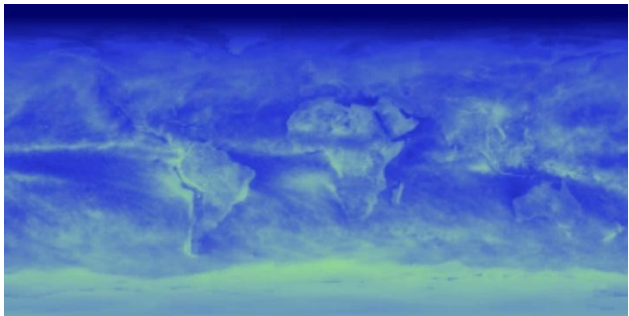


Figure 2.5(c). October 2013, average top-of-the-atmosphere reflected shortwave radiation.

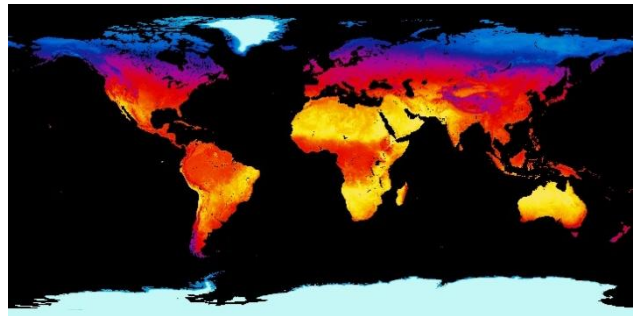


Figure 2.5(d). October 2001-2010, average daytime land surface temperature.

Figure 2.6 shows how individual measurements are interconnected within the “big picture” of Earth’s radiative balance. Some of the measurements are described in subsequent chapters. Other measurements, such as evapotranspiration – one of the mechanisms which provide a path for transporting thermal energy between the surface and the atmosphere – are not yet available from IESRE.

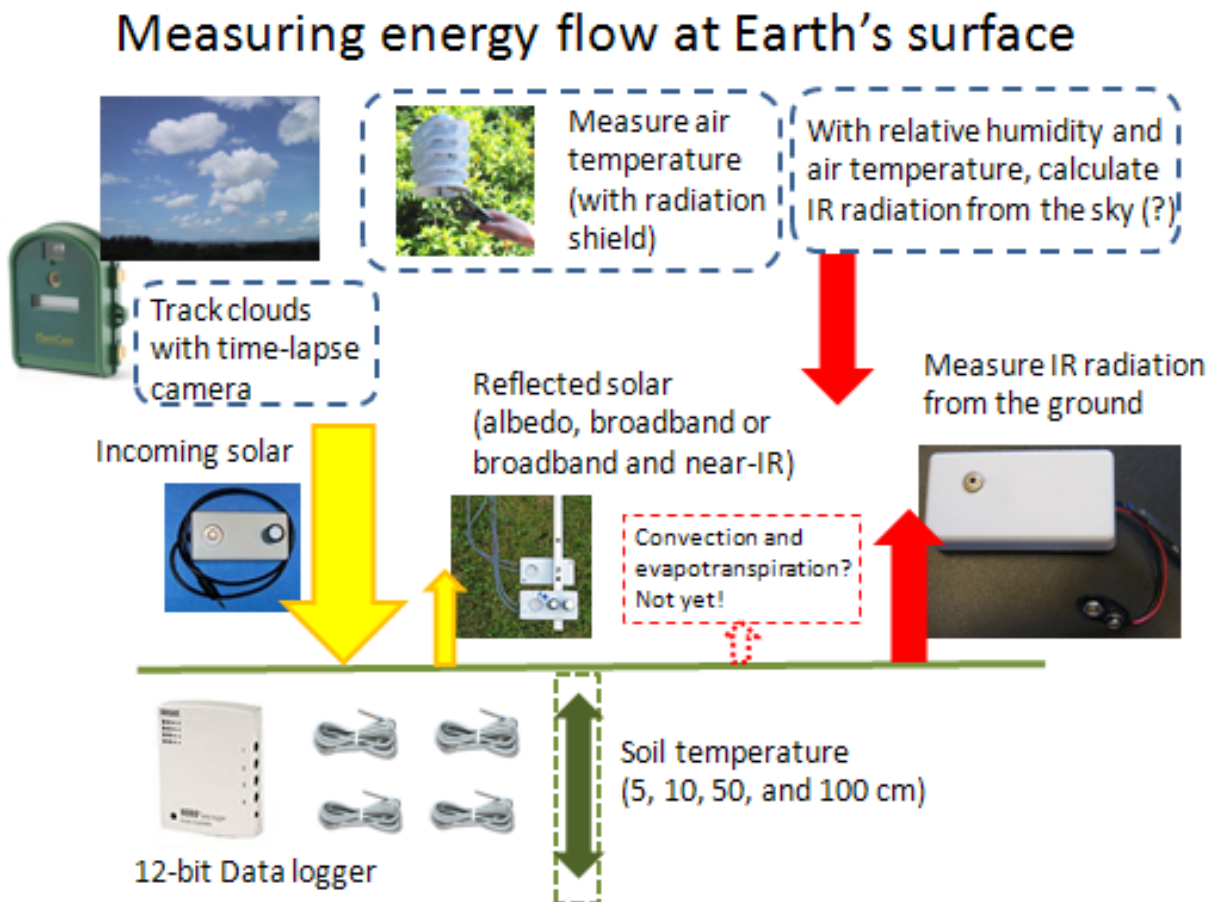


Figure 2.6. Ground-based measurements and Earth's radiative balance.

2.3 Research Question

The single-layer atmosphere described in this chapter can be expanded into a multi-layer atmosphere with increasingly realistic depictions of what happens in the actual atmosphere. Can you develop your own multi-layer model? The American Chemical Society has published excellent online tutorials about single- and multi-layer atmosphere models [ACS, undated].

2.4 Resources

American Chemical Society. ACS Climate Science Toolkit.

<http://www.acs.org/content/acs/en/climatescience/atmosphericwarming/singlelayermodel.html>

<http://www.acs.org/content/acs/en/climatescience/atmosphericwarming/multilayermodel.html>

Cooperative Institute for Meteorological Satellite Studies. *The Earth's Radiation Energy Balance*. Space Science and Engineering Center, University of Wisconsin. <http://cimss.ssec.wisc.edu/wxwise/homerbe.html>

NASAa. <http://neo.sci.gsfc.nasa.gov/>

NASAb. <http://science-edu.larc.nasa.gov/EDDOCS/whatis.html>

NASAc. <http://earthobservatory.nasa.gov/Features/EnergyBalance/page4.php>

3. Recording Data from Sun and Atmosphere Monitoring Instruments

3.1 Data Loggers for Student Research

Many of the research projects described in this document involve collecting data with a data logger. Data loggers record voltage signals and convert them to integer digital values, which may then be converted into other physical units. Data loggers are essential tools for gathering data used in climate science research and I believe that collecting data is absolutely essential to gain ownership of climate science concepts. But, at a time when an essentially infinite amount of “hands-free” information is available in digital form, it is essential not to lose sight of the fact that Earth is an analog system and that data loggers merely provide a way to record analog behavior in a more usable form.

The appropriateness of a data logger for a particular application depends on the resolution of its analog-to-digital (A/D) conversion and the range of voltages that need to be recorded. Suppose a data logger records voltages in the range 0–5V with 12-bit A/D conversion. This means that the input voltage is represented by $2^{12} = 4096$ integer values from 0 to 4095. Thus, the resolution is $5/4096 \approx 1.2\text{mV}$.

Is this adequate? That depends on the input to the data logger. For example, the instruments for measuring incoming solar radiation described in Chapter 4 (pyranometers) produce about 0.25V in full summer sunlight; the maximum solar radiation in summer is around 1000 W/m^2 . 0.25V is $1/20$ of the range of a 5-V data logger so the entire range of insolation will be represented by $4096/20 \approx 205$ values in steps of about 5 W/m^2 . This resolution is probably comparable to the inherent absolute accuracy of this instrument, but it might be too coarse to adequately represent the smaller amounts of solar radiation reflected from relatively dark surfaces such as grass, for example. Sometimes resolution problems can be fixed by amplifying input signals so they cover the full voltage input range of the data logger.

Some data logging systems will automatically interpret stored voltage values based on what kind of sensor is attached to the logger. With others, such as the HOBO loggers discussed below, you must tell the software what kind of sensor is attached when you before you start collecting data.

Some data loggers allow you to assign your own conversion factors to be applied to stored voltage values. For example, for a sensor intended to measure incoming solar radiation (see Chapter 4), a conversion factor might be $4000\text{ (W/m}^2\text{)/V}$, so the values stored in the data logger could be multiplied by 4000 to convert volts to physical units. My own preference is *not* to use this option; I would rather import raw voltage data into a spreadsheet and apply my own conversion factors there.

For the kinds of experiments described in this document, often requiring long-term data collection, loggers should be battery powered to operate in a stand-alone

mode with onboard memory, without being connected to a computer. They have to be rugged enough for use outdoors and they should include software for managing the device and exporting data in a text format – ideally, a .csv file format for import into Excel or some other spreadsheet program.

Table 3.1 summarizes two loggers that IESRE has found to be useful for data collection.⁵ Both record positive voltages only. Both have onboard memory and both communicate with a computer through a USB connection. Both use widely available and easily replaceable batteries which should last for several months of continuous operation. Both are available directly from their manufacturers or from a distributor such as [MicroDAQ](#).

These loggers are not guaranteed by their manufacturers for continuous outdoor use. The HOBO loggers, for example, are specifically advertised for indoor applications. Nonetheless, I have used such loggers in outdoor enclosures for many years. They need not to get wet or be in an environment where moisture will condense on the printed circuit board. If moisture is a potential problem, loggers can be placed in a plastic snap-lid container with rice or cat litter and they should be problem-free.

Cost is definitely a consideration for these data loggers because they are most often used full-time with a particular research project and are therefore not available for other general classroom uses. Programmable multi-channel high-resolution data loggers can cost hundreds or even thousands of dollars, which put them beyond a reasonable price range for student research projects. The prices given in Table 3.1 are for single units at the time this document was written, subject to change, of course. Quantity discounts may be available.

Table 3.1. Two stand-alone data loggers suitable for student climate research.

Logger/ website	Specs	Unit Price	Comments
HOBO UX120-006 Onset Computer Corporation	4 channels, 0–2.5V, 16-bit, 40 μ V resolution. Total of 1.9 million measurements. 1-s minimum sampling interval. 2 AAA batteries	\$139+\$45	Software is extra (HOBOWare Lite, \$45). 0-2.5V, with 0-5V, 0-10V, 0-24V adapter cables available for resolutions of 80 μ V, 160 μ V, 384 μ V. External temperature sensors available (TMC6-HD, \$39). 2.5-mm stereo plugs required to connect sensors to logger. Instantaneous sampling plus statistics over sampling interval.
Track-It Monarch	2 channels, $\pm 0.5\%$ full scale, ± 0.1 mV for	\$59+\$50	Software is free. Voltage input adapter required. Uses screw

⁵ IESRE is not a distributor for any of these loggers, nor does it have any other financial connections to or interests in the companies that make and sell these loggers. They are included in this document only because they are suitable for the data collection projects described herein.

Instrument 500mV adapter,
0–500mV, 0–5V, and
0–10V versions
available.
32,000
measurements each
channel.
2-s minimum
sampling interval.
CR2032 battery

terminals for "bare wire"
connections. Instantaneous
sampling or sample at 2-s
interval and record max, min, or
average over longer interval.

HOBO UX120-006 logger

For many years, IESRE has used HOBO U12-006 four-channel loggers from Onset Computer Corporation.. For sampling at one-minute intervals using all four channels, the logger will capture about 7 days of instantaneous samples. The 12-bit A/D resolution over a 0–2.5V range is suitable for recording the output from IESRE pyranometers (about 0.25V in full sunlight), but it is only barely adequate for smaller signals such as would be obtained when measuring the reflectance of surfaces.

The U12 loggers are now being discontinued. Starting in early 2014, the four-channel U12-006 is being replaced by the 16-bit UX120-006, shown in Figure 3.1. The case is about $10 \times 5 \times 2.5$ cm. When it is recording data, the LCD display panel can be turned off to extend battery life. This logger is only slightly more expensive than the U12-006 – \$140 rather than \$110. It can be used with the latest version of the HOBOWare Lite software; a software update for older versions is available as a free download. It might be worth buying some of the less expensive U12 loggers while they are still available.

In addition to its increased A/D resolution, the most significant UX120 upgrade over the U12 series is its ability to record not only instantaneous measurements, but also the average, maximum, minimum, and standard deviation based on subsamples during a sampling interval – for example, sampling every 10 seconds during a 5-minute interval gives 30 points for generating statistics for that 5-minute interval.

The U12 loggers store up to 64,000 measurements, or 16,000 measurements per channel if all four channels are used. The UX120 will store 1.9 million measurements! Presumably this means that if the statistics option is turned on and all four channels are being used, the storage should be divided by $4 \times 5 = 20$, or 95,000 measurements per channel. With the statistics option turned off, the UX120 will store MANY more measurements than should be recorded between downloads in any situation where instrument performance needs ongoing monitoring.



Figure 3.1. HOBO U120-006.

Like the U12-006 series, the UX120-006 series loggers are intended for indoor use. But, as noted above, outdoor use should not cause problems if the logger environment is properly controlled.

Onset's UX100 loggers include temperature and relative humidity sensors. But IESRE believes that the relative humidity sensors, like those in the U12-013 logger, are not reliable for outdoor use and are therefore not recommended for weather measurements. For temperature measurements, use an external sensor in one of the channels of the UX120-006.

You can download HOBO software for a free 30-day trial, but you must then purchase a product key to continue using it. The HOBOWare Lite version is perfectly acceptable for collecting data from IESRE instruments. Typically, all you need to do with the software is launch the logger to start recording, download the data (in its proprietary binary format) when you're done, and export the data in a .csv file for import into Excel or some other spreadsheet.

Any sensor connected to the external inputs must use a 2.5mm stereo plug even though only two leads are connected; the middle ring is never connected to IESRE sensors. It is possible to make these cables, but the small plugs are difficult to work with. A good solution is to use commercial audio cables such as the Hosa CMM-510.⁶ This 10' cable has a 2.5mm stereo plug at each end. Cut it in half to get 5' cables for two sensors.

Track-It logger

This two-channel logger will store up to 32,000 pairs of voltage values at intervals as short as 2 seconds. The case, including the input module, is about $10 \times 2.5 \times 1.5$ cm. The version shown in Figure 3.2 has an LCD display, but a less expensive version with no display is perfectly suitable for the purposes discussed in this document. The logger is purchased separately from the voltage interface modules. The 500mV version is ideal for recording data from IESRE pyranometers, including when they are used in pairs to measure surface reflectance, and it is also suitable for pyranometers with much lower output voltages, such as the Kipp & Zonen SP-Lite.⁷



Figure 3.2. Track-It Logger with LCD display and voltage input module.

The Track-It can be programmed to sample at 2-second intervals and then store the instantaneous maximum, minimum, *or* average value over a longer interval. Unlike the UX120, you can select only *one* of these values. For example, insolation data collected at one-minute intervals could be the average of 30 two-second samples during that time rather than the instantaneous value at each minute. Such an option may be useful for eliminating data “outliers” in some measurements, but it does not equal the sophistication of the UX120 loggers. Choosing this option will

⁶ One source of these cables is [AValive](http://www.avalive.com/).

⁷ <http://www.kippzonen.com/>

reduce battery life because of the high sampling rate during the recording interval. Consult the user's guide for more information.

The free software is adequate, but less intuitive than the (not free) software for HOBO loggers. Data can be exported in a `.csv` text file format. The screw terminals for connecting sensors are much more convenient than the 2.5mm stereo plugs needed for the HOBO loggers.

3.2 Organizing Your Data

Once you start logging data, it will not take long to collect a *lot* of it. Collecting data at one-minute intervals produces 1440 records per day. Many of the experiments discussed in this document involve multiple sites, too. How should you organize your data?

You should create a folder on your computer that will contain all the data for a project. When you save data, you should devise a consistent file-naming convention that will result in an orderly computer-based filing system. If you do this, it will be easy to find data when you need it. If you don't, you will waste a lot of time trying to figure out what happened to the data you collected six months ago! I use this format:

```
SiteName_ProjectYYYYMMDD.xxx
```

This naming convention will store all data for a particular site and project consecutively by date. If necessary, you could add `_HHMMSS` if time of day is also important. All modern personal computer operating systems support long file names, so you can include whatever you believe is important in the file name. The file extension should of course be appropriate to the application to be used with the file. Typically, files from data loggers saved in a text format should be given a `.csv` extension so they can be opened directly into a spreadsheet.

For the kinds of projects described in this document, spreadsheet software such as Excel is an essential tool for data analysis. You should apply a consistent naming convention to spreadsheet files just as recommended for data files. As noted above, data downloaded from loggers are originally in a proprietary format which can then be converted to `.csv` files. I always retain these `.csv` files even after I have used them to create `.xls` (or `.xlsx`) files.

Typically, data logger files exported to `.csv` files will save a date and time stamp in a format which Excel will convert to its own internal "date" format as opposed to accepting it as text. It is possible to use this date as the x-axis value for graphs of time series data. However, I find it much more useful to convert dates and times into decimal days. Figure 3.3(a) shows a `.csv` file created from HOBOWare software for the HOBO loggers described above. The shaded columns and cells in Figure 3.3(b) show how the date format has been converted to a decimal day. The Excel formulas for columns C and D, row 4, are shown in rows 1 and 2.

	A	B	C	D	E	F
1	Plot Title: IESRE #2					
2	#	Date Time, GMT-05:00	A-BB	A-nearIR	B-BB	B-nearIR
3	1	8/25/2013 8:43	1.59158	1.45482	1.33089	1.21978
4	2	8/25/2013 8:44	1.27534	1.13553	1.01465	0.86081
5	3	8/25/2013 8:45	1.15018	0.99084	0.8779	0.72772
6	4	8/25/2013 8:46	1.0641	0.89499	0.78938	0.64347
7	5	8/25/2013 8:47	0.14591	0.11355	0.33578	0.384
8	6	8/25/2013 8:48	0.14042	0.10989	0.1514	0.1105

Figure 3.3(a). Data from HOBO logger, converted to .csv file.

	A	B	C	D	E	F	G	H	I	J
1			(column C) TEXT(B4,"mm/dd/yyyy hh:mm")							
2	Plot Title: IESRE #2		(column D) VALUE(MID(c4,4,2))+VALUE(MID(c4,12,2))/24+VALUE(RIGHT(c4,2))/1440							
3	#	Date Time, GMT-05:00			A-BB	A-nearIR	B-BB	B-nearIR		
4	1	8/25/2013 8:43	08/25/2013 08:43	25.3632	1.59158	1.45482	1.33089	1.21978		
5	2	8/25/2013 8:44	08/25/2013 08:44	25.3639	1.27534	1.13553	1.01465	0.86081		
6	3	8/25/2013 8:45	08/25/2013 08:45	25.3646	1.15018	0.99084	0.8779	0.72772		
7	4	8/25/2013 8:46	08/25/2013 08:46	25.3653	1.0641	0.89499	0.78938	0.64347		
8	5	8/25/2013 8:47	08/25/2013 08:47	25.3660	0.14591	0.11355	0.33578	0.384		
9	6	8/25/2013 8:48	08/25/2013 08:48	25.3667	0.14042	0.10989	0.1514	0.1105		

Figure 3.3(b). Date and time converted to decimal days.

It is a good idea always to use local standard time when recording data, rather than switching back and forth between standard and daylight saving time. This means that solar noon is always near local clock noon rather than 1:00 pm, and the conversion to Universal Time (UT), as is often required in scientific work, is the same regardless of the time of year. But, as you probably know, your clever computer will almost certainly switch automatically between standard and daylight saving time. And, typically, data logger software will use your computer's calendar/clock to create the time stamps in data files.

What to do? When my east coast location changes from EST to EDT, I simply tell my computer I am in the central time zone so it sets the time back by one hour. Then, in the fall, I switch back to east coast time. This might confuse recipients of my time-stamped e-mails, but that's a price I am willing to pay for consistent times in my data files!

4. Insolation: Total Solar Radiation at Earth's Surface

4.1 Background

Energy from the sun provides the input to Earth's climate system. Insolation, measured in units of watts per square meter (W/m^2), is defined as the total solar power per unit area (irradiance) reaching a horizontal surface at Earth's surface – recall from Chapter 2 that about 29% of the solar irradiance reaching the top of Earth's atmosphere is reflected back to space and 71% reaches the surface or is absorbed in the atmosphere.

Insolation varies with the seasons – reaching a maximum during the summer and falling to a minimum during the winter. At some high northern or southern latitudes, the sun never sets during the summer and never rises during the winter. Insolation varies with sky conditions. The primary factor is cloud cover, but air pollution, dust, and smoke can also affect insolation.

Insolation is measured with an instrument called a pyranometer. Some research-grade pyranometers, which use what are called thermopile detectors, cost several thousand dollars. Less expensive pyranometers used for routine solar monitoring use silicon-based photodiodes. These instruments are still referred to as pyranometers, but they might more accurately be described as “surrogate pyranometers.”

The primary drawback of silicon photodiode-based pyranometers is that their spectral response is not uniform across the range of incoming solar radiation, as shown in Figure 4.1(a). Silicon photodiode detectors have a

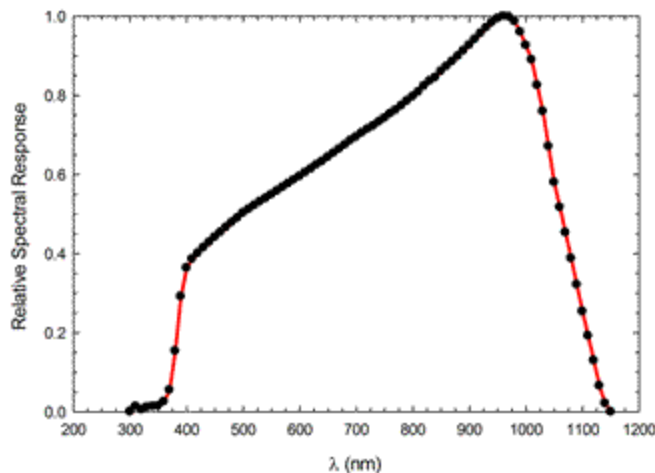


Figure 4.1(a). Typical normalized spectral response for silicon photodiodes.



(b) IESRE pyranometer

strong response peak in the near-IR around 1000 nm. There is a strong atmospheric water vapor absorption band at around 940 nm, so these detectors are over-sensitive to changes in water vapor in the atmosphere and under-sensitive to visible light. Nonetheless, silicon photodiode pyranometers have been used for decades for routine solar monitoring.

IESRE has developed a silicon photodiode pyranometer, shown in Figure 4.1(b), which contains less than \$10 in parts and, when properly calibrated, will produce

results comparable to commercial silicon-based pyranometers costing hundreds of dollars. You can build these instruments yourself with kits from IESRE [IESREa].

Despite their low cost, these instruments are extremely reliable. After five years of continuous data collection with one instrument, there was no significant change in its output when it was re-calibrated. These instruments are so inexpensive that it is practical to use several of them for monitoring differences in solar radiation that can occur even over small areas.

Pyranometers assembled from an IESRE kit must be calibrated against a reliable standard. IESRE will calibrate them for you if you don't have access to a pyranometer that is already calibrated. (Your local university should have one somewhere!) Across the wide range of commercial and research pyranometers, there is a correspondingly wide range of calibration procedures, ranging from "first principles" calibrations with devices that capture solar radiation in a device which then measures very precisely the amount of heat generated by that radiation, to procedures which transfer calibrations from more sophisticated (and expensive) pyranometers to less sophisticated ones. IESRE pyranometers use the second method to calibrate instruments against more expensive commercial silicon-based pyranometers which, in turn, have been calibrated against even more expensive instruments.

There is a detailed online protocol for collecting pyranometer data that contains more background information and practical implementation details [IESREb].

4.2 Clear-Sky Insolation Models

For many insolation studies, it is required to compare measured insolation to what would be expected under clear, cloud-free skies. Part of this calculation rests purely on Earth-sun geometry – the sun's position relative to Earth's surface. For example, the sun's elevation angle at solar noon is higher in the summer than in the winter. The other part of the calculation requires knowledge about how Earth's atmosphere reduces the amount of solar radiation that would otherwise reach the surface.

IESRE has written an online version of a simple clear-sky insolation model [IESREc, d] used by Duchon and O'Malley [1999]. This model takes into account, in a simplified fashion, the effects of light scattering by molecules in the atmosphere (Rayleigh scattering), gas absorption and scattering, aerosols, water vapor, and barometric pressure.⁸ The online application will generate clear-sky insolation and other values such as the time of local solar noon for a specified location and date.

An implementation of the widely used clear-sky insolation model by Bird and Hulstrom [1981] is also available [IESREe]. This model produces results that differ by a few watts per square meter from the Duchon and O'Malley model. It requires similar but more detailed input assumptions about the atmosphere.

⁸ The required pressure is the so-called "station pressure" – sea level pressure corrected for site elevation. See <http://www.instesre.org/Aerosols/pressure.htm>.

Finally, an application that will generate clear-sky insolation at one-minute intervals for a specified location and date is also available [IESREf]. That interval is consistent with the sampling interval we recommend for recording insolation. Output for both the Duchon and O'Malley models is included. The application creates on-screen comma-delimited output that can be copied and pasted into a file for import into a spreadsheet.

4.3 Measuring Insolation

In order to be consistent with the definition of insolation, a pyranometer must be mounted level in a location where there are minimal obstructions to the horizon. Sites surrounded by trees or buildings may be suitable for some kinds of measurements, but not for insolation. Often, flat-roofed buildings are good sites for monitoring insolation, although they are bad sites for meteorological measurements in general. (Air temperatures measured on building roofs will *not* be representative of local air temperatures!)

Once a site has been established, insolation should be recorded continuously. Sampling at one-minute intervals produces 1440 points per day and will provide a good representation of insolation over diurnal and shorter time scales. The sampling and statistics capabilities of the loggers discussed in Chapter 3 provide additional useful information about insolation. Averaging over the sampling interval will help to smooth the data, as there can sometimes be large instantaneous spikes in insolation due to the motion of clouds across the sky.

Figure 4.2 shows some typical insolation data, with one-minute instantaneous sampling. This is not a very good site for measuring insolation, but it is adequate for illustrative purposes. The morning and afternoon shadowing at this site is particularly obvious on April 27th, a clear day, when the insolation values rise and drop quickly as the sun rises above and drops below obstructing trees. The solar noon clear sky model values are in good agreement with measured values. On clear days, the obstructions around the horizon do not cause major reductions to solar radiation reaching the site around solar noon. On the 28th and 30th there is evidence of sunlight reflecting off the sides of clouds, resulting in instantaneous insolation values above the clear-sky value – a common occurrence. The 29th was heavily overcast with rain all day.

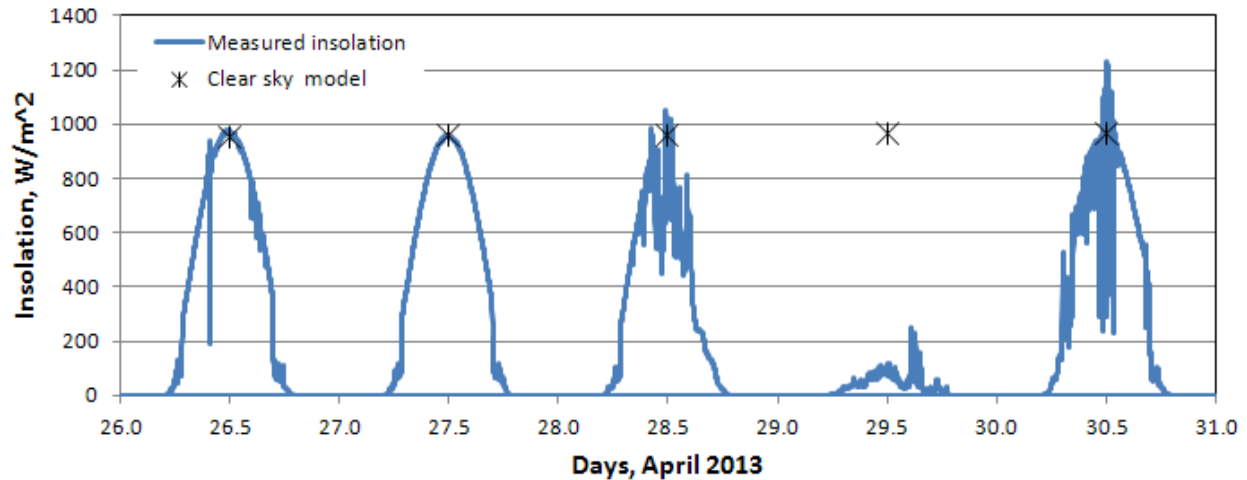


Figure 4.2. Insolation, April 2013, Worcester, PA (40.2°N, 75.3°W, 125 m).

4.4 Measuring Solar Radiation for Other Purposes

Pyranometers can also be used to measure incoming solar radiation in a variety of circumstances. Sites which are not free from obstructions around the horizon are still interesting. Solar radiation is reduced by the presence of shadowing from buildings or natural features. Soil temperatures respond to the energy input from solar radiation, so it would be of interest to compare insolation and the temperature of similar soil types under and away from shadowing. In urban gardens, the placement of crops relative to buildings may be determined by which part of a garden receives the most sunlight.

The orientation of solar panels as required to maximize the availability of energy to heat water or produce electricity has been studied at great length. This is basically a geometry problem and, as such, it is not particularly interesting for a research project that will produce new data. See, for example the [Solar Electricity Handbook]. However, measuring solar radiation at different orientations to the sun is a worthwhile inquiry project that requires careful attention to the scientific process, and it is also useful for learning about using instrumentation.

Figure 4.3 shows insolation data (from a Kipp & Zonen SP-Lite pyranometer) during November, 2011, from the same site as Figure 4.2, along with data averaged from two IESRE pyranometers mounted in the plane of solar photovoltaic panels on the sloping roof of my house (about 30°). The rooftop pyranometers measure higher levels of incoming solar radiation because the panels, which face approximately south, are pointed more directly at the sun. This effect is more pronounced in the winter than in the summer, when the maximum noontime solar elevation is higher. From the top of our roof, shadowing from trees is also nearly absent. Figure 4.3 makes clear why solar panels should be mounted at an angle facing south (in the northern hemisphere) and not horizontally.

For optimum performance, solar panels should be on mechanical trackers which follow the sun. However, such devices are expensive and, of course, they require their own electricity to power motors for moving the panels. For most applications,

active trackers are not considered to be worth the added expense and system complexity.

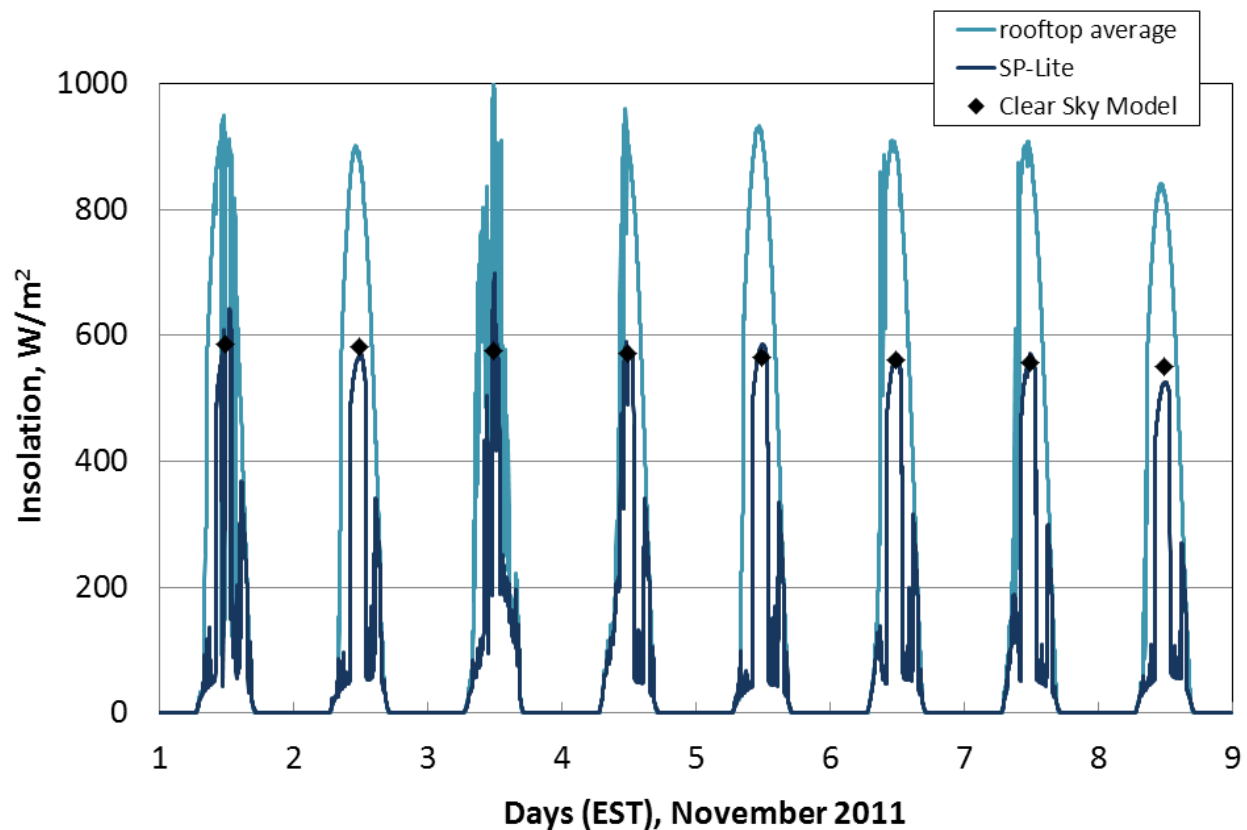


Figure 4.3. Insolation (horizontal pyranometer) vs. pyranometers on sloping roof.

4.5 Insolation and Clouds

Even the most casual examination of diurnal cycles of insolation shows the dominant influence of clouds. Overcast skies lower insolation, more or less uniformly depending on the uniformity of the cloud layer. Scattered cumulus clouds can cause sharp dips in instantaneous insolation when a cloud passes over the sun, and also sharp spikes when sunlight reflects off the sides of individual clouds.

Perhaps this variability can be used to learn something about the nature of cloud cover over a site. Changes in cloud patterns can be both a cause and an effect of climate change. If so, quantitative statistical information about clouds based on pyranometer data would be extremely useful.

The use of pyranometer data to predict cloud type was considered in a paper by Duchon and O'Malley [1999]. That paper compared pyranometer-based cloud type predictions against human observations. At that time there was not the intense interest in the statistics of cloud patterns that exists now because of the profound effects clouds have on climate and climate models.

Basically, relating insolation to clouds involves comparing measured insolation values to modeled clear-sky values. Figure 4.4 shows some pyranometer data from a

site at 40.2°N, 75.3°W. Some shadowing in the early morning and late afternoon is clearly evident at this site. At other times of the day, a clear-sky model seems to provide a reasonable representation of insolation for the site. On day 32 (July 2), perhaps there were some thin uniform cirrus clouds. Or, perhaps there were more aerosols than were accounted for in the model. As noted by Duchon and O'Malley [1999], it is not possible to separate the effects of aerosols from thin uniform cirrus with just pyranometer data.

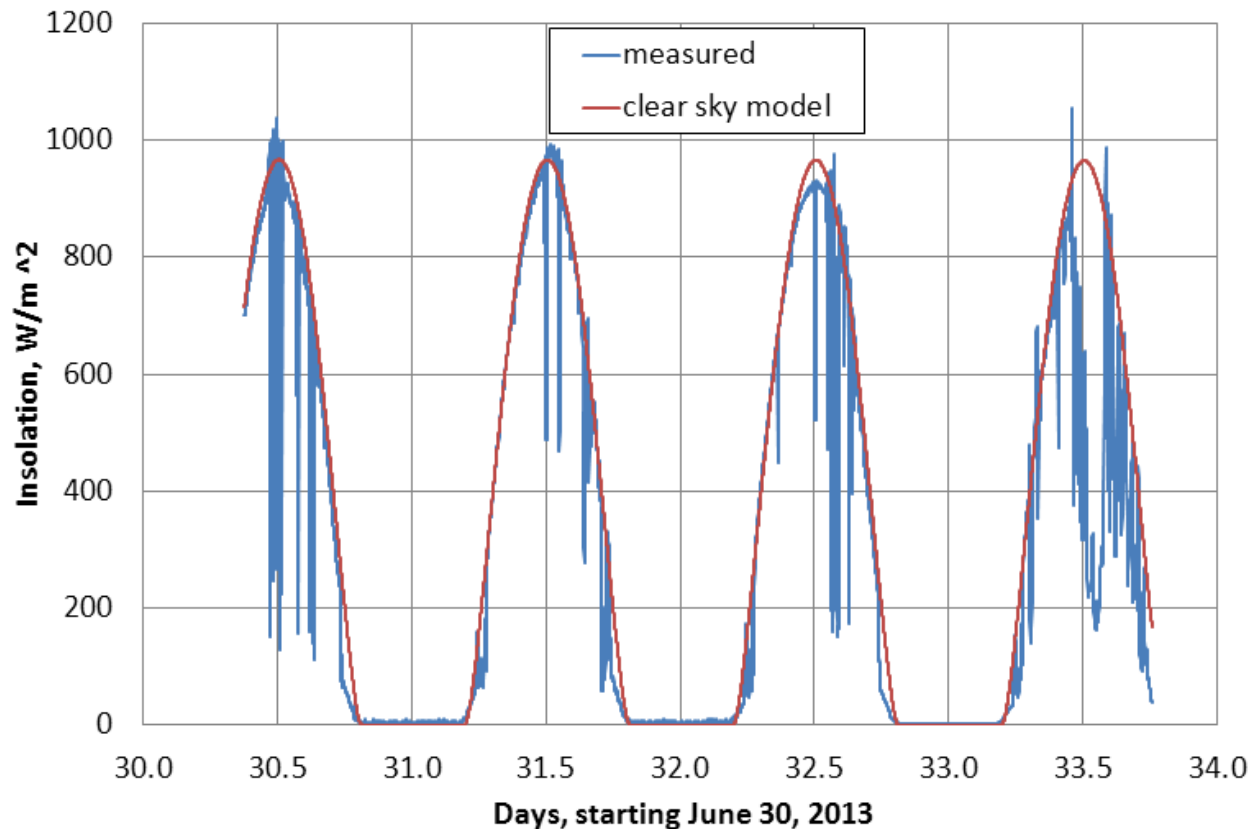


Figure 4.4. Insolation, June-July 2013, Worcester, PA (40.2°N, 75.3°W, 125 m).

From these data, we graph the ratio of the range of the measured data over the clear-sky range for each clock hour as a function of the ratio of the mean of the measured data to the clear-sky mean for each clock hour. It may turn out that for data based on instantaneous measurements, it might be better to calculate a “standard deviation” for all 60 one-minute samples during the hour. “Standard deviation” is in quote marks because a standard deviation calculation implies values normally distributed about a mean – definitely not the case here where, during an hour, clear-sky insolation varies within a range that depends on the local time; the range is small around noon and maximum in mid-morning and mid-afternoon when solar elevation angle is changing the fastest. But, a standard deviation calculation will help to minimize the effect of “outliers” – extreme values that can cause the range calculation not to be representative of what was actually happening during the hour. (See also Section xx in Chapter xx.)

A one-hour interval might seem arbitrary, but it will make it easy to compare these results with hourly pyranometer data from NOAA's Climate Reference Network, which will be discussed in Chapter 9.

Figure 4.5 shows $(\text{observed range})/(\text{clear sky range})$ plotted against $(\text{observed mean})/(\text{clear sky mean})$ and for the nearly four days of data in Figure 4.4. Data from early morning and late afternoon, where shadowing from trees is evident, are excluded. The values in the lower right hand corner, with x-axis values near 1 and low y-axis values, correspond to clear hours where the observed insolation is nearly identical to the clear sky model. Going to the left along the x-axis, there is evidence of thin uniform cirrus clouds, with a low range ratio. The x-axis values around 0.3 correspond to the cloudy and but not uniformly overcast conditions starting around noon on the 4th day. The high y-axis values between $x = 0.8-1.0$ correspond to data from day 1, with its very large insolation range – almost certainly cumulus clouds passing in front of the sun.

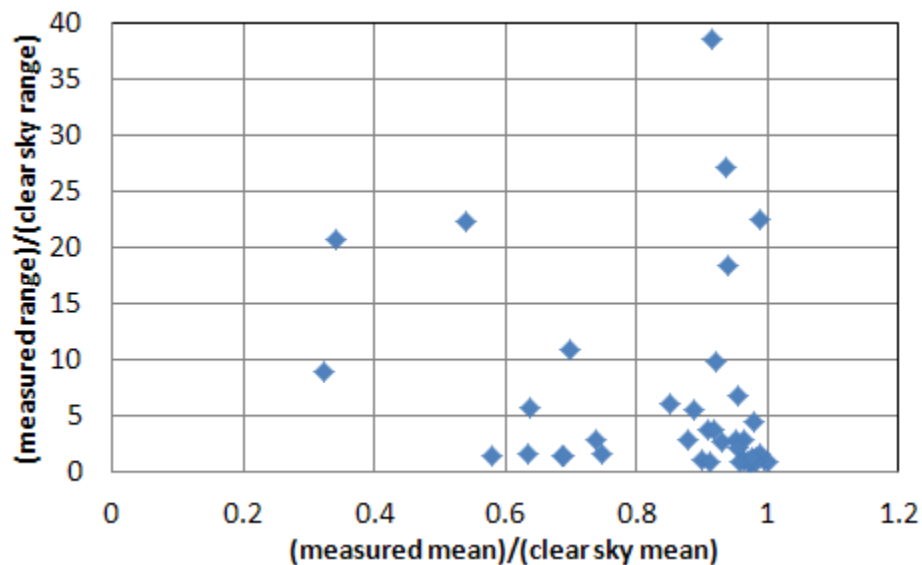


Figure 4.5. Clustering of insolation mean and range values, from data shown in Figure 4.4.

For this relatively small amount of data, it is easy to associate the x-y values on the graph with hours in the data. Repeating this calculation with larger amounts of data, over a month, a season, or a year, will produce more “clumping” of the data at various locations on the graph, depending on the nature of the cloud cover. Differences in the distribution of these values among sites provide a visual indicator of differences among sites. Over time, changes in the distribution patterns will provide a visual indication of changes in cloud patterns over a site.

Note that this method is biased in the sense that it produces the strongest response to clouds when they actually block the sun. Thus it is conceivable that, depending on where they are in the sky, some clouds will produce very little change in insolation or, conversely, that these clustering statistics will not accurately represent cloud properties across the entire sky.

4.6 Quantifying the Effects of Clouds and Tree Canopies on Insolation

It is clear that cloud cover has by far the most significant impact on insolation. Given a clear sky model of insolation, is it possible to establish a quantitative relationship that describes reductions in insolation as a function of cloud cover without necessarily involving cloud type? Given such a model one could predict insolation as a function of cloud cover or, inversely and perhaps more usefully, predict cloud cover based on measured insolation.

It is often the case that older research papers, written before the personal computer revolution, can open the door to research possibilities that are rendered much more practical with modern computing power and technology. A 1977 paper by R. K. Reed provides an excellent example. Reed gave an empirical relationship between the ratio of observed insolation to clear-sky insolation over open ocean as a function of cloud cover and solar elevation angle:

$$S_{\text{Elev}} = 1353s \cdot (0.61 + 0.20s)$$

$$S/S_{\text{Elev}} = 1 - 0.62C + 0.0019\text{Elev}_{\text{noon}}$$

where s is the sine of the solar elevation angle, C is the cloud cover in tenths and $\text{Elev}_{\text{noon}}$ is the solar elevation angle at solar noon.

Comparisons with other equations relating insolation to cloud cover are also presented in Reed's paper:

Kimball (1928)

$$S/S_{\text{Elev}} = 1 - 0.71C$$

Berliand (1960), cited in Kondratyev (1969)

$$S/S_{\text{Elev}} = 1 - aC + 0.38C^2$$

where a varies with latitude

Laevastu (1960)

$$S/S_{\text{Elev}} = 1 - 0.60C^3$$

Tabata (1964)

$$S/S_{\text{Elev}} = 1 - 0.716C + 0.00252\text{Elev}$$

It is not clear why these equations should apply only over open ocean. Perhaps it is due to the fact that the ocean provides a uniform surface over which clouds can form. Perhaps it is simply a matter in the pre-satellite era of not having opportunities to actually observe clouds over the open ocean.

The interesting point about these equations is that the cloud cover from none to overcast is specified to the nearest tenth based on a protocol for human observations. However, digital cameras can provide instant photos of the sky and time-lapse cameras can easily produce multiple images and videos of cloud cover throughout the day. Readily available image processing software then makes it possible to convert images to an estimate of cloud cover in those images. Granted, these photos will be only for a part of the sky. But, it is also possible to stitch together multiple images or use a "fish eye" lens to photograph the entire sky.

Figure 4.6(a) shows a sky photo. Figure 4.6(b) shows this image saved as a two-color (black and white) image using IrfanView, a popular freeware image processing program [IrfanView].



Figure 4.6(a). Full-color sky image.



Figure 4.6(b). IrfanView Conversion to B/W image.

Unfortunately, IrfanView's conversion of a full color image to a B/W image sometimes plays tricks, as shown in Figure 4.7. In this image of an overcast sky, the darker and lighter areas are reversed. This is a strange result, but this image can't be classified into clear and cloudy areas in any case.



Figure 4.7(a). Full-color overcast sky image.

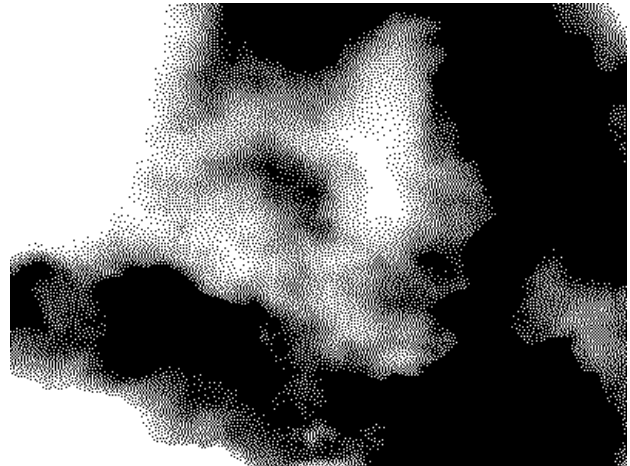


Figure 4.7(b). Inappropriate(?) IrfanView conversion to B/W image.

Assuming that the B/W image provides a fair division of the sky between clear and cloudy, you then need to count the black and white pixels. Save the image as a .bmp file with an image width evenly divisible by 8. (This is easy with IrfanView, using the "Resize" option.) If you understand how .bmp files are formatted, it is not difficult to write a program to count black and white pixels. The code below is written in PHP, a language which can be used online or on your own computer if you have installed a server such as Apache.

```
<?php
// Written by David Brooks, February 2013. (C) IESRE, 2013.
// Counts black and white pixels in a two-color (black/white) .bmp file.
```

```

// The target image should have a width in pixels that evenly divisible by 8.
// 504 pixels is a good choice -- the height doesn't matter.
// IrfanView will resize images and save them as two-color files.
// PHP scripts can be executed from a "localhost" created by a
// server such as Apache.
// Assume target file is in the same directory as this script.
$filename="BWtest.bmp"; $in=fopen($filename,"r");
echo "file header:<br />";
$i=0; $ch=array();
while ($i<14) {
    $ch[$i]=ord(fgetc($in)); echo $ch[$i]." "; $i++;
}
echo "<br />";
$filesize=$ch[4]*65536+$ch[3]*56+$ch[2]; $offset=$ch[11]*256+$ch[10];
echo "file size, offset to image: ".$filesize." ".$offset."<br />";
echo "file information:<br />";
$i=0;
while ($i<48) { // Read to last byte before start of image.
    $ch[$i]=ord(fgetc($in)); echo $ch[$i]." "; $i++;
}
echo "<br />";
$wt=$ch[6]*65536+$ch[5]*256+$ch[4]; $ht=$ch[10]*65536+$ch[9]*256+$ch[8];
echo "image width, height, size: ".$wt." ".$ht." ".$wt*$ht."<br />";
echo "image size from header: ".$ch[22]*65536+$ch[21]*256+$ch[20]."<br />";
echo "bits per pixel: ".$ch[14]."<br />";
// Read file, one row at a time.
$w=0; $b=0;
$w=0; $b=0;
for ($r=1; $r<=$ht; $r++) {
    for ($c=1; $c<=$wt/8; $c++) {
        $ch=fgetc($in);
        // Read the byte and convert to unsigned integer.
        $num=ord($ch); $bit=1;
        for ($m=0; $m<=7; $m++) {
            if (($num & $bit) == $bit) $w++; else $b++; $bit*=2;
        }
    }
    $ch=fgetc($in); // Read end-of-row byte.
}
echo "black, white pixels: ".$b." ".$w."<br />";
fclose($in);
?>

```

The output from this program for the B/W image shown in Figure xx(b) is:

```

file header:
66 77 198 62 7 0 0 0 0 0 54 0 0 0
file size, offset to image: 462422 54
file information:
40 0 0 0 248 1 0 0 58 1 0 0 1 0 24 0 0 0 0 0 144 62 7 0 194 30
    0 0 194 30 0 0 0 0 0 0 0 0 0 0 0 0 0 0 0 0 0 0 0 0
image width, height, size: 504 314 158256
image size from header: 474768
bits per pixel: 24
black, white pixels: 125161 33095

```

If you are interested in the output other than the last line, there is plenty of information online about the format of .bmp files, including on IESRE's website [IESREg]. Suffice it to say that having the file width (in pixels) evenly divisible by 8 is a choice suggested by the file format, in which B/W pixels are given values of 0 or 1 and stored row-by-row in 8-bit bytes.⁹

The procedures that apply to analyzing sky images can also be applied to tree canopies. Figure 4.8 shows IrfanView's conversion of a tree canopy (taken with a camera pointed straight up) to a B/W image. Although you might quibble over the details, this conversion seems to give a reasonable representation of open sky under these trees; they are deciduous trees so, of course, the amount of open sky will vary with the seasons.



Figure 4.8(a). Full-color tree canopy image.



Figure 4.8(b). Conversion to B/W image.

ImageJ, a freeware program from the National Institutes of Health [NIH], provides many more image processing options that will be useful for this kind of project.

4.7 Inquiry and Research Questions

(Inquiry)

- How does insolation vary during the day, with weather and with the seasons?
- How does insolation vary in microclimates such as urban gardens?
- How does the orientation of solar collectors influence the amount of energy available for conversion into heat or electricity?

(Research)

- How does air quality affect insolation at your site? Is it possible to use sky images to separate aerosol effects from other effects such as cirrus clouds? In some parts of

⁹ Full-color .bmp images require 3 bytes, or 24 bits, per pixel, so their files are approximately 24 times as large as a corresponding B/W image.

the U.S., particularly the southwest, large dust clouds from Asia and smoke from fires are common. There are models which forecast and track these events [NRL; NASA]. Perhaps you can see their effect on insolation on cloud-free days. (The presence of clouds will overwhelm effects of air quality.) This project depends critically on the quality and stability of pyranometer calibrations, as the effects of air quality on insolation are likely to be small compared to cloud effects.

- The overview in Section 4.5 of how to analyze pyranometer data based on Duchon and O'Malley's 1999 paper provides a starting point for research on cloud statistics. You will need to collect pyranometer data over several seasons at your site. Then you can look at the statistics over a month, a season, or a year.

Pyranometer data from the Climate Reference Network (see Chapter 6) provides hourly averaged data from about 125 sites around the U.S. Using these largely unexploited data to characterize cloud patterns at USCRN sites would be a valuable contribution.

- Compare instantaneous one-minute samples with instantaneous samples at a much shorter interval averaged over a minute or some longer time period. What is gained or lost by time-averaging samples? What might the implications be for these differences in terms of insolation statistics or solar power applications?

- Section 4.6 provides a starting point for analyzing insolation under cloudy skies and tree canopies. There is always a need for actual on-the-ground data to supplement insolation models that take cloud cover into account. The U.S. National Renewable Energy Laboratory has published several versions of its *National Solar Radiation Data Base* [NREL]. The 10-km gridded data are based on actual and modeled data. Measured hourly insolation from more than 1400 stations in the U.S. are also available. How do your data compare with NREL's?

- Insolation under vegetative canopies is of interest in agriculture and climate science because if climate is warming, it will affect the timing of plant development and of budburst and senescence in areas with deciduous trees. Is it possible that local measurements of insolation under tree canopies can be correlated with satellite-based global analyses of seasonally changing vegetation coverage?

4.8 Resources

[Bird, R. E., and R. L. Hulstrom. A Simplified Clear Sky Model for Direct and Diffused Insolation on Horizontal Surfaces. SERI/TR-642-761, Solar Energy Research Institute, Golden, Colorado, February 1981.](#)

Duchon, Claude E., and Mark S. O'Malley. *Journal of Applied Meteorology*, **38**, pp 132-141, 1999.

IESREa. July 2013.

<http://www.instesre.org/construction/pyranometer/pyranometer.htm>

IESREb. August 2011.

<http://www.instesre.org/Solar/PyranometerProtocol/PyranometerProtocol.htm>

IESREc. November 2010.

<http://www.instesre.org/Solar/insolation.htm>

IESREd. November 2010. <http://www.instesre.org/Solar/InsolationInstructions.htm>

IESREe. June 2011. <http://www.instesre.org/Solar/BirdModelNew.htm>

IESREf. Clear-sky insolation model with text output.

<http://www.instesre.org/Solar/ClearSkyModelOnline.htm>

IESREg. How to read bitmap (.bmp) files. March 2013.

http://www.instesre.org/howto/BW_image/ReadingBitmaps.htm

IrfanView. <http://www.irfanview.com/>

Calibration of Radiation Instruments at PMOD/WRC.

<http://www.pmodwrc.ch/pmod.php?topic=calibration>

Monterey Naval Research Laboratory.

<http://www.nrlmry.navy.mil/aerosol/#currentaerosolmodeling>

Myers, Daryl R., Thomas L. Stoffel, Ibrahim Reda, Stephen M. Wilcox, Afshin M. Andreas. Recent Progress in Reducing the Uncertainty in and Improving Pyranometer Calibrations. *Journal of Solar Energy Engineering*, **124**, February 2002.

NASA.

http://acdb-ext.gsfc.nasa.gov/People/Colarco/Mission_Support/

http://acdb-ext.gsfc.nasa.gov/People/Colarco/Mission_Support/aod_floop/

NIH. <http://rsbweb.nih.gov/ij/download.html>

NREL. National Solar Radiation Data Base.

http://rredc.nrel.gov/solar/old_data/nsrdb/1991-2010/

Reda, Ibrahim. Calibration of a Solar Absolute Cavity Radiometer with Traceability to the World Radiometric Reference. NREL/TP-463-20619, January 1996.

<http://www.nrel.gov/rredc/pdfs/20619.pdf>

Reed, R. K. On Estimating Insolation Over the Ocean. *Journal of Physical Oceanography*, **2**, 482-485, May 2007.

Solar Electricity Handbook.

<http://solarelectricityhandbook.com/solar-angle-calculator.html>

5. Surface Reflectance

5.1 Background

As discussed in Chapter 4, very inexpensive pyranometers developed by IESRE can be used to measure insolation. Surface reflectance can be measured with two pyranometers – in this application such instruments would more likely be referred to as radiometers. One radiometer faces up and the other faces down. An advantage of this measurement is that neither instrument requires an absolute radiometric calibration, as is required for measuring insolation. It might be desirable for the upward-facing instrument to have such a calibration, but it is optional.

Reflectance varies over a wide range for different surfaces [International Building Performance Simulation Association – USA Affiliate]. Especially for vegetated surfaces and snow [IBPSA; Warren, 1982; author and date unknown], broadband reflectance is different from near-IR reflectance. Tabulated values of surface reflectance are just approximations or averages because surface reflectance depends on sky and surface conditions and sun-surface geometry.

When measurements of reflected radiation are made from space, scientists need “bidirectional” reflectance models to interpret these data in terms of surface reflectance. These models take into account the solar elevation relative to the surface and the solar azimuth relative to the line of sight from the orbiting spacecraft. It takes a *lot* of data to derive such models and mathematical modeling is required to fill in the total range of angles. From the ground you may be able to derive “directional” reflectance models which depend only on solar elevation.

The photodiode used in IESRE’s pyranometers is also available in a version that is physically identical, but responds only to near-infrared radiation. The spectral response of both detectors is shown in Figure 5.1. The near-IR version (PDB-C139F) is the detector with the black housing. Providing an absolute calibration for the near-IR detector is a problem because there is no standard against which to compare it.

In principle, knowing the spectral response of such a device, a radiative transfer model could be used to determine what it should “see” under clear-sky conditions.¹⁰ See the research project outlined in Section 5.5.

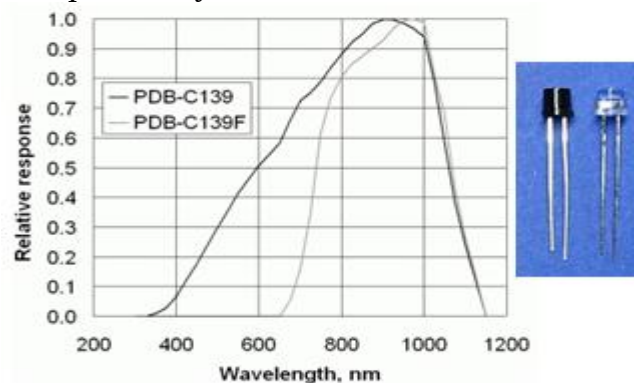


Figure 5.1. Spectral response of broadband and near-IR silicon photodetectors.

¹⁰ A discussion of radiative transfer models is beyond the scope of this document. There are many online sources of information.

5.2 Setting Up an Experiment

Figure 5.2 shows a surface reflectance experiment with a two-channel radiometer, but the procedure is the same for a one-channel radiometer. Because of the trees, this site is not a very good choice for measuring insolation, but it is a reasonable site for measuring surface reflectance. The two radiometers are connected to the four-channel HOBO U12-006 data logger described in Chapter 3. The long arm is facing south, so the tripod does not shadow the ground under the sensors.



Figure 5.2. Experiment setup for measuring broadband and near-IR surface reflectance.

As noted above, radiometers for measuring surface reflectance do not require an absolute radiometric calibration. What is needed is the relative signal from two identical sensors. You could imagine using just a single sensor, switching back and forth between the up and down position. But, this is not a practical solution!

The practical solution is to use two sensors and calibrate one relative to the other. Mount two instruments, A and B, side by side and record data for a day. You could start by pointing both instruments up. Later, you could point them both down. Designate the A instrument as the reference which will be pointed up in the

experiment. The B instrument will be pointed down at the surface during the experiment. Determine the value $C_{B \rightarrow A}$ which, when multiplied times the output of the B instrument, causes the adjusted output voltage of the B instrument to agree with the reference instrument. Then:

$$\text{reflectance} = (B_{\text{volts}} \cdot C_{B \rightarrow A}) / A_{\text{volts}}$$

Figure 5.3 shows results from calibrating two two-channel instruments. Figure 5.3(a) shows the outputs from the four sensors. Figure 5.3(b) shows the results of multiplying the B broadband output by 0.93 and the B near-IR output by 1.05. The relative calibration of the broadband channels is nearly perfect and, as should be the case, the same regardless of whether the instruments are pointing up or down. These data are instructive because there appear to be some problems with the A near-IR sensor. The conversion factor of 1.05 provides a fine fit in the morning, but later in the day differences appear between the A- and B-nearIR channels. Perhaps there is a loose connection that produces some electronic noise on the A-nearIR channel. Perhaps the problem lies with the output of the B-nearIR channel. This problem is obvious only because both instruments were viewing the same scene; it probably would have been missed otherwise. Regardless of the cause, this is a real-life problem that needs to be resolved before these instruments can be used. It is only after completing a successful calibration, with all problems resolved, that you can be confident about your reflectance measurements.

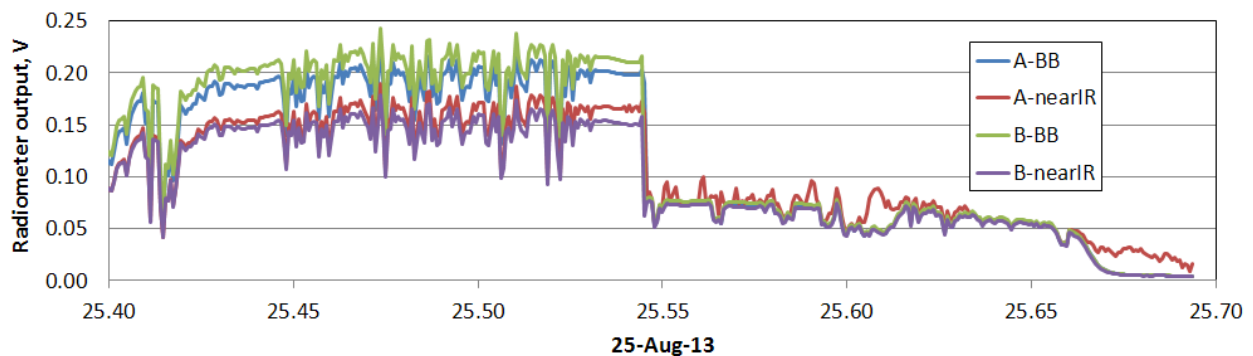


Figure 5.3(a). Raw data for relative calibration of two radiometers.

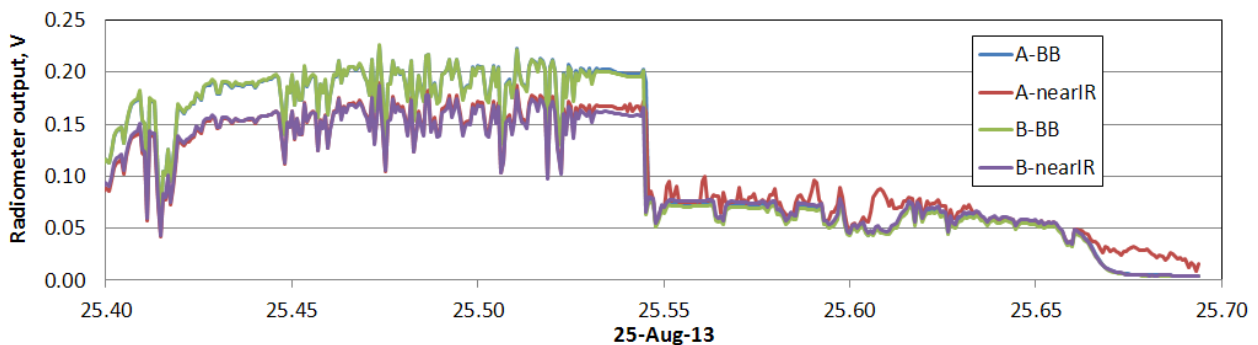


Figure 5.3(b) Relative calibrations applied to two radiometers. NASA2010/RelativeCalibrations_20130825

It is important to remember that the detectors in these pyranometers collect radiation from the entire hemisphere above (or below) them. So, the downward-facing pyranometer "sees" not just the surface directly under it, but also radiation from around the entire site, with decreasing sensitivity as the line of sight moves from directly down to horizontal. This may include buildings, upward-sloping surfaces, sky, and trees – obstructions which provide varying inputs to the downward-pointing sensor as the sun moves across the sky.

Clearly, site selection is very important for reflectance measurements. A large expanse of homogeneous surface is the best choice. You might consider limiting the influence of a hemispherical field of view by moving the detector closer to the surface. This shouldn't cause a problem if the surface being measured is homogeneous and representative of the larger area around it. It might be tempting physically to limit the field of view of the downward-pointing sensor(s). But this would mean that the relative calibration procedure described above wouldn't work.

The point of the relative calibration is to ensure that the calibrated output of the downward-pointing sensor is exactly the same as the upward-pointing sensor when both are pointed in the same direction. Two instruments with identically restricted fields of view won't work because the upward-pointing sensor needs always to view incoming radiation from the entire sky – all the radiation that will reach the ground. As is always the case for experimental research, tradeoffs are required. In this case, the tradeoff is between measuring a representative surface and limiting radiation from places other than that surface.

5.3 Reflectance Data

Figure 5.4(a) shows reflectance data obtained by mounting two two-channel radiometers on the end of a long hollow 12mm square aluminum tube (Figure 5.4(b) and holding it out in front, roughly parallel to the ground, while walking from a flagstone patio, across a gravel driveway, onto grass, and back. The interesting point about these data is that the broadband (labeled "total") and near-IR (labeled IR) reflectances are essentially the same over manmade surfaces, but significantly different over a vegetated surface.

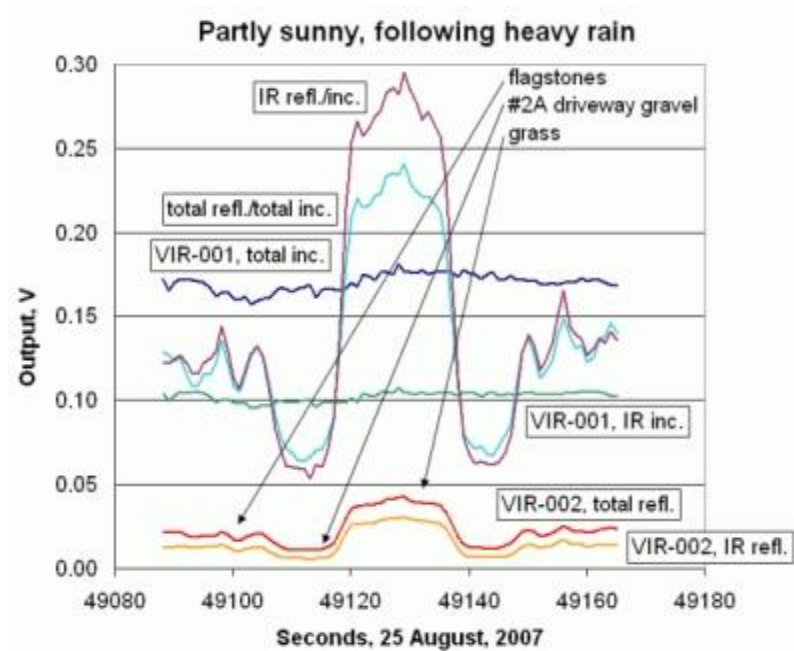


Figure 5.4(a). Broadband and near-IR reflectance over three different surfaces.



Figure 5.4(b). Two-channel radiometers.

Figure 5.5 shows an example of daytime broadband and near-IR reflectance over grass in the northern hemisphere fall. For these data, taken during a clear day (except for one small mid-afternoon "blip" due to reflections from the side of a small cloud somewhere in the sky), there is obviously a relationship between time of day (sun elevation angle) and surface reflectance. This is not at all surprising.

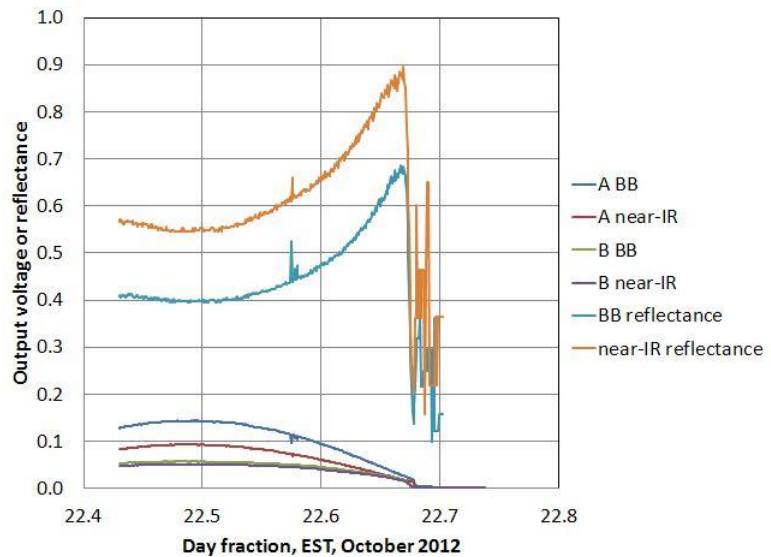


Figure 5.5. Broadband and near-IR reflectance over grass, 40.2°N, 75.3°W.

The response of surfaces to incoming solar radiation is complicated. The distribution of solar radiation falling on a surface depends on a combination of diffuse radiation from the sky and direct radiation from the sun. In a clear sky, about 85% of the radiation around mid-day is direct radiation.

A surface reflects some of the incoming radiation, acting more or less like a mirror, depending on its characteristics, and scatters some of it, acting like a rough diffusing surface. This behavior influences how much radiation the downward-

facing detector sees. It may never see some of the "mirror-reflected radiation" and under cloudy skies and at different times during the day it will receive relatively more of the scattered radiation. During a clear day, the constantly changing interactions between a surface subjected to both direct solar radiation and diffuse sky radiation, changing with solar position, means that surface reflectance will have a range of values rather than being a single number.

In late afternoon (at about 22.67 days), this site starts to fall into shadow, with the proportions of sunlit and shadowed surface changing quickly and, in the midst of these changes, the upward-facing detector falling into shadow. At these low signal levels, rather than looking like a continuous function, the reflectance values vary among several "discrete" values, due to the limited resolution of the data logger that converts the analog output of the detectors to a digital value. These values can be ignored in any analysis of the properties of the surface being studied. At a different site, with a larger expanse of homogeneous surface and fewer obstructions around the horizon (there are lots of trees and bushes around this site, and a two-story house about 10 m behind the location from which the photo was taken), it might be possible to extend the analysis to smaller solar elevation angles (earlier and later in the day).

5.4 Indices for Monitoring the Health of Vegetation (and Snow?)

Understanding the health of vegetation on Earth's surface is important for climate scientists, but also for other reasons. From a climate change perspective, global space-based measurements are needed to track the shifting characteristics of vegetation (such as crops and forests) in response to climate change. These changes can be both a result of and a cause of climate change. For example, these measurements can be used to monitor the status of tropical forests such as the Amazon, which are so important to the environmental health of our planet, or the progress of desertification in sub-Saharan Africa in response to changing land use and weather patterns.

It is not only the environmental health of our planet that depends so critically on the health of vegetation. There are political and economic impacts, too. Areas where droughts or other natural disasters significantly impact agriculture can quickly become politically unstable trouble spots. Entire populations can be stressed by changes in growing conditions, leading to refugee problems that may require a response from the international community. Sometimes, especially in areas where "mono-crop" agriculture is dominant, very small changes in climate can produce very large changes in the success of agricultural operations — critical to global food supplies and to the stability of countries whose economies depend heavily on agriculture. Indeed, although it is easy to take it for granted, the status of vegetation impacts all of our lives, regardless of whether climate is changing or not!

Since the beginnings of Earth science conducted from space, scientists have looked at vegetation. Basically, vegetation is green, so this provides a clue. But, more descriptive data are needed.

In order to monitor the health of vegetation, scientists have defined the Normalized Difference Vegetation Index (NDVI):

$$\text{NDVI} = (\text{NIR} - \text{VIS}) / (\text{NIR} + \text{VIS})$$

where NIR and VIS are the surface reflectances in the near-infrared and visible. Mathematically, the NDVI can have values between -1 and $+1$. An example of a satellite-derived global NDVI map is given in Figure 5.6 [NASA].

The NDVI is based on the observation that vegetation reflects solar radiation differently in the visible and near-IR regions of the electromagnetic spectrum. The reflectance of dense healthy vegetation is relatively higher in the near-IR and lower in the visible than unhealthy or more sparse vegetation. As the visible reflectance decreases, the NDVI moves toward 1. Over bare soil, VIS and near-IR reflectance are about the same, so NDVI moves toward 0. Under some conditions, it is possible for NDVI to be less than 0.

Locally, this same measurement can be used to monitor changes in vegetation over a small area on the ground, in response to time of year, temperature, precipitation, and soil conditions. If you are already measuring broadband and near-IR reflectance, calculating a vegetation index requires no additional data and only one additional column of calculations in a spreadsheet, so there is no reason not to do it.

Remember that the NDVI compares visible and near-IR radiation, while IESRE's radiometers use a near-IR detector and a broadband detector that *includes* the same portion of the near-IR spectrum. There is no way to separate out the visible component based just on the data. However, you can define a "broadband" vegetation index:

$$I_{\text{broadband}} = (\text{NIR} - \text{broadband}) / (\text{NIR} + \text{broadband})$$

Figure 5.7 shows some reflectance data and $I_{\text{broadband}}$ calculations from May 2013 over a healthy grass lawn that had received plenty of springtime rain. Note that the reflectances change significantly during the day, as a function of sun elevation angle, but the index value changes only a little. $I_{\text{broadband}}$ has an average value of about 0.175. This is probably smaller than the NDVI over the same surface because the broadband channel includes all of the near-IR signal, too. But, what is the significance of this index? Will its value change enough with the seasons or with

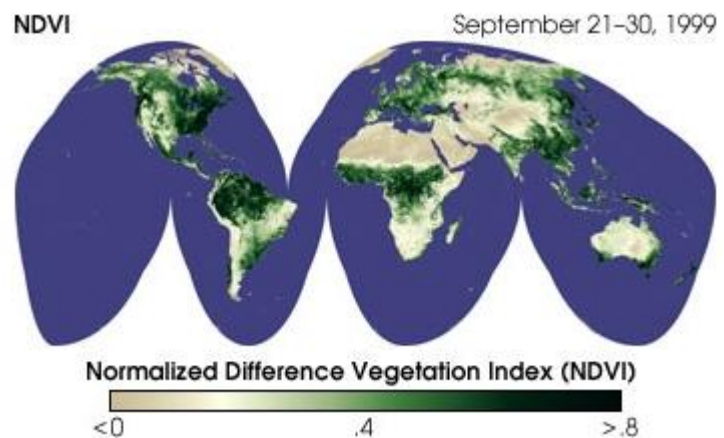


Figure 5.6. Satellite-derived global NDVI map.

weather conditions such as a summer drought to make it a useful stand-in for the NDVI? That is still an open question!

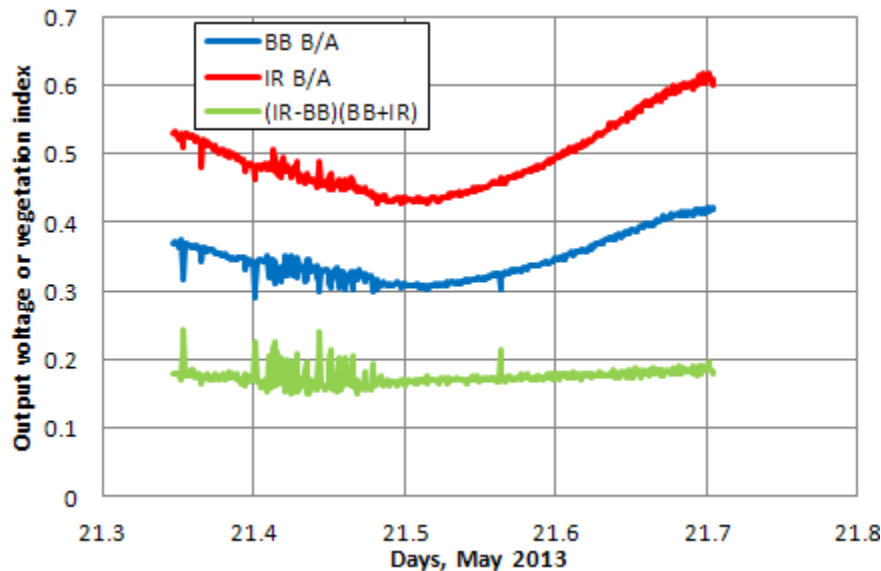


Figure 5.7. Reflectance and $I_{\text{broadband}}$ over grass, 40.2°N, 75.3°W.

Snow too?

Exactly the same measurements and calculations can be done over snow. As noted above, snow should reflect solar radiation differently in the visible and near-IR, changing with the “health” of the snow cover – its depth, age, moisture content, air temperature, melting, and soot deposits.

5.5 Inquiry and Research Questions

(Inquiry)

- Before undertaking research projects, collect some one- or two-channel reflectance data over a surface. Make sure the upward- and downward-pointing radiometers are properly calibrated relative to each other. Take photos of the surface at the experiment site, ideally near the same time of day. If you are using two-channel radiometers, calculate $I_{\text{broadband}}$. Do the reflectance data and calculated index make sense?
- Collect one- or two-channel data over two different surfaces, not necessarily simultaneously, and compare the results.

(Research)

- How do the reflectances of vegetated and manmade surfaces differ over seasons? Collect data simultaneously at two or more sites with different surfaces.
- How do the reflectances of surfaces depend on sun, sky, and surface conditions? Can you develop a mathematical model for these dependencies, starting with a

surface-dependent model for clear-sky reflectance as a function of solar elevation angle?

- How does the reflectance of manmade surfaces affect our environment and the efficiency with which structures can be heated and cooled? How could construction materials with high reflectances be used to modify urban heat island effects? What could be the role of green (vegetated) roofs?
- Can you devise an experiment that will test the effects of different roofing materials on the temperature in an enclosed space under those materials?
- Section 5.4 discussed the possibility of using a broadband vegetation index based on the detectors used in IESRE's radiometers, one of which is a broadband detector and the other of which responds only to near-IR radiation, as a stand-in for the VIS/NIR NDVI. In order to compare this broadband index with an index corresponding to the NDVI, you need a second instrument (VIS/NIR) which is identical except for the addition of a "low-pass" filter to block near-IR radiation from reaching the broadband detector. The specifications for the 12.5mm-diameter NT55-234 filter from Edmund Optics are:

Front Surface: T=85%, 480nm-680nm; T=50%, 680nm-740nm; T=10%, 740nm-1200nm

The filter blocks 90% of near-IR radiation, while passing almost all visible radiation.

Figure 5.8 shows such an instrument.¹¹ It is identical to the two-channel radiometer discussed in this chapter except for the 12.5mm-diameter (0.5") filter mounted over the broadband photodiode, under a 12.5mm Teflon® diffuser. The filter is shown over the photodiode in the inset image. The near-IR detector with its 9.5mm (0.375") diameter Teflon® diffuser, the standard diameter for unfiltered photodiodes in IESRE radiometers, is on the right.



Figure 5.8. Two-channel radiometer with IR cutoff filter over broadband photodetector.

At the time this document was written, the NT55-234 filters cost over \$40 each – almost four times the cost of all the other two-channel radiometer parts combined. So, even though this is still a relatively inexpensive radiometer by research standards, the question of whether VIS/NIR index provides significantly more useful information about the health of vegetation than the broadband/NIR index is well worth asking.

Figure 5.9 shows some data collected at 40.2°N, 75.3°W, with a VIS/NIR instrument. Figure 5.9(a) shows results from June 15, 2011, when the grass was healthy and green. The output from the individual channels varies quite a bit

¹¹ This instrument may be available on special order from IESRE.

during the day, but the NDVI values remain relatively constant. Late in the afternoon, shadowing of this site by trees produces erratic results which can be ignored. For this surface the NDVI is about 0.47-0.48.

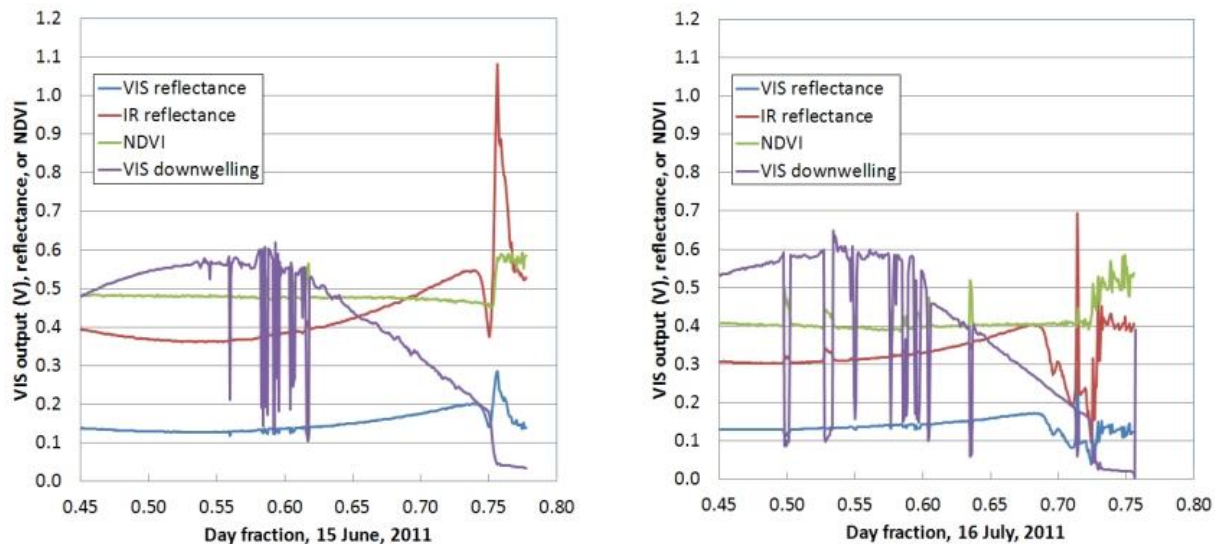


Figure 5.9. VIS and near-IR reflectance, and NDVI over a grassy surface, 40.2°N, 75.3°W.
 (a). Ample rain earlier in month. (b). No rain for several weeks.

During the next several month, as often happens this time of year, there was no rain. This grassy area has only a very thin layer of topsoil over shale, so it does not retain moisture well. With no rain, the soil quickly dries out and the grass turns brown. We would expect the NDVI to decrease as a result. Figure 5.9(b) shows that by July 16, the NDVI has decreased to a value of about 0.40. Note that the VIS reflectance is about the same, but the near-IR reflectance has decreased significantly. The change in NDVI is significant, but not really large. Much more data are required to determine how to interpret this measurement as an indicator of the health of vegetation (or the “health” of snow).

For comparison, it is interesting to collect these data over a surface with no vegetation. The graph below shows the NDVI calculation over a gravel driveway adjacent to the grassy surface. For this surface, there should be little difference in the VIS and IR reflectivity so the NDVI should much smaller than the value over a vegetated surface. The data shown in Figure 5.10 (from a very cloudy day) give NDVI values of about 0.8 – a result that is very different from a vegetated surface! Note that the NDVI is relatively

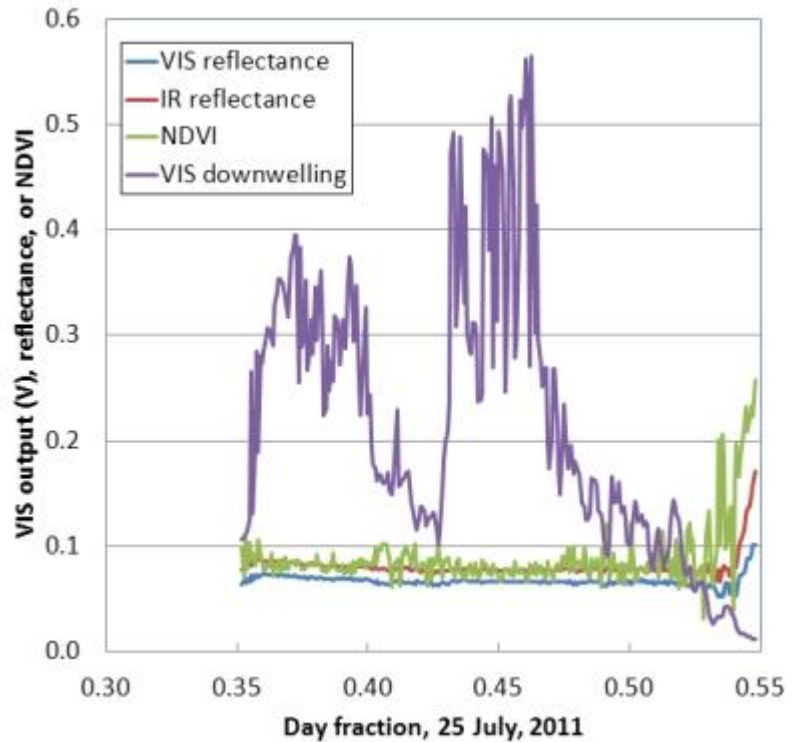


Figure 5.10. NDVI calculation over gravel.

constant even though the incoming radiation (tracked with the VIS channel) varies over a very large range of values.

- Measuring the reflectance of snow is more challenging than other surfaces in most places because it is so weather-dependent. But, if you live in an area where snow is reasonably predictable during the winter, you can plan ahead for such measurements, using a two-channel radiometer and calculating the broadband and NIR reflectances and the broadband/NIR index discussed in Section 5.4. Because the properties of snow are so different from other surfaces, the behavior of snow reflectance as a function of solar elevation angle and sky conditions should be very interesting [IBPSA]. Ideally, you should compare this behavior against data from the same surface during other seasons.

• It might be interesting to try to derive absolute radiometric calibrations for the near-IR photodetectors used in the two-channel radiometers discussed in this chapter. Figure 5.11 shows the radiation received by the broadband (PDB-C139) and near-IR (PDB-C139F) photodiodes based on the SMARTS radiative transfer model [NREL], under clear skies at a solar elevation angle of 30° (relative air mass = 1/sin(solar elevation)). The normalized spectral response of the two detectors has been taken from Figure 5.1. Other assumptions about the atmosphere, including water vapor, are also required as input to the model.

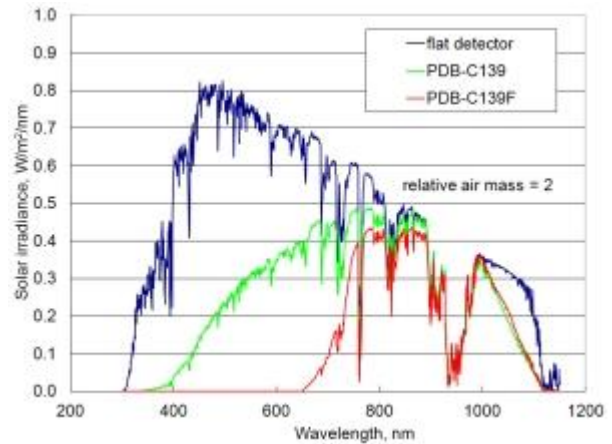


Figure 5.11. Clear-sky irradiance received by broadband (PDB-C139) and near-IR (PDB-C139F) silicon photodiodes.

For the conditions depicted in Figure 5.11, the ratio of total radiation received by the near-IR detector to the total radiation received by the broadband detector is $R = \dots$. In principle, this information could be used to calibrate the near-IR channel in a two-channel radiometer by using a calibrated broadband pyranometer as a reference. Use the SMARTS model to generate data under clear skies over a range of assumed relative air masses. The calculated values of R will depend on the air mass and the assumed total atmosphere precipitable water vapor – $R_{m,WV}$. Then find a calibration constant $C_{m,WV}$ for a pair of broadband and near-IR sensors from:

$$C_{m,WV} \cdot \text{near-IR}_{\text{output volts}} = R_{m,WV} \cdot \text{BB (W/m}^2\text{)/V}$$

What to do about this relationship under cloudy skies is an open question. It is certain that the ratio of received near-IR to broadband radiation will be different than it is under clear skies.

5.6 Resources

(Author Unknown) Department of Civil & Environmental Engineering. Optical Properties of Snow. The University of Utah.

<http://www.civil.utah.edu/~cv5450/Remote/AVIRIS/optics.html>

(IBPSA) International Building Performance Simulation Association – USA Affiliate. Ground Reflectance.

http://www.bembook.ibpsa.us/index.php?title=Ground_Reflectance

NASA. Measuring Vegetation (NDVI and EVI).

<http://earthobservatory.nasa.gov/Features/MeasuringVegetation/>

National Renewable Energy Laboratory. SMARTS Simple Model of the Atmospheric Radiative Transfer of Sunshine. <http://www.nrel.gov/rredc/smarts/about.html>

Warren, Stephen G. Optical Properties of Snow. *Review of Geophysics and Space Physics*. Vol. 20, No. 1, pp 67-89, February 1982.

6. Surface and Sky Thermal Radiation

6.1 Background

As noted in Chapter 2, Earth's maintains its radiative balance by absorbing solar radiation and re-emitting it in the form of thermal radiation. Surface temperature and radiated thermal power are related through the Stefan-Boltzmann equation (Equation 1 in Chapter 2):

$$\text{radiated power} = \epsilon\sigma T^4$$

Handheld “non-contact” IR thermometers for measuring the temperature of objects (Figure 6.1) are widely available. Point one at a surface, squeeze the trigger, and the output from a thermopile sensor¹² is converted to a temperature displayed in °C or °F. These devices use the Stefan-Boltzmann equation to convert thermal radiation to a temperature. Typically, they assume an emissivity of 0.95, which is reasonable for many surfaces [The Engineering Toolbox].

These devices are interesting for characterizing surfaces, but they provide only instantaneous measurements. It would be much more useful to be able to monitor surface radiating temperature continuously.



Figure 6.1. Handheld non-contact IR thermometer.

6.2 Continuously Monitoring Surface Radiating Temperature

An instrument to record surface radiating temperature is more complicated than the pyranometer discussed in Chapter 2, so it deserves a more detailed discussion.

The Excelitas TPS 1T 0134 OAA060 thermopile sensor¹³ is a self-contained module with a built-in op amp, pre-calibrated for converting voltage to temperatures in °C. It is relatively expensive by the standards of other IESRE sensors – about \$25 each. The spectral response is shown in Figure 6.2. It produces a voltage output in the range of 0-4.5 V, corresponding to a temperature range from –27°C to 60°C. Some extreme conditions may produce surface temperatures outside this range.

¹² <http://en.wikipedia.org/wiki/Thermopile>

¹³ <http://www.excelitas.com/pages/product/Thermopile-Detectors-Sensors-and-Array-Modules.aspx>

The full-width half-height field of view of this device is 60° , which means that it “sees” thermal radiation mostly within a 60° cone directly under it. The sensor output is converted to temperature using a manufacturer-supplied polynomial:

$$T(^{\circ}\text{C}) = -0.002603V^6 + 0.04802V^5 - 0.38431V^4 + 1.8498V^3 - 6.835V^2 + 32.71V - 26.75$$

The conversion is shown in Figure 6.3.¹⁴ In order to use this sensor with 0–2.5V loggers used for other IESRE instruments (see Chapter 3), a voltage divider is required.¹⁵ Use two equal 1% resistors with a summed value of at least 50k Ω . (Standard carbon film resistors are typically 5%, and not accurate enough for this purpose, although it is possible to test samples from a batch of such resistors until you find two that are equal.) For loggers with a range of at least 0–5V, no voltage divider or other circuitry is required as long as the logger has a high enough input impedance. Both the loggers described in Chapter 3 have very high input impedances.

The completed instrument is shown in Figure 6.4 with two possible circuit diagrams. Unlike pyranometers, which are passive devices “powered” by the sun, the thermal sensor with its integrated op-amp needs an external power supply. The instrument shown in Figure 6.4 has a standard 9V battery clip, but an input up to +12V or even a little higher (as from a 12V solar power panel, for example) would also be OK. If in doubt, check a data sheet for the LM78L05 voltage regulator. The voltage regulator will not operate with a supply voltage less than about 7V. Even a high-quality 9V battery will power this device continuously for only a few days. 6 D cells in series will last much longer. Another option is to use rechargeable 9V NiMH batteries.

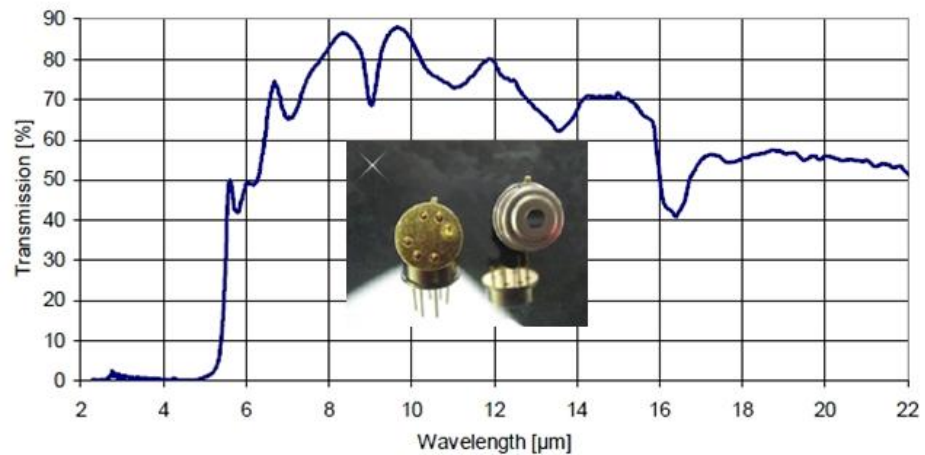


Figure 6.2. Spectral response of the TPS 1T 0134 OAA060 thermopile sensor.

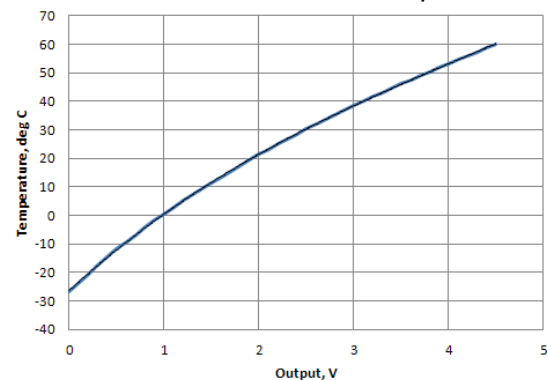


Figure 6.3. Voltage-to-temperature conversion for the TPS 1T 0134 OAA060 sensor.

¹⁴ Why the manufacturer provides a 6th order polynomial for this conversion is a mystery!

¹⁵ Onset sells voltage input adapter cables that act as voltage dividers, including a 0–5V cable, but I would rather divide the voltage myself.

A pc board for building this instrument is available from IESRE. The circuit could also be built on perfboard, but this is a little risky considering that the sensors are relatively expensive (~\$25 each).

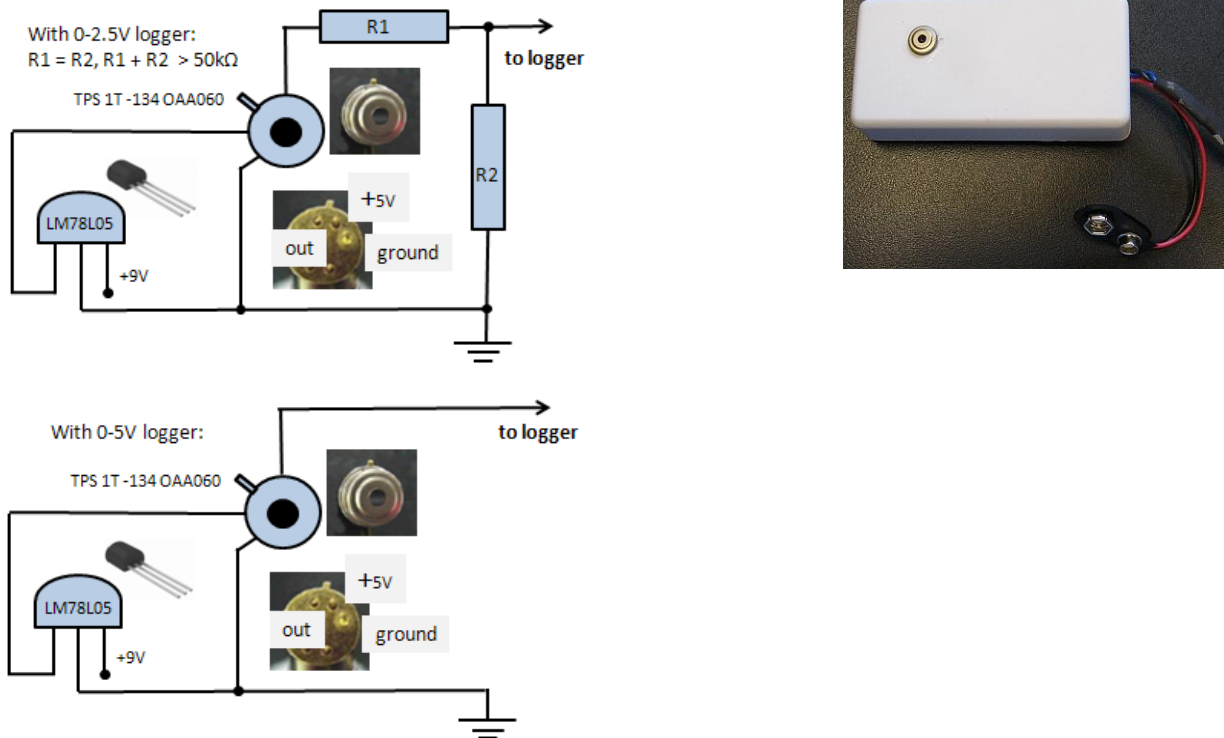


Figure 6.4. Thermopile sensor with circuits for interfacing with a data logger.

In general, it is a good idea to maintain a healthy skepticism about “pre-calibrated” sensors. Figure 6.5 shows some data collected with three thermopile sensors initially looking down at a concrete floor in a basement and then outdoors at a brick walk. Two of the sensors appear essentially identical while the third one – the blue line – gives results a little lower than the other two. Starting around day 10.4, the rms differences among the three sensors marked white, black, and red (based on the color coding of their cables in the experiment setup) are white–red = 0.44°C , red–black = 0.55°C , black–white =

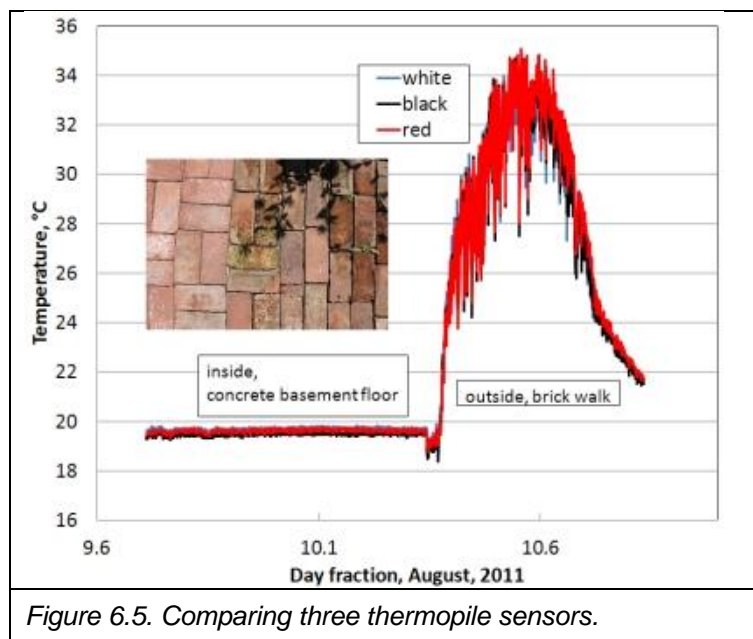


Figure 6.5. Comparing three thermopile sensors.

0.45°C. Even though the three sensors cannot measure *exactly* the same surface because they cannot be *exactly* co-located, the differences among them are almost certainly real. Whether or not the differences are significant depends on the application. But, in any case, any research project involving comparing results among several sensors needs to determine the relative performance of those sensors ahead of time and make adjustments as needed.

6.3 Comparing Radiating Temperature of Surfaces

A basic application of these thermopile devices is to compare the heat-retention properties of various surfaces. Figure 6.6 shows surface radiating temperatures measured over a grassy surface and a brick walk, plus air temperature at a site bordering the grassy surface. The grassy surface heats up quickly in the morning and cools down faster than air temperature at night. The brick walk has greater thermal inertia. Its temperature rise lags a little behind air temperature in the morning. It retains heat for a considerable time at night and never drops as low as the air temperature. This behavior can be expected to depend not only on the surface, but on soil moisture content, winds, and sky conditions.

On a local scale, this experiment helps to explain why maximum temperatures at temperate latitudes in the northern hemisphere don't usually occur until July or August, after the maximum noontime elevation angle of the sun on the summer solstice on June 20th or 21st: Earth's surface responds to increasing solar input, but the thermal inertia of the system (more like brick than grass in its properties) causes a lag in the gradual warming of the ground in response to rising temperatures. In the winter, the coldest temperatures usually occur after the winter solstice on December 21st or 22nd, as the cooling of the ground lags behind dropping temperatures.

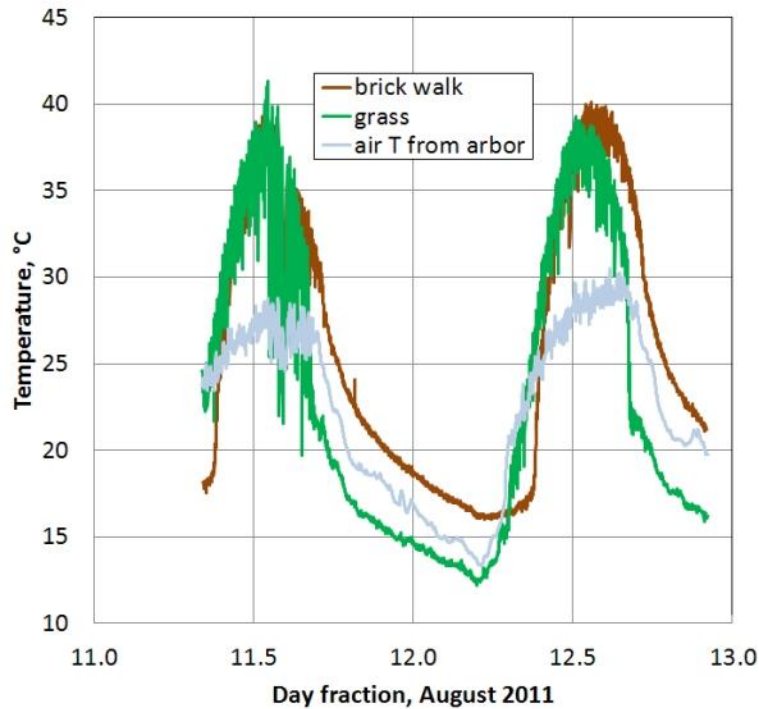


Figure 6.6. Air temperature and surface radiating temperatures over grass and brick.

6.4 Infrared Radiation from the Nighttime Sky

Can the TPS 1T 0134 OAA060 be used to monitor thermal radiation from the sky? If so, what does the measurement mean?

It is not clear that the Excelitas sensors are suitable for continuous outdoor monitoring. The housing may not be entirely moisture-proof and the transmission properties of the window covering the thermopile detector may not be stable under prolonged exposure to the sun. However, nighttime use is another matter. On rain-free nights it should be OK to point these devices up at the sky for prolonged periods. It is still possible that dew collecting on the sensor could cause problems, and, of course, predicting precipitation-free nights is an imperfect process.

Ideally, a second sensor should be pointed down to measure surface radiating temperature at the same time. Taken together, these two sets of data give an interesting picture of incoming and outgoing thermal radiation at Earth's surface.

Figure 6.8 shows radiation for two nights in August 2013 at 40.2°N, 75.3°W, converted into a temperature. August 2nd started out partly cloudy. By shortly after midnight the sky appears to be overcast. The sky was certainly overcast by daylight on the 3rd. Just after 9:00 on the 3rd, shortly after bringing the sensors inside, it started to rain. At dusk on 4th and at first light on the 5th, the sky was clear. There is evidence of some scattered cumulus clouds, having some small effects on the sensor output.

In Figure 6.8, the sensor outputs have been converted to a temperature, but what does this mean for the sky-viewing sensor? The sensor captures the IR

radiation from the sky within its 60° field of view. The temperature conversion is based on the assumption that the sensor is pointed at an actual blackbody surface (or a graybody with an emissivity close to 1). For overcast skies, it might be reasonable to assume that the thermopile sensor is measuring the temperature of the cloud base "surface." But in general, the sensor doesn't see a real "surface" at all when it looks at the sky. Not only is the emissivity of the sky with or without clouds unknown, but it is not even necessarily true that the sky or clouds behave like blackbodies or graybodies.

Uncertainty about interpreting data from a sky-pointing thermopile sensor does not make the data less interesting or useful, but it is important to be careful what you call the result of the voltage-to-temperature conversion. Referring to this value as an "apparent temperature" (my preference) or an "effective temperature" is much more appropriate. It is likely, by the way, that the apparent temperature of a cold clear winter sky will often be less than -26.75°C , resulting in an output of 0 V.

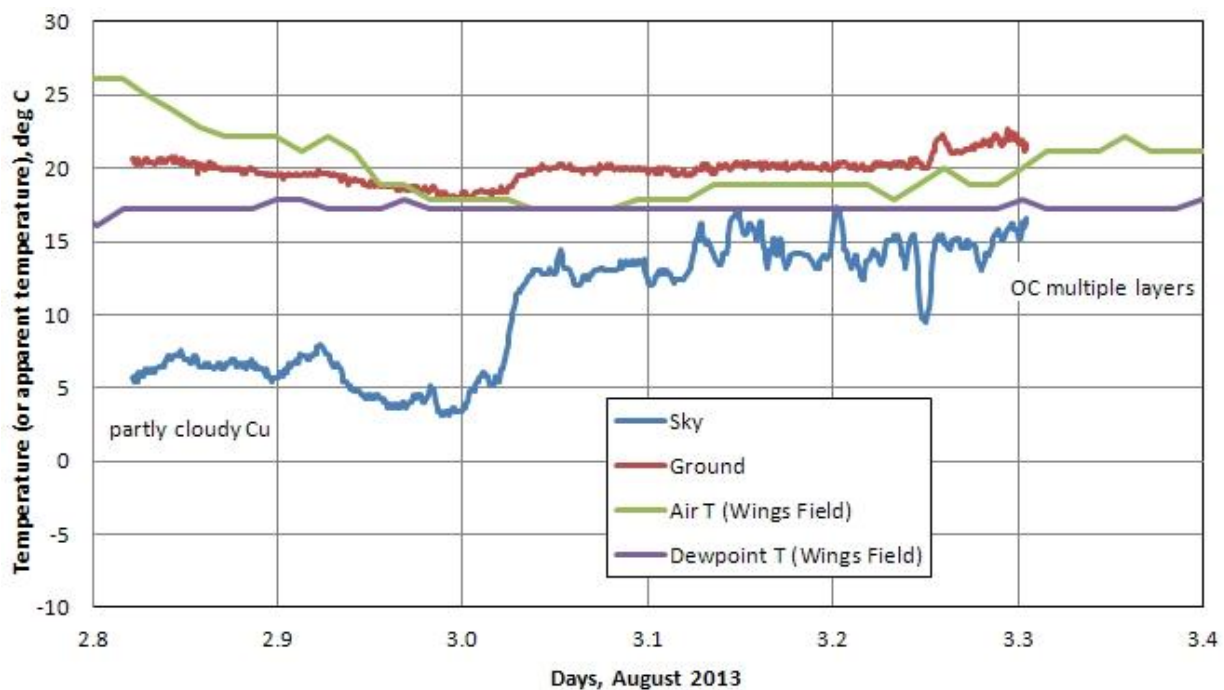


Figure 6.8(a). Surface temperature and apparent sky temperature under partly cloudy/overcast skies, 40.2°N , 75.3°W .

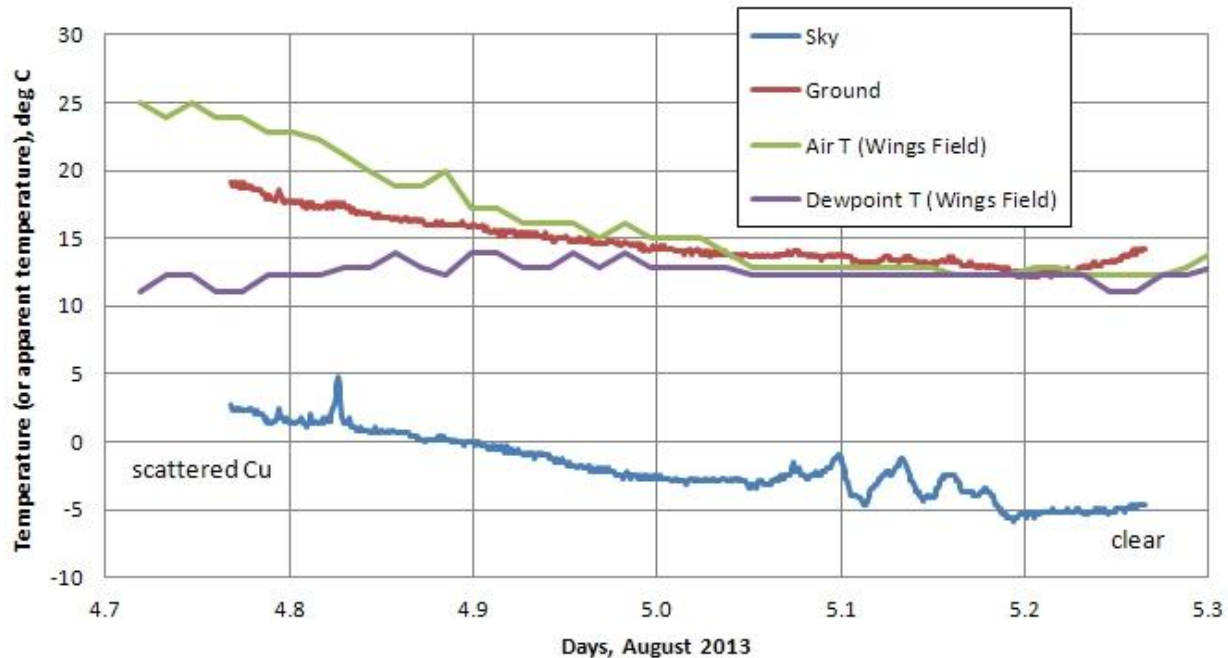


Figure 6.8(b). Surface temperature and apparent sky temperature under mostly clear skies, 40.2°N, 75.3°W.

Regardless of how one interprets the output from these thermopile sensors when they are pointed up at the sky, Figure 6.8 shows that the data can be used to track clouds in the nighttime sky. Of course, this is not possible with visual observations at night unless there is enough moonlight to see clouds.

Air and dewpoint temperatures from a nearby small commercial airport are included in Figure 6.8 because these values are needed for models to estimate thermal radiation from the sky – see Section 6.6.

6.5 Monitoring the Daytime Sky

Although there may be some problems with long-term exposure of the Excelitas sensors to sunlight, daytime sky radiation measurements are interesting enough to consider this measurement. An obvious advantage of daytime measurements is that you can compare instrument output with photographic and visual images of the sky.

Investigating the long-term stability of thermopile sensors under the conditions described here represents uncharted territory and you are invited to try it. The sensor should be oriented so that it faces north angled down from the zenith sky so the sun is never within the sensor's field of view, as shown in Figure 6.9.

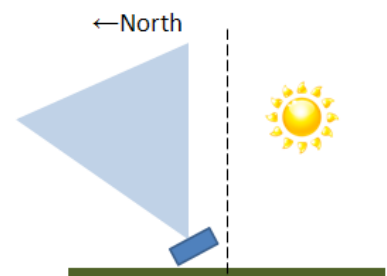


Figure 6.9. Proper orientation for sky-viewing sensor during daytime in northern hemisphere.

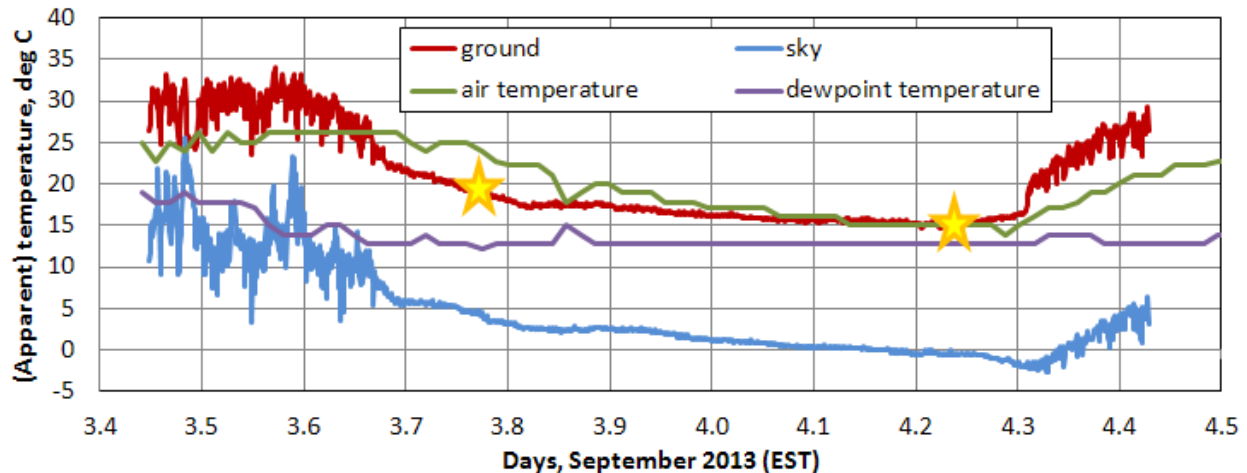


Figure 6.10. Day-night-day thermopile measurements, 40.2°N, 75.3°W.

At temperate latitudes, pointing the sensor at an elevation of 60° should be acceptable even during June, when the noontime sun is at its maximum elevation angle. Figure 6.10 shows some day-night-day data from the same site as Figure 6.8. The gold stars indicate approximate sunset and sunrise times on the 3rd and 4th. Note that in both Figures 6.8 and 6.10 the nighttime sky apparent temperature falls below 0°C. Also notice in Figure 6.10 the slight jump in ground temperature just after day 4.3 (~7:00 am EST), when shadows from trees move past the sensor site to put it in sunlight.

A further refinement would be always to orient the sensor at an elevation angle a fixed angular distance away from the solar noon elevation – an angle that changes during the year. This value can be calculated as a function of day of year and latitude with this online application: <http://www.instesre.org/Solar/insolation.htm>.

Because the long-term stability of these thermopile sensors under exposure to sunlight is not established, you should have an additional “reference” sensor that is used for periodic indoor checking of your outdoor sensors.

6.6 Converting Temperature to Radiated Power

The apparent or actual surface temperatures shown in Figures 6.8 and 6.10 are not an end in themselves. In the context of investigating radiative balance, those values need to be converted to radiated power – irradiance. Conversion of surface temperature to irradiance is a straightforward application of the Stefan-Boltzmann equation, using an emissivity of 0.95 for grass and many other surfaces. As noted above, converting the apparent sky temperature to irradiance is *not* straightforward.

Several authors have modeled longwave clear-sky radiation L_{clr} , using the familiar form of the Stefan-Boltzmann equation with local air temperature T_0 and an effective emissivity which may be much less than 1, based on empirical data or theory [Crawford and Duchon, 1999; Flerchinger *et al.*, 2009]. Flerchinger gives this simple formulation for L_{clr} :

$$L_{\text{clr}} = \epsilon_{\text{effective clear}} \sigma T^4$$

Where T is air temperature in units of kelvins. Both Flerchinger *et al.* and Crawford and Duchon reference other authors who have provided formulas for calculating clear-sky emissivity. Emissivity depends on air temperature and atmospheric water vapor content. Because water vapor is rarely directly available, most of the calculations summarized in Flerchinger rely on dewpoint temperature, which is related to water vapor [Reitan, 1963; Smith, 1966] and which can be calculated from air temperature and relative humidity. Hence, the emissivity models involve various combinations of air temperature T , atmospheric water vapor pressure e_w , and atmospheric water vapor. Here is one example [Brutsaert, 1975], quoted in Flerchinger, which requires only air temperature ($^{\circ}\text{C}$) and relative humidity:

$$\epsilon_{\text{effective clear}} = 1.723 \cdot [e_w / (T + 273.15)]^{1/7}$$

$$e_w = 6.11 \times 10^{[7.5T_d / (237.7 + T_d)]} \text{ kPa}$$

$$A = 17.27T / (237.7 + T) + \ln(\text{RH}/100)$$

$$T_d = 237.7A / (17.27 - A) \text{ } ^{\circ}\text{C}$$

Calculations for vapor pressure and dewpoint temperatures can be found online [NOAAa, b, c, d]. The values of $\epsilon_{\text{effective clear}}$ vary quite a bit depending on which model is used, so it is worth exploring some of the other models, too.

Figure 6.11 show thermal irradiance for the data from Figure 6.10, assuming the skies were clear – a reasonable assumption at least during the night. The red line shows thermal irradiance from the surface using a Stefan-Boltzmann calculation with the measured surface temperature and an emissivity of 0.95. The solid blue line shows thermal irradiance from the sky using a Stefan-Boltzmann calculation with the measured apparent sky temperature and an emissivity of 1. The dashed blue line shows results from the model given above, using the air temperature and dewpoint values graphed on Figure 6.10.

The striking point about Figure 6.11 is the close agreement of the modeled sky radiation, based just on air and dewpoint temperatures, with the radiation calculated from the measured apparent sky temperature; the latter calculation is based on the completely unwarranted assumption that the sky can be treated approximately as a blackbody “surface” with an emissivity of 1.

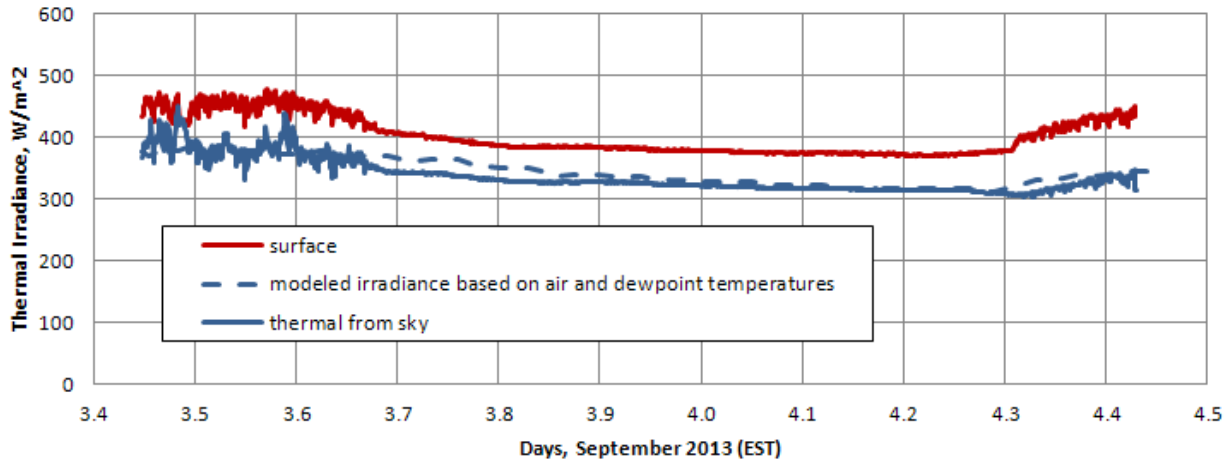


Figure 6.11. Thermal irradiance from the surface and sky.

Of course, it is not sufficient just to be able to calculate clear-sky thermal radiation from the sky. Other authors cited by Flerchinger have derived modifications to clear-sky emissivity based on cloud cover. Increasing cloud cover increases the clear-sky emissivity, based on the assumption that a cloud base has an emissivity close to 1 regardless of whether clouds actually behave like graybodies. Formulating emissivity models for non-clear skies is an excellent research topic.

6.7 Inquiry and Research Questions

(Inquiry)

- Collect and compare some thermal radiation data over two different surfaces under different weather conditions (not when it's raining). Can you relate the data and the differences between surfaces to weather conditions?

(Research)

Many of these research projects should be done in combination with surface reflectance of the surfaces being studied and air temperature above the surfaces.

- How do the thermal radiating properties of roofs depend on roofing material?

This question should be examined in combination with other measurements such as air temperature above the roof and the reflectance of the surface.

- How does precipitation affect thermal properties of a vegetated surface? What is the relationship between surface radiating temperature, air temperature, and soil temperature over vegetated surfaces?

Ideally, you should measure soil moisture directly. There are protocols for determining soil moisture in collected samples, but equipment for continuous *in situ* monitoring of soil moisture is relatively expensive.

- How does surface radiating temperature vary over the seasons and what, if anything, does this tell us about seasons that air temperature does not?

- A paper by Mims, Chambers, and Brooks [2011] has shown that a handheld non-contact IR thermometer pointed at the clear zenith sky can be used to estimate total column water vapor – an important parameter for understanding climate change due to greenhouse gases. Can the thermal sensor described in this chapter be used to determine an “all weather” mathematical model for this relationship? Is the model different for daytime and nighttime measurements? Are the results any better than a model based just on dewpoint temperature? This project can be done effectively only if you have access to an independent source of water vapor data, such as from AERONET (<http://aeronet.gsfc.nasa.gov/>) or GPS-MET (<http://gpsmet.noaa.gov/cgi-bin/gnuplots/rti.cgi>) sites. See Chapter 8 for more information about water vapor measurements.

- Can you use thermal sensor output to quantify cloud amount and type?

It is clear that thermal radiation from the sky varies with cloud cover, but it is not so clear how to interpret this behavior in terms of cloud type and amount. Considering the discussion in Chapter 4 about using pyranometer data to analyze cloud properties during the day, is it possible to link these two projects to provide a more comprehensive method of quantifying cloud properties?

- The discussion in Section 6.6 suggests many possibilities for research into the relationship between data from a sky-pointing thermopile sensor and thermal radiation from the sky. The surprising agreement between modeled and measured clear-sky irradiance shown in Figure 6.11 needs to be tested under other clear-sky conditions, and then extended to other sky conditions.

6.8 Resources

Brutsaert, W. On a derivable formula for long-wave radiation from clear skies. *Water Resources Research*, **11**, 742-744, 1975.

Crawford, T. M., and C. E. Duchon. An Improved Parameterization for Estimating Effective Atmospheric Emissivity for Use in Calculating Daytime Downwelling Longwave Radiation. *Jour. Appl. Meteorology*, **38**, 474-480, 1999.

The Engineering Toolbox.

http://www.engineeringtoolbox.com/emissivity-coefficients-d_447.html

http://www.engineeringtoolbox.com/radiation-heat-emissivity-d_432.html

Flerchinger, G. N., Wei Xiaio, Danny Marks, T. J. Sauer, Qiang Yu. Comparison of algorithms for incoming atmospheric long-wave radiation. *Water Resources Research*, Vol. 45, W03423, doi: 10.1029/2008WR007394, 2009.

Mims, Forrest M., Lin Hartung Chambers, David R. Brooks, Measuring Total Column Water Vapor by Pointing an Infrared Thermometer at the Sky. *Bull. Amer. Meteor. Soc.*, 92, 10, 1311-1320, 2011.

NOAAa. http://www.srh.noaa.gov/epz/?n=wxcalc_vaporpressure

NOAAb. <http://www.srh.noaa.gov/images/epz/wxcalc/vaporPressure.pdf>

NOAAc. <http://www.hpc.ncep.noaa.gov/html/dewrh.shtml>

NOAAD. <http://www.srh.noaa.gov/images/epz/wxcalc/wetBulbTdFromRh.pdf>

Reitan, C. H. Surface dew point and water vapor aloft. *Journal of Applied Meteorology*, **2**, 776-777, 1963.

Smith, W. L., Note on the relationship between total precipitable water and surface dew point. *Journal of Applied Meteorology*, **5**, 726-727, 1966.

7. Sky Photography

7.1 Background

Whenever you want to find out about the weather, probably the first thing you do even when you're indoors is look at the sky. Is it blue and clear? Hazy? Raining? Gray and overcast? Cloudy? What kinds of clouds are visible? It is clear from our every-day experience that the appearance of the sky is important to our assessment of the state of our local environment. Is it possible to find ways of quantifying these observations?

Sky photography allows you to build a permanent record of the state of the atmosphere. Any photograph of the sky provides useful information about the atmosphere when the photo was taken. But, if you photograph the sky over long periods of time, following an established protocol, these photographs can also provide quantitative information about the changing state of the atmosphere. The interpretation of many ground-based measurements is greatly facilitated by a record of the condition of the sky.

As opposed to other data collection-based research projects discussed in this document, much interesting sky photography can be done with no special equipment. All you need is a digital camera and a plan for creating a consistent record of a set of scenes over an extended period of time. Possible targets for your photos include views of the sky extending up from the horizon and views of distant objects.

Regardless of what scene you are viewing, it is important to consider lighting conditions. A distant mountain or building will look much different depending on whether the surface facing you is in sunlight or shadow. The sky will look much different if the sun is in front of you, in your camera's field of view, or behind you. So, it is important to identify scenes where appropriate lighting is possible and to collect data at times of the day where those scenes will be lit in approximately the same way over extended periods of time.

Another consideration in sky photography is camera settings. Typically, modern digital cameras operate by default in "auto" mode, where firmware in the camera automatically sets a shutter speed and f-stop before you snap the photo. It may even choose an ISO setting – a number related to "real" film having varying sensitivity to light. This is very convenient for most photography and usually results in the best-looking image for any given scene. But, once you start taking sky photographs, consistency and repeatability are the goals. Hence, it is preferable always to use the same camera with the same manual settings. This is the only way reliably to track changes in sky conditions over time. Some digital cameras allow you to select settings manually and some don't. Less expensive point-and-shoot cameras may not have this feature, while more expensive cameras will; check the specs.

If your camera has a range of resolution settings, you should use the highest available resolution. Although it is tempting to use photo-processing software to

“improve” your images, that is not appropriate for this kind of work. Do not resize or “sharpen” your images, or adjust the brightness, contrast, or color saturation. It may be appropriate to crop the image, depending on which features are of interest.

7.2 Sky Brightness Measured from the Horizon

Figure 7.1 shows an example of how to analyze a sky photograph. This image was taken looking north from the grounds of a school in Chiang Rai, Thailand’s northernmost Province, in January 2010. The analysis is done with the freeware ImageJ program.¹⁶ The “Line” box is checked on the ImageJ toolbar and the cursor has been used to draw a straight line vertically from the bottom of the photo to the top. ImageJ’s “Plot Profile” tool from the “Analyze” option on the toolbar is then used to plot the sky brightness along this line. ImageJ converts the image to a grayscale, with brightness levels from 0 (black) to 255 (white) and plots the values as a function of distance above the horizon, in units of pixels. The data represented in this graph can be saved as a comma-delimited (.csv) text file.

For this project, distance from the horizon is measured in units of image pixels. It is important always to use the same camera at the same resolution setting, so “500 pixels from the horizon” always means the same thing.

This analysis represents quantitatively what is qualitatively obvious from looking at the photo. The sky is mostly clear, but there is a layer of haze close to the ground that causes the sky to be a little darker near the horizon. The decrease in brightness near the horizon, with the maximum brightness somewhat above the horizon, is often associated with urban smog, although that seems an unlikely source in this case because there are no major cities nearby and north of Chiang Rai.

The shape of the brightness curve and the location of the maximum can be used to describe the state of the lower atmosphere. Under some very clear or very hazy sky conditions, there may be no peak at all in the brightness curve. Under hazy conditions, the brightness may not fall off as rapidly with distance above the horizon.

The information contained in these images can be used to do real research with what might at first look like “just” pictures of the sky. Long-term and/or seasonal changes in the shape of the graphs may be indicators of climate change. It is important for this work to develop a consistent way of naming and storing images. If your camera has an option to include a date and time stamp on the image, you should use it.

¹⁶ Free download from National Institutes of Health. <http://rsbweb.nih.gov/ij/download.html>

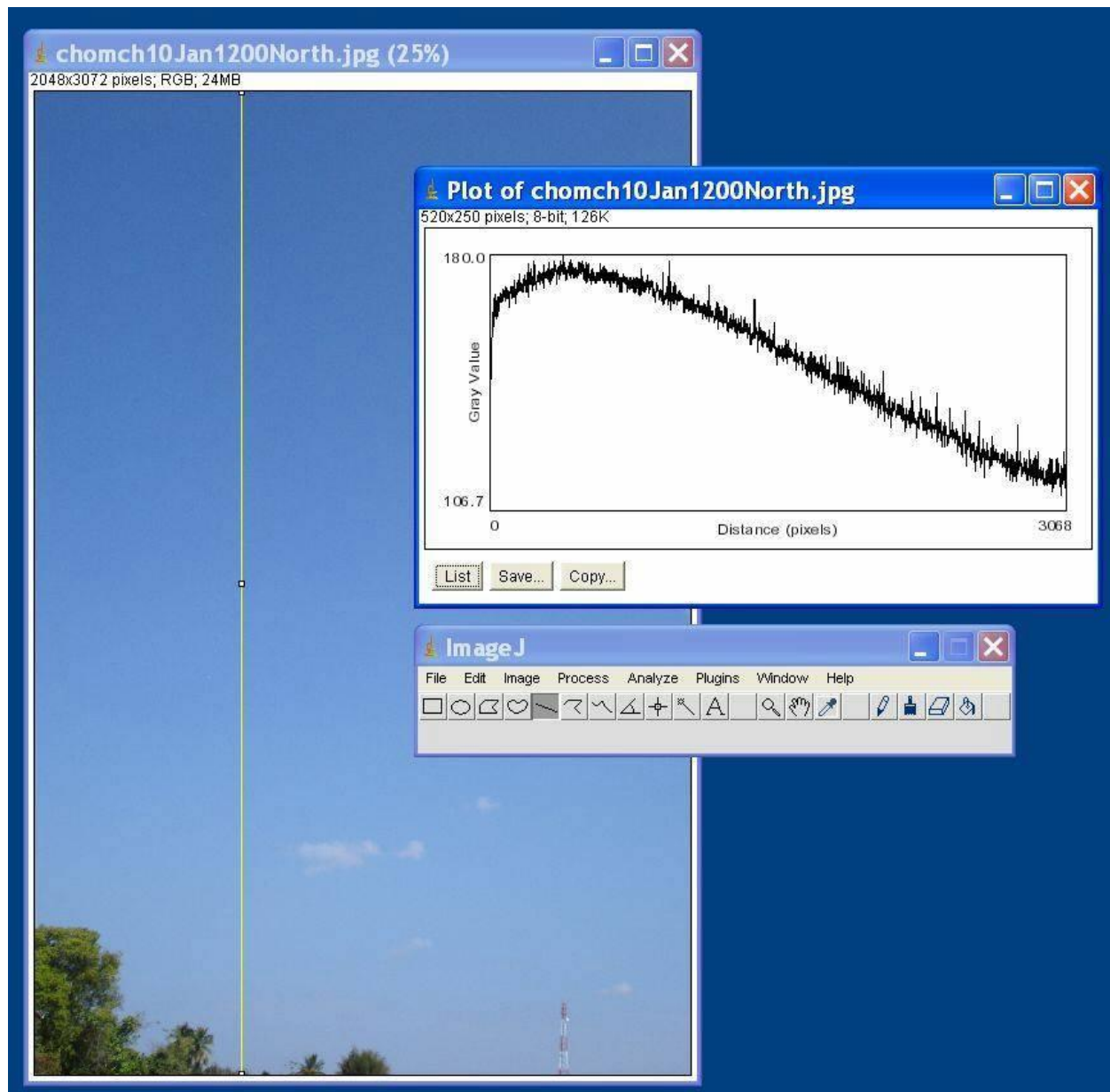


Figure 7.1. Analyzing sky image from Thailand.

7.3 Horizontal Visibility

Figure 7.2 shows another application of sky photography. The scene is the Manhattan (New York City) skyline as seen from the rooftop of the science building at Queens College, Flushing, NY on June 30, 2011. (The Empire State Building is at the left.) The sky was relatively clear on this day. ImageJ's "Histogram" tool (under the "Analyze" tab) has been used to determine the average brightness of pixels in a rectangle on the dark building at the right and a rectangle of sky of about the same size to the left of that building. The ratio of the mean building/sky brightness (on a grayscale of 0–255) is $133.21/170.55 = 0.78$.

Horizontal visibility is affected by particulates suspended in the atmosphere (aerosols), relative humidity, and smog over the city. The smaller the building/sky brightness ratio, the better the horizontal visibility. In the limit for conditions with very poor horizontal visibility, buildings at this distance will disappear against the sky and the ratio will reach a value of 1.0. These kinds of images could be used in conjunction with the images discussed in the previous section to study long-term and/or seasonal changes in weather and climate. Studies of horizontal visibility using this technique should be done using the same distant object(s) under roughly the same lighting conditions (time of day) and with the same manual camera settings.

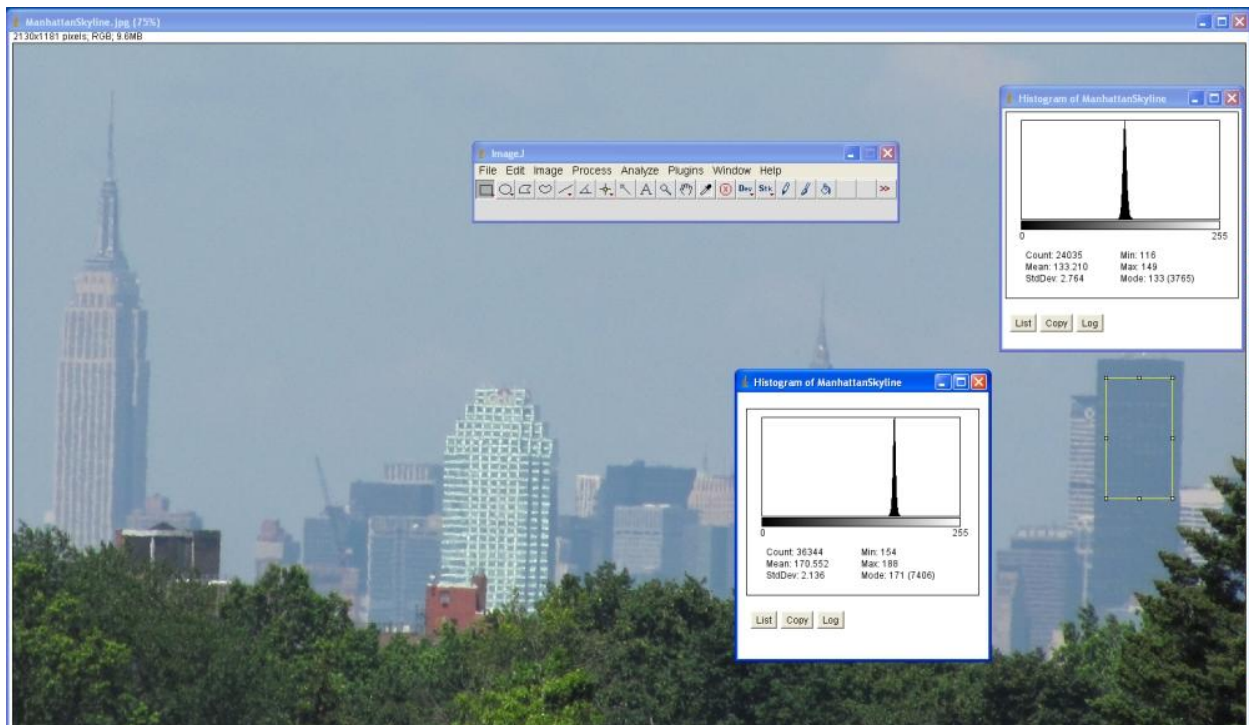


Figure 7.2. Analyzing haze over the Manhattan, NY, skyline.

7.4 Photographing the Solar Aureole

The photography described in the previous two sections of this chapter relate to the lower atmosphere. Chapter 4 discussed measuring insolation – solar radiation that passes through the entire atmosphere on its way to Earth’s surface. Insolation is affected by the presence of aerosols – solid or liquid particulates suspended in the atmosphere. Aerosols cause scattering of sunlight – the more aerosols, the more scattering.

There is another more direct way to observe the effects of particulates in the atmosphere. Scattering of sunlight produces the solar aureole, which appears as a whitish ring around the sun. The size of the aureole is related to the amount of scattering. With very clean air, and/or at high-elevation observing sites, the aureole

is very small. In hazy skies, the aureole can be very large and bright. This is true on typical summer days in temperate and tropical climates.

Digital photography offers a very simple and direct way to analyze aureoles. The measurements requires only a digital camera with manual controls for setting focus, exposure, and f-stop and ImageJ software (as discussed previously) for measuring the brightness of the sky along a line drawn horizontally outward from the edge of the sun. At this point, before proceeding, please take seriously this warning:

NEVER, under any circumstances, look directly at the sun, even with dark sunglasses or through a camera's optical viewfinder. Doing this can permanently damage your vision! There are very dense filters available designed specifically for viewing the sun, and there are viewers which project a reflected image of the sun, but no other methods are safe!

In order to photograph the sky around the sun, it is absolutely necessary to block the solar disk itself. Otherwise, the light from the sun will "wipe out" the rest of the image. Also, pointing your camera directly at the solar disk can permanently damage the camera's light sensors.

The solution is to build a simple fixture that blocks light coming directly from the solar disk. Figure 7.3 shows such a fixture, mounted on a standard camera tripod. The mounting bracket is made from a 66-cm long piece of 1/4" × 1" aluminum bar stock, available at hardware and building supply stores. The camera is mounted at one end of the bar with a 1/4"-20 screw, using the standard threaded tripod mount found on cameras. Another hole further down the bar is tapped for a 1/4"-20 screw, to attach it to the tripod. In between, a small hinge supports a sheet of thin aluminum approximately the same size as the camera body. This protects the camera from the sun while the setup is being positioned.



Figure 7.3. Setup for photographing the solar aureole.

Drill and tap a #8 or similar machine screw hole in the end of the bar. Fasten a penny with epoxy to a short piece of #14 copper wire and attach it with the screw and a washer. When the camera shown in Figure 7.3 is turned on with its lens extended, the end of the lens is about 61 cm from the penny. The penny should just cover the solar disk, leaving only the solar aureole and the sky around it. The shadow cast by the penny should just cover the camera's lens. Spray paint all these metal surfaces flat black to minimize light reflections.

To position the penny relative to the camera lens, paste a paper label to the side of the aluminum sheet facing away from the camera. With the camera turned off, flip the aluminum sheet down out of the way. Adjust the tripod so the shadow from the penny is centered over the camera's lens cover. Then flip the sheet into the "up" position and draw a circle around the shadow cast by the penny.

Manually set your camera to its shortest exposure and smallest available aperture (largest f-stop), and focus it at infinity. The camera shown in Figure 7.4 is a Canon PowerShot A530 set at 1/1600 s and f-5.6¹⁷. The camera retains these settings once they are set in manual mode, but the focus at infinity must still be set manually each time the camera is used.



Figure 7.4. Ready to take photograph of solar aureole.

To take a photo of the aureole, position the aluminum sheet in the "up" position to keep sunlight off the camera face, as shown in Figure 6.3. Then adjust the tripod so the sun's shadow is centered on the circular target. When the position is set, flip the aluminum sheet down out of the way and take the picture, as shown in Figure 7.4. Only a few seconds are required to align the penny's shadow and take a photo, during which time the sun will not have moved significantly. I usually take three quick photos and select the one that shows the aureole the most symmetrically oriented around the shadow from the penny. At a shutter speed this fast, a little "jiggle" from the tripod won't be a problem if you move it slightly.

¹⁷ This camera is no longer made, but similar models with full manual control may still be available..

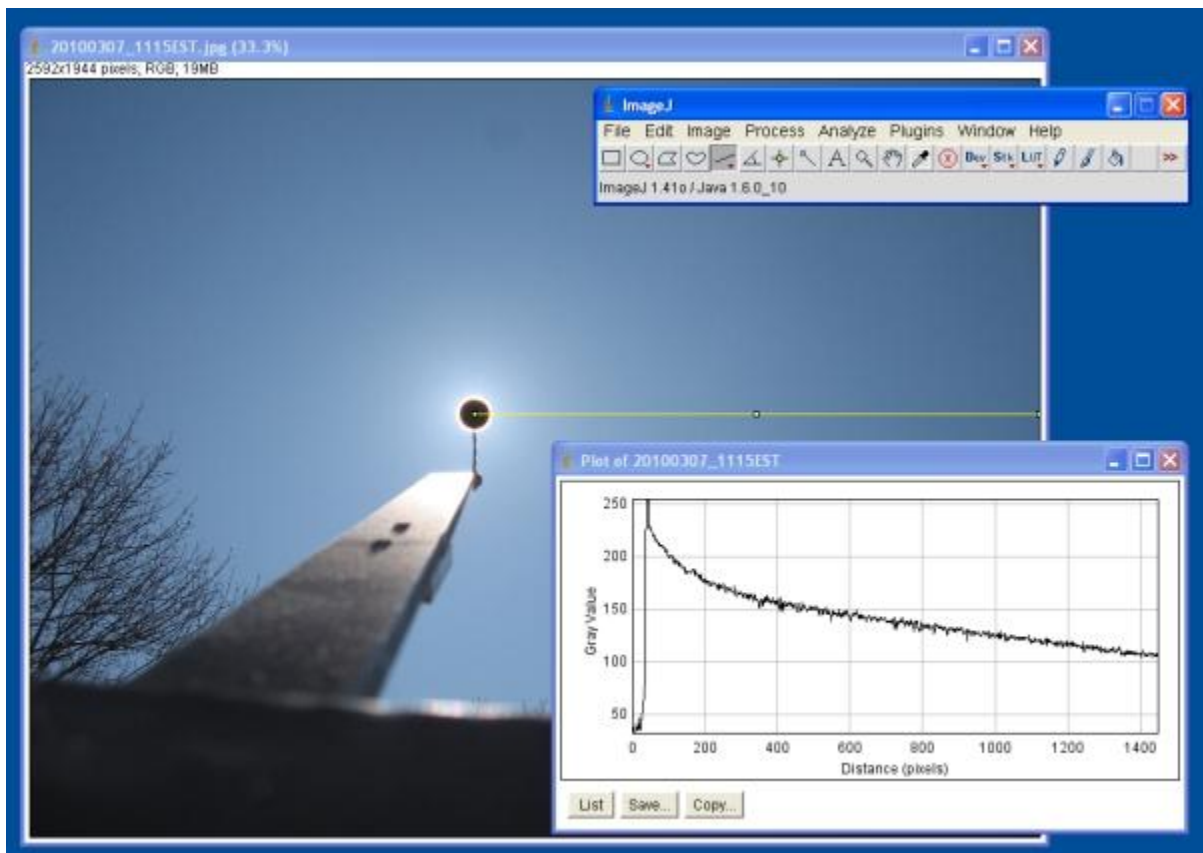


Figure 7.5. Aureole photo, 12:25 EDT, 07 March 2010, processed with ImageJ software.

Figure 7.5 shows ImageJ processing for an aureole image taken on a typical clear day in early spring. The density plot shown in Figure 7.5 will help to determine when the penny is correctly positioned to cover only the solar disk. The distance from the lens to the penny is right when the density plot on a very clear day reaches a value of 255—the maximum brightness the image will record—just at the edge of the disk. If there is a wider band of 255 values around the shadow, then the disk is too small. If the density doesn't reach 255, then the disk is too large. For your camera, you may need to use a disk of a different size placed at a different distance from the lens.

Figure 7.6 shows density plots for two aureoles taken six days apart. The top plot was taken during a day on which some early morning cirrus clouds appeared to dissipate by mid-day. However, the aureole photo showed what appeared to be the remains of some very thin and wispy cirrus clouds around the sun. In any case, the size of the aureole is clearly larger than it is in the lower photo, which is associated with the bottom density plot. This photo was taken following the very dramatic passage of a cold front. The day before the photo was taken, air temperature dropped from 18°C around midday to 1°C by late afternoon, with high winds.

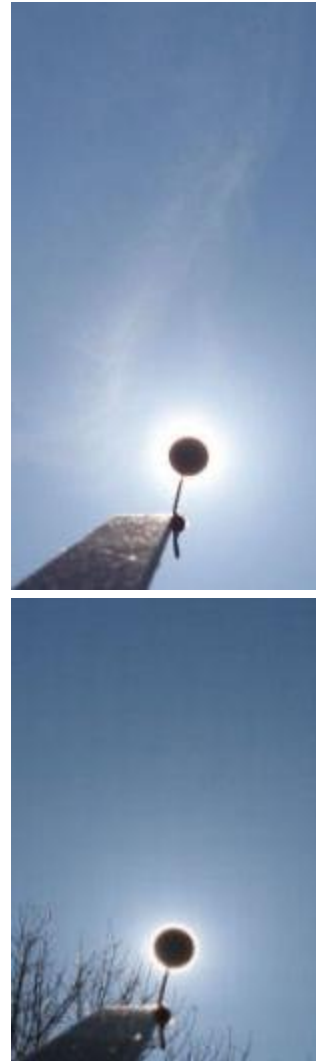
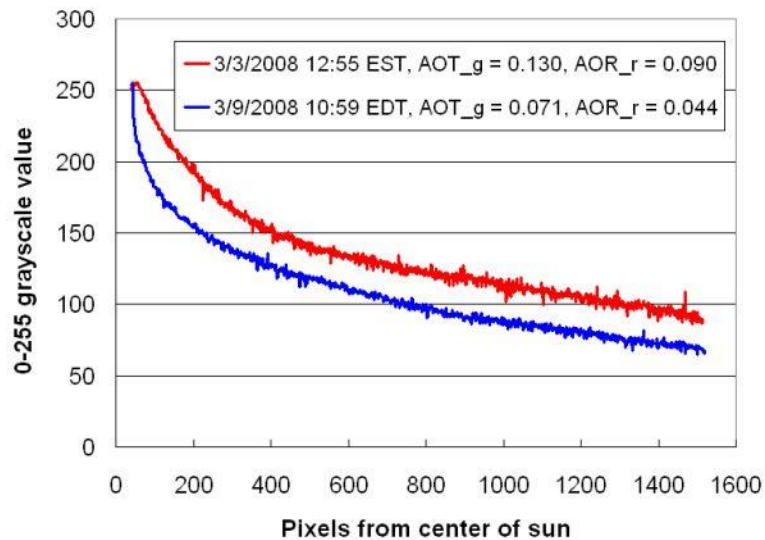


Figure 7.6. Aureole photos taken under different sky conditions.

The aerosol optical thickness values at 505 nm and 625 nm were obtained with a two-channel LED-based sun photometer developed for the GLOBE Program [GLOBE; Brooks, 2010]. The values are significantly smaller on March 9 than on March 3. If cirrus clouds really were present over the sun during the measurement on March 3, then the AOT values might be suspect. The very rapid decrease in the aureole density seen on March 9 is observed only under conditions of very clean skies with very low AOT values.

For the purpose of comparing and analyzing aureole images, it is important always to use the same camera, because different cameras process light differently and have a different field of view, and always to use the same exposure and f-stop. (Both images in Figure 7.6 were taken at 1/1600 s, f-5.6.) If the camera is allowed to use its automatic exposure settings, you will not be able to compare images taken at different times under different sky conditions. If you can afford it, it is a good idea

to devote a camera exclusively to this project, so it can be left permanently mounted on the fixture.

Figure 7.7 shows another interesting set of aureole images taken before, during, and after Hurricane Earl passed almost unnoticed on its way north along the Atlantic coast in early September, 2010. Earl didn't cause much damage, but it did pick up large amounts of dust from the Sahara desert blown across the Atlantic Ocean to the Caribbean. The solar aureole on August 31 is typical for a hazy late summer day. On September 5, the sky is full of dust; the purplish/pinkish border around the outer edge of the aureole is typical for relatively large particulates such as dust. By September 5, the dust is gone and the post-Earl sky is exceptionally clear. Note the extreme differences in sky color – these images were all taken with the same camera and the same manual settings as the previous images! More details about this event can be found at Brooks [2010].

Although it is perfectly clear from the images shown here that there is a relationship between aerosols and the solar aureole, quantifying this relationship is not easy. A great deal of work during the 1970's and 80's was done by Deepak and others, using "real" film before the advent of digital cameras. There are many references in Deepak, Box, and Box [1982].



August 31, 13:45 EDT.



September 4, 12:44 EDT.



September 5, 11:24 EDT.

Figure 7.7. Solar aureole before, during, and after Hurricane Earl, September 2010

7.5 Cloud Observations and Photography

Cloud photography is closely related to sky photography, but the inquiry and research goals are different. Clouds can be both causes and effects of a changing climate and understanding the role of clouds is one of the major challenges for climate analysis and modeling [ISCCP, 2013]. Scientists are interested in both cloud cover amount and type. Figure 7.8(a) shows a variety of afternoon clouds – cumulus, altocumulus, and cirrus.

Contrails form behind aircraft when the water vapor from their engine exhausts condenses. In some parts of the world with heavy air traffic, contrails are a significant source of cloud cover. (See, for example [Chambers, undated].) Figure

7.8(b) shows a short-lived contrail from a commercial jet in the sky above the image in Figure 7.8(a) at about the same time. How long contrails last and whether they persist and stay “tight” or spread provides useful information about the atmosphere at the altitude where they occur. Commercial jets on long flights cruise at around 30,000-40,000 ft (roughly 9-12 km), and on shorter flights at lower altitudes around 25,000-30,000 ft (7.5-9 km).



Figure 7.8(a). Late-afternoon clouds, 40°N, 75°W.

Figure 7.8(b). Short-lived commercial jet contrail, 40°N, 75°W.

Research into the relationship between clouds and insolation was discussed in Chapter 4. Any project exploring this relationship should include date- and time-stamped sky photographs to provide records of actual cloud conditions.

NASA’s CloudSat [Colorado State University, 2013], launched in 2006, continues to collect data from its near-polar sun-synchronous orbit at an orbit inclination of 98.2° and an altitude of 705 km.¹⁸ With these orbit parameters, CloudSat repeats its ground track on Earth’s surface every 16 days. Daytime overflights over the U.S. always occur around 13:00–13:30 local time. Information about when CloudSat will fly over a particular site can be found online [NASA, 2005]. Moving around Earth at a speed of about 7.5 km/sec, CloudSat can provide only a “snapshot” of what is happening underneath it at a particular site.¹⁹ There is need to provide ongoing “ground truth” for CloudSat data, to help scientists determine whether what they infer from space matches actual cloud conditions as seen from the ground. Sky photos, along with insolation data before, during, and after the overflight of a site can help with this process. With multiple cloud layers, the view of clouds from the ground may be significantly different from what a satellite-based instrument will see from orbit. Hence, ground observations may be

¹⁸ CloudSat is one of several “A-Train” Earth-observing satellites which closely follow one another along the same sun-synchronous orbit track. See <http://atrain.nasa.gov/> and <http://atrain.nasa.gov/publications.php#RefHandbook>.

¹⁹ See <http://hyperphysics.phy-astr.gsu.edu/hbase/orbv3.html> for site which will calculate orbital velocity for a spacecraft orbiting at a specified altitude above Earth’s surface.

able to provide additional information about clouds that cannot be detected from orbit.

NASA's Students' Cloud Observations On-Line (S'COOL) project [NASA, 2013] provides a way for schools and students to relate local cloud observations to satellite-derived cloud data. Note, however, that because of the 16-day cycle of cloud retrievals over a particular site, determining any kind of quantitative relationship between ground observations and satellite-derived cloud data is a long-term project.

Real-time imagery from NOAA's GOES satellite shows cloud cover viewed in the visible and IR over various regions of the globe [NASA, continuous online update; NOAA, continuous online update]. You can find out more about satellite-based meteorology in learning modules from the University of Wisconsin website [CIMSS, undated].

7.6 Inquiry and Research Questions

(Inquiry)

- Select a direction in which to collect images of the sky with the horizon at the bottom of the image. Use ImageJ to determine the brightness variation along a line vertically up from the horizon. During the course of several weeks, monitor the changes in this curve. Be careful to restrict the images to conditions where there are no clouds in the sky where the brightness curve is drawn.
- Find a distant object, natural or manmade, and use ImageJ to determine the object-to-sky brightness ratio over several weeks. Graph the ratio. Do the scene images provide any clues as to the cause of changes in the ratio?

For both these inquiry projects, record metadata (“data about data”) in the form of your own description of sky conditions and anything else you believe might be relevant.

- Following a protocol such as <http://www.globe.gov/documents/348614/348678/clouds.pdf> record cloud type and amount. Use a cloud identification chart such as one of these:
http://asd-www.larc.nasa.gov/SCOOOL/PDF/Cloud_ID.pdf
http://www.globe.gov/documents/367957/0/cloud_chart_canada.pdf

Some cloud types, such as “puffy” white cumulus clouds, are very easy to identify. Some other types require practice. (They may never look exactly like the photos on cloud identification charts!) In order to improve the quality of your cloud type identifications, it is a good idea to ask for help from a local meteorologist or atmospheric scientist.

If you see contrails where you live, keep a record of the date and time of sightings for a few weeks. Is there a pattern to when contrails appear? (Commercial aircraft may regularly fly over your site at the same time every day.) Note whether the contrails are short-lived, persistent, or persistent and spreading.

(Research)

- How is the shape of the sky brightness curve related to other measures of air quality such as horizontal visibility or an air quality index? (See [AirNow]). Can you derive a mathematical model for the shape of the sky brightness curve along a line vertically up from the horizon? What parameters need to be considered in defining the mathematical model? Can these parameters be associated with some other measures of air quality?
- Can you derive a mathematical model that relates the object-to-sky brightness ratio to an air quality index or some other measure of local air quality? Does the model depend on which component of air quality defines the air quality index at a particular time? Perhaps consistently using a single component of air quality, such as particulates, will yield a better correlation with the ratio than the air quality index, which is calculated based on the worst of the component parameters. If you live near a major airport, you may be able to access horizontal visibility data online.
- Can you find a relationship between insolation and horizontal visibility or the shape of the sky brightness curve along a line vertically up from the horizon?
- Can you find a relationship between the extent and brightness shape of the solar aureole and air quality, water vapor, or aerosol optical thickness? Note that the 1982 paper by Deepak, Box, and Box cited in Section 7.4 uses the characteristics of the solar aureole to determine the size distribution of aerosols, but not necessarily the total concentration of aerosols. Nonetheless, it is apparent that at least a rough correlation does exist.
- The cloud projects discussed in Section 7.6 are best done in collaboration with others. Sites in different locations will allow you to obtain more data correlated with satellite overflights. If you can present a plan for collaborative research that has a convincing strategy for long-term success, you may be able to solicit support from cloud scientists. One such project is to supplement sky photographs during the early afternoon satellite overflights with insolation data extending 15 or more minutes before and after the overflight.

For this project, the typical one-minute interval for recording insolation data should be shortened to just a few second to provide higher time resolution data before and after the overflight time. Ideally, you could start recording at one-minute intervals early in the day, decrease the sampling interval around the overflight time, and then continue with one-minute sampling for the rest of the day. Use the Satellite Overpass Closest Approach Predictor [NASA, 2005] to determine overflight times.

7.7 Resources

Acknowledgement: My friend and colleague, Forrest Mims, has been taking sky photographs for many years, and he has inspired my much more recent interest in this topic. You can find more about Mims' work at

http://www.sunandsky.org/Sky_Photos.html, undated.

AirNow. Air Quality Index (AQI) – A Guide to Air Quality and Your Health. May 2013. <http://www.airnow.gov/?action=aqibasics.aqi>

Brooks, David R. Measuring Aerosol Optical Thickness, 2010.

http://www.instesre.org/Aerosols/Aerosols_home_page.htm

Brooks, David R. Hurricane Earl and Saharan Dust, September 2010.

<http://www.instesre.org/Solar/AureolePhotography/Earl.htm>, 2010.

Chambers, Lin. The GLOBE Contrail Protocol: A Student-Scientist Partnership. (Undated PowerPoint.)

http://science-edu.larc.nasa.gov/contrail-edu/pdf/resources/presentations/CSU_Monterey_Bay.pdf

Colorado State University Department of Atmospheric Science. CloudSat.

<http://cloudsat.atmos.colostate.edu/>, updated 21 November 2013.

Cooperative Institute for Meteorological Satellite Studies (CIMSS), University of Wisconsin-Madison Space Science and Engineering Center (SSEC). Satellite Meteorology for Grade 7-12.

<http://cimss.ssec.wisc.edu/satmet/>, undated.

Deepak, A., G. P. Box, and M. A. Box. Experimental validation of the solar aureole technique for determining aerosol size distributions. *Applied Optics*, **42**, 2236-2242, 1982.

GLOBE Program.

www.globe.gov, <http://www.globe.gov/web/atmosphere-climate/protocols>

International Satellite Cloud Climatology Project (ISCCP). Cloud Climatology.

<http://isccp.giss.nasa.gov/role.html>, updated March 11, 2013.

Mims, Forrest M. Solar Aureoles Caused by Dust, Smoke, and Haze. *Applied Optics*, **42**, 492-496, 2003.

Mims. http://www.sunandsky.org/Sky_Photos.html

NASA. GOES Project Science. <http://goes.gsfc.nasa.gov/>, continuously updated.

NASA. Satellite Overpass Closest Approach Predictor.

<http://www-angler.larc.nasa.gov/cloudsat/closest.html>, updated July 6, 2005.

NASA. Students' Cloud Observations On-Line (S'COOL).

<http://scool.larc.nasa.gov/>, updated 18 October 2013.

NOAA. Geostationary Satellite Server. <http://www.goes.noaa.gov/>, continuously updated.

Building Performance Simulation Association – USA Affiliate. Ground Reflectance.

[http://www.bembook.ibpsa.us/index.php?title=Ground Reflectance](http://www.bembook.ibpsa.us/index.php?title=Ground_Reflectance)

NASA. Measuring Vegetation (NDVI and EVI).

<http://earthobservatory.nasa.gov/Features/MeasuringVegetation/>

National Renewable Energy Laboratory. SMARTS Simple Model of the Atmospheric Radiative Transfer of Sunshine. <http://www.nrel.gov/rredc/smarts/about.html>

Warren, Stephen G. Optical Properties of Snow. *Review of Geophysics and Space Physics*. Vol. 20, No. 1, pp 67-89, February 1982.

8. Atmospheric Water Vapor

8.1 Background

Although human-induced warming of the lower atmosphere is correctly associated with the release of increasing amounts of carbon dioxide into the atmosphere since the start of the Industrial Revolution in the last half of the 19th century, it is important to remember that water vapor (WV) and not CO₂, is the predominant greenhouse gas responsible for maintaining habitable conditions on Earth's surface.

The distribution of WV varies significantly around the globe in both space and time. Monitoring water vapor from space, initially related to tracking clouds and weather, has a long history, dating back to the TIROS 2, 3, and 4 satellites launched in 1960, 1961, and 1962 [CIMSS, undated]. Currently, global and regional visible, IR, and water vapor images from GOES satellites, such as the water vapor image shown in Figure 8.1 are continuously updated and are widely available online [for example, NASA Earth Science Office; NOAA National Weather Service]. Although these WV images may look like “photos,” the gray-scale representation of WV content is based on processed data from satellite sensors over a range of wavelengths.

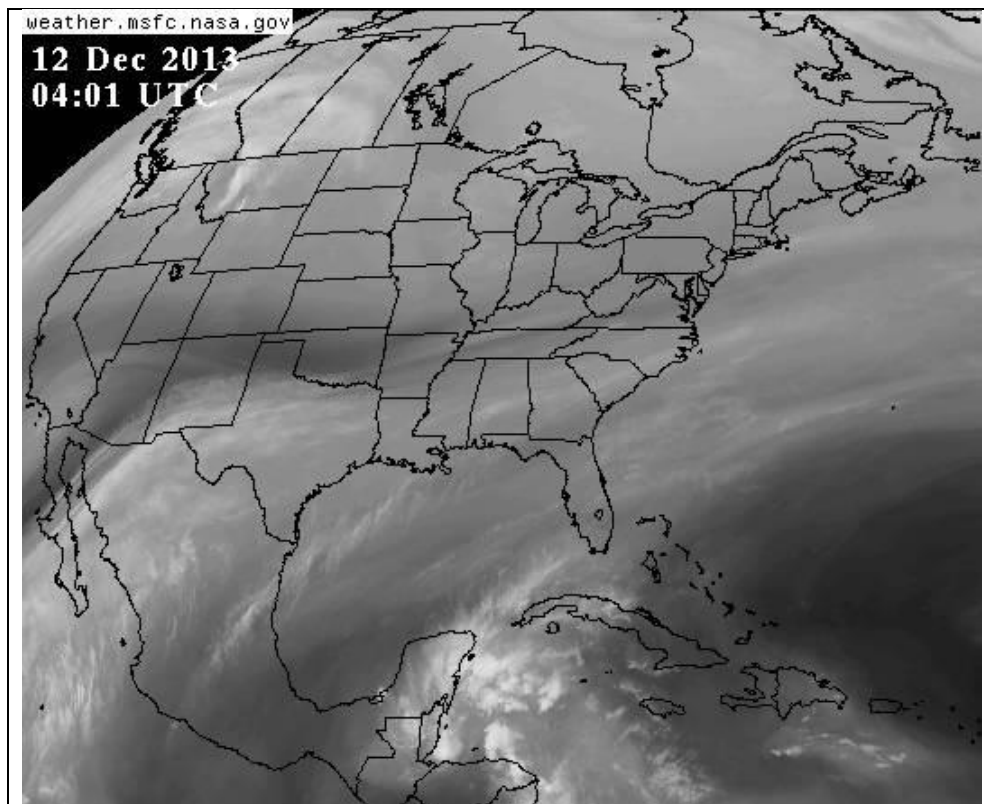


Figure 8.1. GOES East water vapor image (weather.msfc.nasa.gov).

8.2 Measuring Atmospheric Water Vapor

Quantitatively, total atmospheric water vapor is measured in units of centimeters of water (cm H₂O). Imagine holding a cylindrical cup in your hand, pointed straight up, and then magically condensing all of the water vapor in a cylinder the same diameter as the inside of the cup, extending upward through the entire atmosphere, into the cup. The depth of water in your cup would be the total atmospheric water vapor, also called the total precipitable water vapor or integrated precipitable water (IPW).

Figure 8.2 shows a 12-year record of water vapor data collected by Forrest Mims, as cited in Brooks, *et al.*, 2003. The strong seasonal cycle, with maximum values in the summer, is clearly evident.

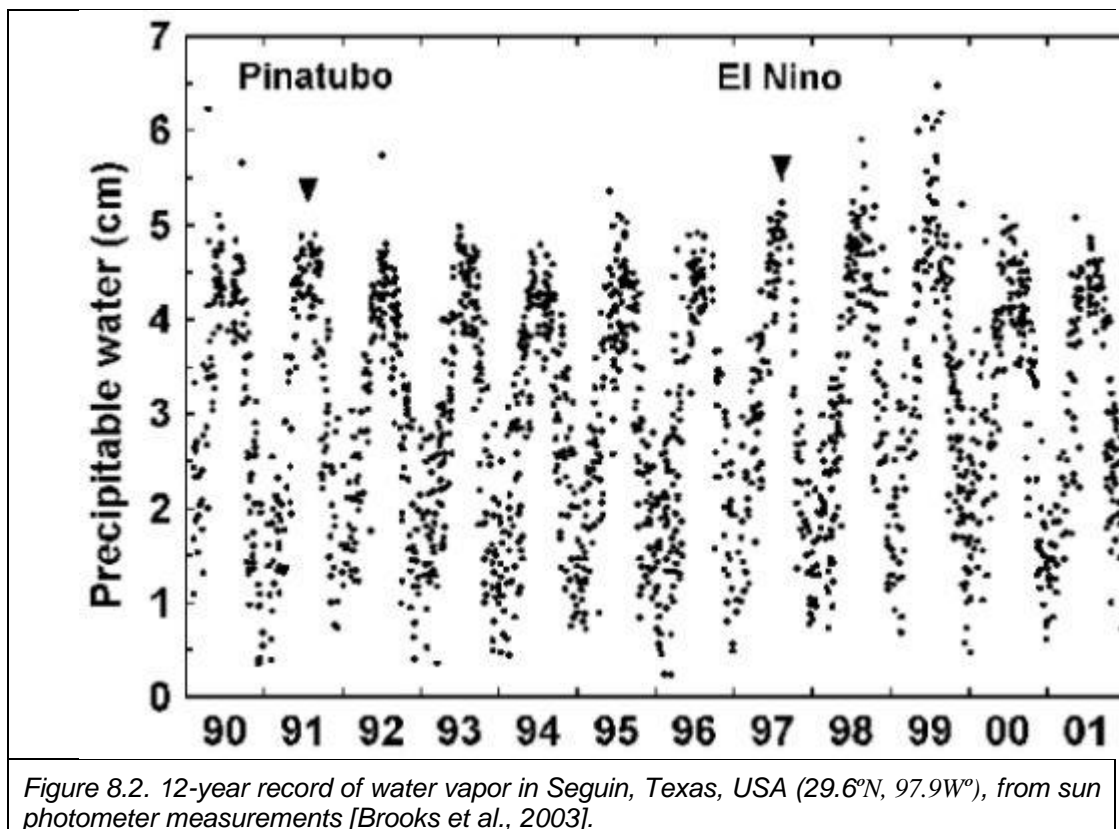


Figure 8.2. 12-year record of water vapor in Seguin, Texas, USA (29.6°N, 97.9W°), from sun photometer measurements [Brooks *et al.*, 2003].

Ground-launched balloon soundings are often used to measure the vertical distribution of water vapor through the atmosphere. This is an expensive procedure that is very weather dependent and not regularly done at a great number of locations. Scientists would *like* to have other options for measuring IPW. Telemetry signals from Global Position Satellites (GPS) are now being used to provide real-time IPW data at hundreds of GPS-MET sites around the country [NOAA Earth System Research Laboratory]. Some of NASA's Aerosol Robotic Network (AERONET) sites also provide real-time IPW data [NASA AERONET].

Some formulas for estimating IPW, based on dewpoint temperature as calculated from air temperature and relative humidity values measured at conventional weather stations, date back to the 1960's [Reitan, 1963; Smith, 1965]. Reitan's formula is very simple:

$$\ln(\text{IPW}_{\text{Reitan}}) = 0.1102 + 0.0614T_{d,F}$$

where \ln is the natural (base e) logarithm.

Smith's formula for locations in the northern hemisphere is in the same form, but it uses latitude- and season-dependent parameters, as shown in Figure 8.3:

$$\ln(\text{IPW}_{\text{Smith}}) = 0.1133 - \ln(\lambda + 1) + 0.0393T_{d,F}$$

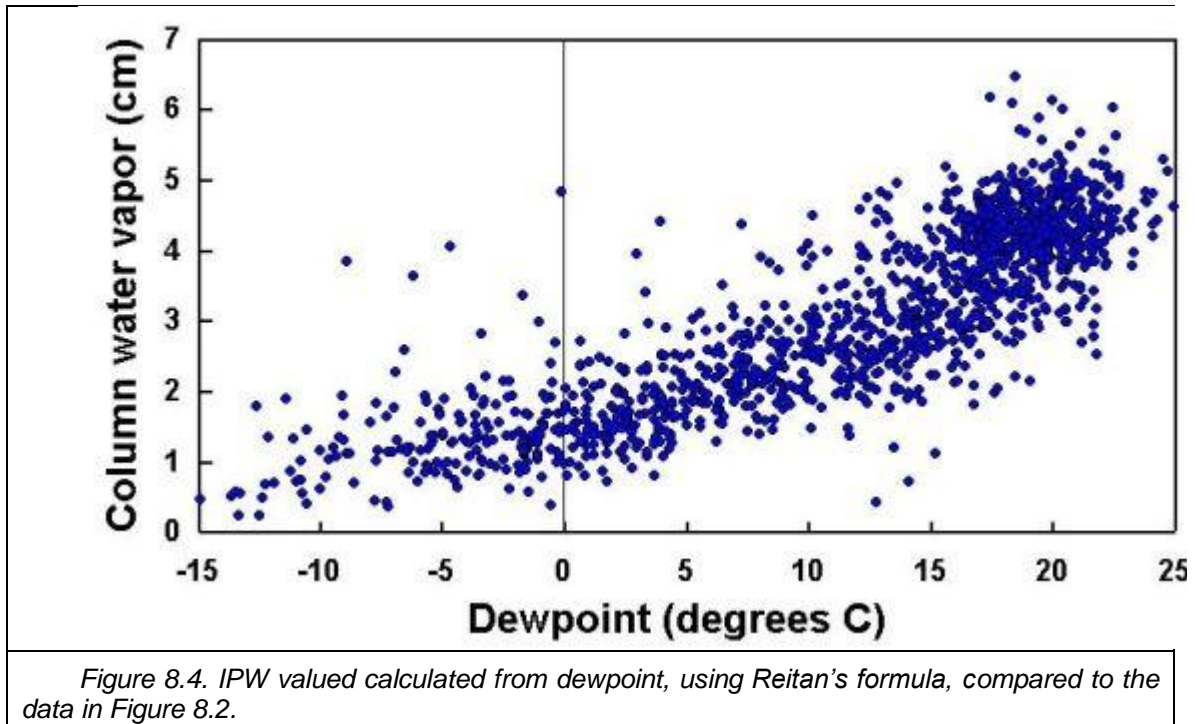
$T_{d,F}$ means that, as was the convention at the time, temperatures are in degrees Fahrenheit rather than Centigrade. See the equations in Section 6.5 for Centigrade dewpoint temperature calculations. The conversion from Centigrade to Fahrenheit is:

$$T_{d,F} = (9/5) \cdot T_{d,C} + 32$$

These formulas require only information that can accurately be determined on the ground. These dewpoint-based IPW approximations tend to be more accurate under conditions where the atmospheric conditions are stable, that is, when the dewpoint temperature has had a chance to stabilize. But, at best, they are *just* approximations; it is not really possible to believe that values based just on atmospheric conditions at Earth's surface would always be in complete agreement with, for example, WV values from balloon soundings integrated through the atmosphere. Figure 8.4 shows IPW based on Reitan's formula compared to the measured data in Figure 8.2. Values based on Smith's formula would be a little different, but the overall results would be very similar.

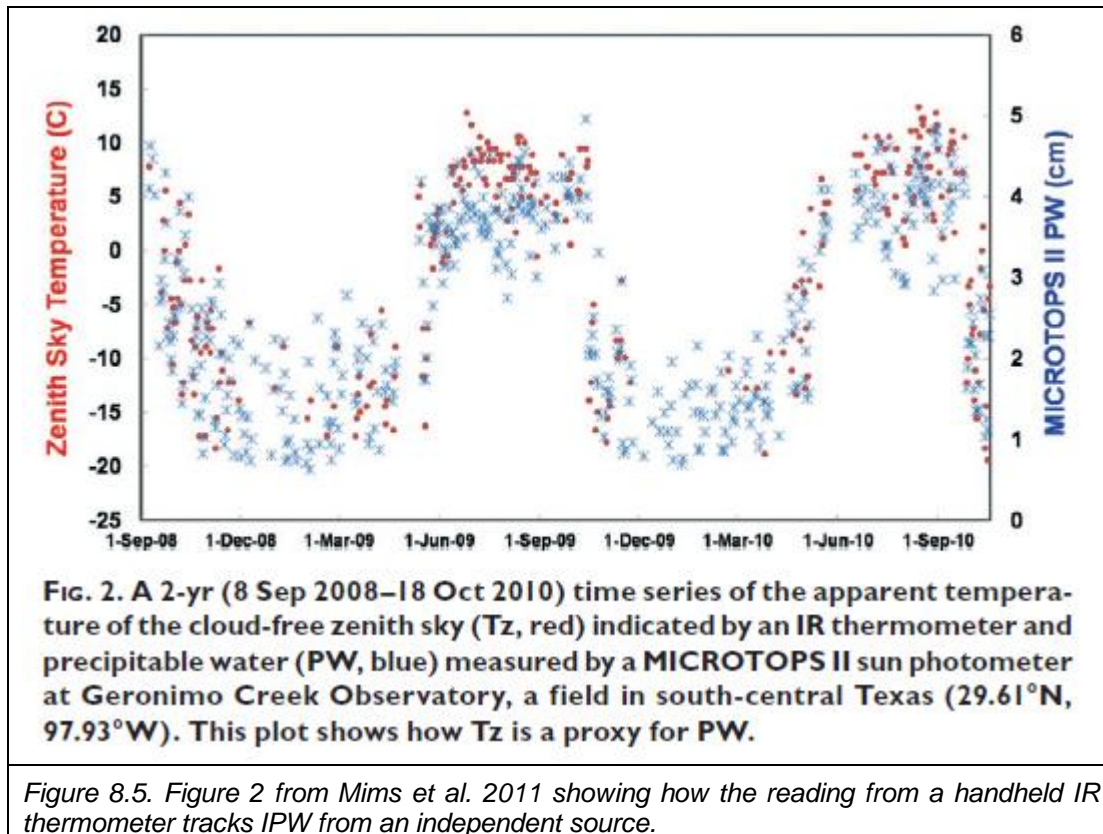
Season latitudinal zone (deg N)	Winter	Spring	Summer	Fall	Annual average
0-10	3.37	2.85	2.80	2.64	2.91
10-20	2.99	3.02	2.70	2.93	2.91
20-30	3.60	3.00	2.98	2.93	3.12
30-40	3.04	3.11	2.92	2.94	3.00
40-50	2.70	2.95	2.77	2.71	2.78
50-60	2.52	3.07	2.67	2.93	2.79
60-70	1.76	2.69	2.61	2.61	2.41
70-80	1.60	1.67	2.24	2.63	2.03
80-90	1.11	1.44	1.94	2.02	1.62
Northern Hemisphere average	2.52	2.64	2.62	2.70	2.61

Figure 8.3 Table 1 from Smith [1965].



Based on his preliminary work with near-infrared light-emitting diodes in the early 1990s [Mims, 1992], Forrest Mims pioneered the use of LED-based sun photometry to measure IPW [Mims, 2002] (See Figure 8.2) and this technique has been used in water vapor sun photometers developed a decade ago for the GLOBE Program [Brooks, Mims, and Roettger, 2007].

More recently, Mims and colleagues described how to measure IPW by pointing an inexpensive handheld infrared thermometer (See Figure 6.1) toward the zenith sky when there are no clouds within the instrument's field of view [Mims, Chambers, and Brooks, 2011]. Figure 8.5 shows the relationship between IPW and readings from an IR thermometer. Especially if you are fortunate to live near an AERONET or GPS-MET, which provide an independent source of IPW data, this is a project on which much interesting work remains to be done.



8.3 Inquiry and Research Questions

(Inquiry)

- Find a few of the GPS-MET and/or AERONET sites nearest your location. Download and graph IPW data for several days. What can you observe about diurnal and daily patterns. Does IPW appear to be related to the movement of weather patterns across your site? If so, how? Compare the water vapor values from these sources with the values calculated using the Reitan or Smith equations (see Section 8.2) for calculating IPW based on air temperature and relative humidity.
- Point a handheld IR thermometer such as the Kintrex IRT0421 or the less expensive Kintrex IRT0401 at the same point in the sky at different times of the day (including during the night, if possible), over a period of at least several days and a range of weather conditions. How does the “temperature” reading change? Temperature is in quotation marks because, as discussed in Section 6.4, the interpretation of readings from IR sensors is not obvious when they are pointed at the sky. What do you think the “temperature” values mean? Are there sky conditions that appear to lie outside the range of your IR thermometer?

(Research)

- It is possible that there may be a predictable relationship between the Reitan/Smith IPW calculations (See Section 8.2) and IPW from independent sources. Can you find such a relationship?
- The two Kintrex IR thermometers mentioned above have different specifications, including a much different field of view. Apart from zenith measurements under cloud-free skies, it would be interesting to compare data from these two instruments over a range of sky conditions and try to explain the differences. As suggested in Chapter 6, there may be other interesting relationships between sky conditions and IR thermometer readings.
- The 2011 Mims, Chambers, and Brooks paper suggests avenues for further research into the use of handheld IR thermometers for tracking water vapor:

“Scans across cloud-free skies at MLO and the Texas site demonstrate that the method may be used to estimate PW by pointing the IR thermometer toward the sky at known angles away from the zenith. This method will be explored to permit measurements of PW when either the sun or clouds are near the zenith and when Tz falls below the minimum range of the IR thermometer on very cold, dry days and at alpine sites.”

At the time this document was written the suggested research had not yet been done. Hence, this is an excellent student research project.

- Relatively little is known about the temporal and spatial distribution of IPW at the mesoscale – roughly 100 to 1000 km, larger than localized storms, but smaller than large (synoptic scale) weather patterns such as fronts. Because traditional means of measuring IPW are expensive, there is no system in place to provide routine mesoscale data. Such data are important for modeling mesoscale meteorology to improve weather forecasts and, on a longer time scale, to improve the representation of water vapor in climate models. Coordinated regional measurements of IPW using handheld IR thermometers would be a significant undertaking, but it would be an extremely valuable contribution from student research.

8.4 Resources

Brooks, D. R., F. M. Mims III, R. Roettger. Inexpensive Near-IR Sun Photometer for Measuring Total Column Water Vapor. *J. Atmospheric and Oceanic Technology*, **24**, 1268-1276, 2007.

Brooks, D. R., F. M. Mims III, A. S. Levine, D Hinton. The GLOBE/GIFTS Water Vapor Monitoring Project: An Educator's Guide with Activities in Earth Sciences, NASA EG-2003-12-06-LARC, 2003.

Cooperative Institute for Meteorological Satellite Studies. Water Vapor Imagery Tutorial. Space Science and Engineering Center, University of Wisconsin – Madison.

<http://cimss.ssec.wisc.edu/goes/misc/wv/>, undated.

Mims, F. M. III, L. H. Chambers, D. R. Brooks. Measuring Total Column Water Vapor by Pointing an Infrared Thermometer at the Sky, *Bull. Amer. Meteor. Soc.*, **92**, 10, 1311-1320, 2011.

Mims, F. M. III. Sun photometer with light-emitting diodes as spectrally selective detectors, *Applied Optics*, **31**, 6965-6967, 1992.

Mims, F. M. III. An inexpensive and stable LED Sun photometer for measuring the water vapor column over South Texas from 1990 to 2001, *Geophys. Res. Lett.*, **29**, 13, 20-1 – 20-4, 2002.

NASA AERONET.

http://aeronet.gsfc.nasa.gov/cgi-bin/type_piece_of_map_opera_v2_new, continuously updated.

NASA Earth Science Office.

<http://weather.msfc.nasa.gov/GOES/goeseastconuswv.html>, updated continuously.

NOAA Earth System Research Laboratory. Ground-Based GPS Meteorology.

<http://gpsmet.noaa.gov/cgi-bin/gnuplots/rti.cgi>, continuously updated.

NOAA National Weather Service.

<http://www.weather.gov/satellite#wv>, updated continuously.

Reitan, C. H. Surface Dew Point and Water Vapor Aloft, *J. Applied Meteorology*, **2**, 776-779, 1963.

Smith, W. L. Note on the Relationship Between Total Precipitable Water and Surface Dew Point, *J. Applied Meteorology*, **5**, 726-727, 1965.

9. Climate Trends

9.1 Background

As is well known, the distinction between weather and climate is that climate is weather averaged over time. (“Climate is what we expect, weather is what we get” – attributed to Robert Heinlein or sometimes to Mark Twain.) In this chapter, we will discuss three ground-based datasets suitable for studying climate trends. All of them are from the National Oceanic and Atmospheric Administration (NOAA), and each provides a slightly different perspective on climate. All of them provide interesting possibilities for student research. All are large datasets with formidable obstacles to non-specialists who wish to study them. In each case, IESRE has written online applications to get past these obstacles [IESREa, 2013].

In addition to providing historical background for climate, these datasets also provide a context and “reality check” for any measurements you make on your own. Climate baselines can help you identify and assess extreme events.

9.2 30-Year Climate Normals

Typically, climate scientists consider 30 years as an appropriate time over which to average variations in weather and define climate for a particular site. Data collected and averaged or summed in some way over 30 years are referred to as climate normals. Ideally, such data should come from sites which are properly situated, carefully maintained, and environmentally stable over long periods of time. Over 30 years, such sites are not easy to find! In some cases, weather stations are located where they are convenient for people without regard for their long-term interpretation in climate studies. In some cases, observers are interested in local weather without regard to whether it represents “natural” weather in that particular area – airport weather stations are a good example. In many cases, especially around large cities, weather sites are moved from time to time and sites in once remote locations eventually find themselves surrounded by suburban or urban development. Sometimes “official” weather stations are moved from remote locations to urbanized locations such as airports, a choice which is important for meteorologists responsible for aviation weather, but a very poor choice for climate scientists! Nonetheless, the National Oceanic and Atmospheric Administration (NOAA) National Climatic Data Center, has compiled several such datasets [NOAAa, b; Arguez *et al*, 2012] based on data that are available.

Can these 30-year normals be used to detect climate change? Not necessarily. It is always tempting to use these kinds of “official” data sets without thinking too much about the underlying issues. But, NOAA points out that “when the widespread practice of computing Normals commenced in the 1930s, the generally accepted notion of the climate was that underlying long-term averages of climate time series were constant” and it warns that “care must be taken when interpreting changes between one Normals period and the other. Differences... may be due to

station moves, changes in methodology, changes in instrumentation, etc., that are not reflective of real changes in the underlying climate signal.” [NOAAa]

Now, of course, it is widely accepted that climate *is* changing, specifically that Earth is warming. The RealClimate website, maintained by working climate scientists, provides technical details and updates; a recent posting cites a new study which claims that global warming has been underestimated [RealClimate, 2013]. This NASA website [NASA, 2013] cites the claim that “97% of climate scientists agree” that Earth is warming and it includes a list of scientific organizations that publicly share this view. NOAA also accepts climate change as a fact: “Climate change is apparent now across our nation...” [NOAA, 2013]. It seems reasonable to expect that this change *should* be visible in successive 30-year normals that are calculated on a consistent basis. But based on NOAA’s cautions, there is no reason to believe that newer normals will necessarily be consistent with older normals (over an entire state, for example). However, even if the desired consistency does not exist, it is still worthwhile and interesting to compare these datasets because finding and attempting to explain anomalies is a challenging and interesting problem. One thing is certain about these data: any long-term trend in air temperature, up or down, or any other parameter, is going to be small compared to weather-induced fluctuations. This fact explains why understanding Earth’s current climate and predicting its future is so challenging.

NOAA’s climate normals come in several different data formats depending on when and how they were assembled. Normals for 1971-2000 and 1981-2010 have been taken from an online product based on NOAA data and made available by a commercial company, Golden Gate Weather Services.²⁰ The 1951-1980 and 1961-1990 data are directly from NOAA; they have different formats, so each set has its own access and visualization application. Figures 1(a)-(c) show the input screens for these three applications.

²⁰ We gratefully acknowledge the work of Jan Null, who has made these datasets available online at no cost.

1951-80 Climate Normals for the 50 States

This application accesses NOAA 30-year climate normal data for the time span 1951-80. Click [HERE](#) for a brief overview of climate normal datasets. Click [HERE](#) for the detailed NOAA description of the 1951-80 data.

State:	Data Code:
Alabama	10 - average of 30 maximum temperatures
Alaska	11 - highest of 30 maximum temperatures
Arizona	12 - lowest of 30 maximum temperatures
Arkansas	13 - standard deviation of 30 maximum temperatures
California	20 - average of 30 minimum temperatures
Colorado	21 - highest of 30 minimum temperatures
Connecticut	22 - lowest of 30 minimum temperatures
Delaware	23 - standard deviation of 30 minimum temperatures
Florida	30 - average of 30 mean temperatures
Georgia	31 - highest of 30 mean temperatures
Hawaii	32 - lowest of 30 mean temperatures
Idaho	33 - standard deviation of 30 mean temperatures
Indiana	40 - average of 30 precipitations
Iowa	41 - highest of 30 precipitations
Kansas	42 - lowest of 30 precipitations
Kentucky	50 - heating degree days (base 65°F)
Louisians	60 - cooling degree days (base 65°F)

Which data code (choose one)?

Choose output type:

Monthly values: Lon/Lat grid of values

For Lon/Lat grid, select monthly or yearly values:

Jan Feb Mar Apr May Jun Jul Aug Sep Oct Nov Dec Yearly

Figure 9.1(a). Input screen for 1951-1980 NOAA climate normals.

1961-90 Climate Normals for the 50 States

This application accesses NOAA 30-year climate normal data for the time span 1961-90. These data also include values calculated for 1970-90 and 1980-90 spans. Click [HERE](#) for a brief overview of climate normal datasets. Click [HERE](#) for the detailed NOAA description of the 1961-90 data.

Alabama	Element Codes:	Data Codes:
Alaska		
Arizona	minimum temperature	4 - 61-90 normal
Arkansas	maximum temperature	5 - 61-90 standard deviation
California	mean temperature	6 - 61-90 median
Colorado	total precipitation	7 - 70-90 mean
Connecticut	heating degree days	8 - 70-90 mean
Delaware	cooling degree days	9 - 70-90 standard deviation
Florida		10 - 80-90 mean
State: Georgia		11 - 80-90 standard deviation
		12 - 80-90 median

Choose output type:

Monthly values: Lon/Lat grid of yearly values;

Figure 9.1(b). Input screen for 1961-1990 NOAA climate normals.



1971-2000 and 1981-2010 Climate Normals for the 50 States, DC, and territories

Accesses 30-year climate normals by state, for 1971-2000 or 1981-2010. Data are reported by month plus annual average. Station longitude and latitude are included the output. Not all stations record all parameters. Text output is displayed in comma-separated format, which can be copied and pasted into a .csv file.

Select State (other):

- AK - Alaska
- AL - Alabama
- AR - Arkansas
- AZ - Arizona
- CA - California
- CO - Colorado
- CT - Connecticut
- DC - District of Columbia
- DE - Delaware
- FL - Florida
- GA - Georgia
- HI - Hawaii

Select time period: 1971-2000 1981-2010

Parameters (select one):

(°F) Average temperature Maximum Temperature Minimum Temperature

(inches) Precipitation Snow (1981-2000 only)

(65°F base) Heating Degree Days Cooling Degree Days

Select output type:

All data for selected parameter Lon/Lat table for selected parameter and month (or annual mean)

"Bubble Chart" showing differences between sites and statewide mean

Jan Feb Mar Apr May Jun Jul Aug Sep Oct Nov Dec Annual

Radius scaling for temperature: HDD/CDD Precip/snow

[Click here to generate specified output.](#)

Figure 9.1(c). Input screen for 1971-2000 and 1981-2010 NOAA climate normals.

Heating degree and cooling degree days (HDDs and CDDs) are calculated on a base temperature of 65°F:

$$\text{CDD} = \text{MAXIMUM}[0, (T_{\text{average}} - T_{\text{base}})]$$

$$\text{HDD} = \text{MAXIMUM}[0, (T_{\text{base}} - T_{\text{average}})]$$

and accumulated over a month. Annually accumulated CDD and HDD values provide an excellent single-value representation of how warm or cold a year is.

For the bubble chart options, you can change the radius of the circular bubbles, which is useful when the differences across a state relative to the statewide mean are very small or very large.

Figure 9.2 shows an example of some data extracted from the 1981-2010 Climate Normals: annual snowfall in Pennsylvania as a function of site elevation. The data were saved as a .csv file and graphed in Excel. Not surprisingly, there is a relationship between elevation and snowfall, with a few interesting anomalies.

For example, the site at about 700 feet with a snowfall of 100" gets "lake effect" snow from Lake Erie.²¹

Parameter: Snow
 Output type: LonLatGrid
 Month: 13
 Pennsylvania
 Climate Normals (1981-2010)

ALLENTOWN AP , 390, -75.4492 , 40.6508 , 32.9
 ALTOONA FAA AP , 1476, -78.3169 , 40.3000 , 31.7
 BEAR GAP , 1015, -76.4983 , 40.8208 , 31.5
 BEAVER FALLS 1 NE , 760, -80.3133 , 40.7628 , 9.5
 BEAVERTOWN 1 NE , 540, -77.1572 , 40.7739 , 32.3
 BECHTELSVILLE 1ENE , 460, -75.6150 , 40.3783 , 10.1
 BIGLERVILLE , 720, -77.2578 , 39.9356 , 25.9
 BRADFORD 4 SW RSCH 5 , 1660, -78.7144 , 41.8975 , 71.8
 BRADFORD CNTRL FS , 1500, -78.6500 , 41.9500 , 74.1
 BROOKVILLE SEWAGE PLT , 1210, -79.0833 , 41.1500 , 42.5
 BUCKSTOWN 1 SE , 2460, -78.8422 , 40.0631 , 97.8
 BUCKSVILLE , 460, -75.2044 , 40.5003 , 27.7
 BUFFALO MILLS , 1310, -78.6458 , 39.9458 , 39.5
 BUTLER 2 SW , 1000, -79.9167 , 40.8500 , 36.3

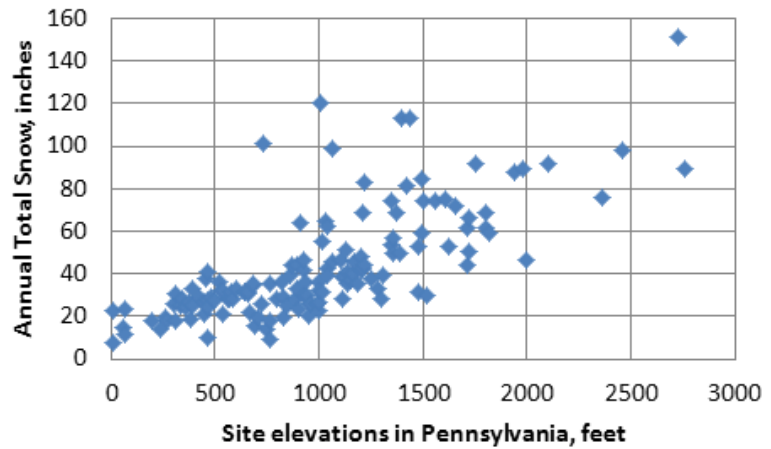
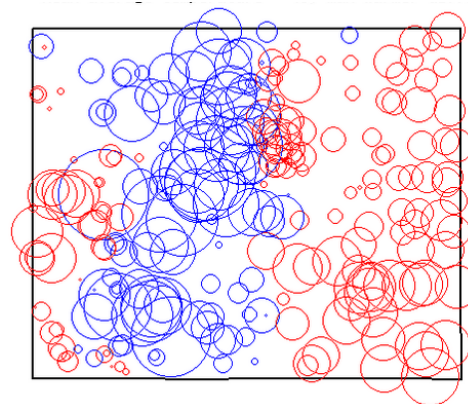
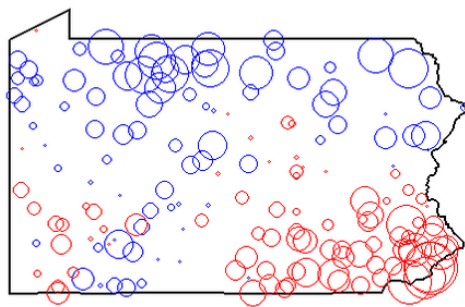


Figure 9.2. Total annual snowfall (month 13) as a function of site elevation, for 1981-2010 Pennsylvania Climate Normals.

Figure 9.3 shows some results from the bubble chart option for Pennsylvania and Colorado. The diameters of the red and blue circles are scaled by the amount the 30-year mean annual temperature for a site is above or below the statewide mean. Site temperatures will be affected by latitude, elevation, and urbanization. The locations of warmer temperatures and cooler temperatures in both these states appear to be influenced by some or all of these factors. Philadelphia in the southeast and Pittsburgh in the southwest is warmer than the rest of the state, but both urban centers are also in the southern part of the state. The Appalachian Mountains run northeast from east of Pittsburgh. In Colorado, the very strong elevation influence of the Rocky Mountains is obvious. See the Research section at the end of this chapter for more comments on this topic.



(a) Pennsylvania

(b) Colorado

Figure 9.3 Site temperatures above and below statewide mean, 1981-2010 Climate Normals.

²¹ <http://www.erh.noaa.gov/er/buf/lakeeffect/lakeintro.html>

9.3 The U.S. Historical Climatology Network

If climate normals can't be relied upon to detect climate change, where can we look? Air temperature and precipitation data from more than 1200 stations around the 48 conterminous states (not including Alaska and Hawaii), some with records extending back into the 19th century, have been collected to build NOAA's U.S. Historical Climatology Network [NOAAc]

USHCN data include monthly mean air temperature (maximum, average, and minimum) and summed precipitation, organized by site in four separate files, one for each dataset. Each line of every file contains the site identification code, year, and the monthly values. The files do not include annual mean temperatures or yearly total precipitation, as these can easily be calculated from the monthly values. A separate file associates each site ID code with its state, name, longitude/latitude coordinates, and elevation. In contrast to some earlier data products like NOAA's climate normals, the USHCN always uses metric units – decimal degrees for longitude/latitude, degrees centigrade for temperature, millimeters for precipitation, and meters for elevation.

These data come in two important versions. One version contains raw data from the observing sites. Not surprisingly, the raw data are of variable quality. In the other version, NOAA has used a variety of techniques designed to remove inconsistencies, as might occur when a station is moved, for example, and other “artifacts” such as urban heat island effects. It is a considerable understatement to say that not everybody agrees with NOAA's analysis and the resulting “corrections.” Some have argued, for example, that removing heat island effects is not justified or that NOAA's data manipulations tend to exaggerate warming trends. But, this is a case of trying to make the best use of what is available – not perfect, but certainly better than not trying at all. There is an extensive list of references dealing with these data, many of which are publications in peer-reviewed journals, on NOAA's USHCN website [NOAAc].

When I had questions about which was the most appropriate version of the three available datasets to use for looking at trends, a NOAA scientist responded [Menne, private communication, 2013]:

“The *.raw files mean that there were no adjustments applied to the data to account for changes in observing practice. The *.tob files are corrected for only one type of change – the time that the thermometers are read and reset. The *.FLs.52i files have the time of observation change adjustments plus adjustments to account for other changes in bias. As such, the *.FLs.52i files are considered the most appropriate for trend analysis since they represent the most complete attempt to remove non-climate-related artifacts in the data. The *.FLs.52i data also contain estimates for missing data and are continually updated and reprocessed (*i.e.*, there is no ‘fixed’ version).”

Figure 9.4 shows a sample of data from the *.raw file for a site in Tucson, Arizona. This site has records dating back to October, 1891. The -9999 values indicate missing values. There are other numbers and letters in the file which provide data quality control information. The data values are given as integers equal to 100 times the temperature in degrees C. Thus, 2159, the monthly mean average temperature value for October, 1891, is interpreted as 21.59°C. The data are always aligned in columns according to a specified format; if this were not true, it would be more difficult to write software for reading the files.²²

```

USH00028815 1891 -9999 -9999 -9999 -9999 -9999 -9999 -9999 -9999 -9999 2159 4 1495 4 695 4 0
USH00028815 1892 959 4 1156 4 1389 4 1592 4 -9999 2620 4 3086 4 2948 4 2728 4 1939 4 1478 4 795 4 0
USH00028815 1893 1072 4 1228 4 1336 4 1758 4 2178 4 2864 4 2948 4 2770 4 2497 4 1862 4 1225 4 1023 4 0
USH00028815 1894 736 4 850 4 1272 4 1817 4 2239 4 2500 4 2953 4 2809 4 2640 2184a 1779 1274 0
USH00028815 1895 1111 1216 1501 1846d 2376 2727 3010a 2822 2711 2047 1281 922 0
USH00028815 1896 1250 4 1194f 4 1637 1769 2307 2985e 2945 2891 2703 2045 1450 1206a 0

```

Figure 9.4. First six records in the monthly mean average air temperature file for a site at the University of Arizona in Tucson, Tucson, AZ.

Figure 9.5 shows the input screen for accessing USHCN data by site. One option generates a comma-delimited table of all the monthly data in the file, with blank values for months with missing data. The other option graphs data for a selected month or for the annual mean or sum, which is calculated by the program.




Retrieve and Display USHCN Data for the Conterminous 48 States

Use this application to investigate data from NOAA's [U.S. Historical Climate Network](#). See [HERE](#) for a detailed description of the data format. Processed data have NOAA-applied adjustments in an attempt to remove "non-climate-related artifacts." See [HERE](#) for a list of stations.

Choose Site:

AL BREWTON 3 SSE

AL FAIRHOPE 2 NE

AL GAINESVILLE LOCK

AL GREENSBORO

AL HIGHLAND HOME

AL MUSCLE SHOALS AP

AL SAINT BERNARD

AL SCOTTSBORO

AL SELMA

AL TALLADEGA

AL THOMASVILLE

AL TROY

AL TUSCALOOSA ACFD

AL UNION SPRINGS 9 S

AL VALLEY HEAD

AZ AJO

AZ BUCKEYE

AZ CANYON DE CHELLY

AZ CHANDLER HEIGHTS

AZ CHILDS

Choose annual average (or total) or month:

Annual

January

February

March

April

May

June

July

August

September

October

November

December

Graph temperature or precipitation

Use raw or processed data.

Select maximum temperature for graph.
(The total range is 40°C.)

30°C 40°C 50°C

Figure 9.5. Input screen to access USHCN data.

²² Column-aligned formats date back to earlier days of programming in FORTRAN, when it was required to provide a format which specified the columns in which data values would be found. Modern programming languages are more flexible, but it is still helpful to have column-aligned values.

Figure 9.6(a) shows one example of raw data from the USHCN – monthly average maximum, mean, and minimum monthly air temperatures for July from 1891 to the present, from the University of Arizona in Tucson, Tucson, AZ. with superimposed linear trend lines. The temperatures, and especially minimum (nighttime) temperatures, are increasing steadily with time on average, but why? Do the increases describe “real” climate warming in the American Southwest? Or does the increasing temperature represent changes in the location of the site, urbanization around the site, other changes in the environment surrounding the site, or characteristics of the site itself? Access to the USHCN data provides an important window into the difficult data quality questions being considered by climate scientists around the world as they struggle to separate climate change signals from weather and other effects.

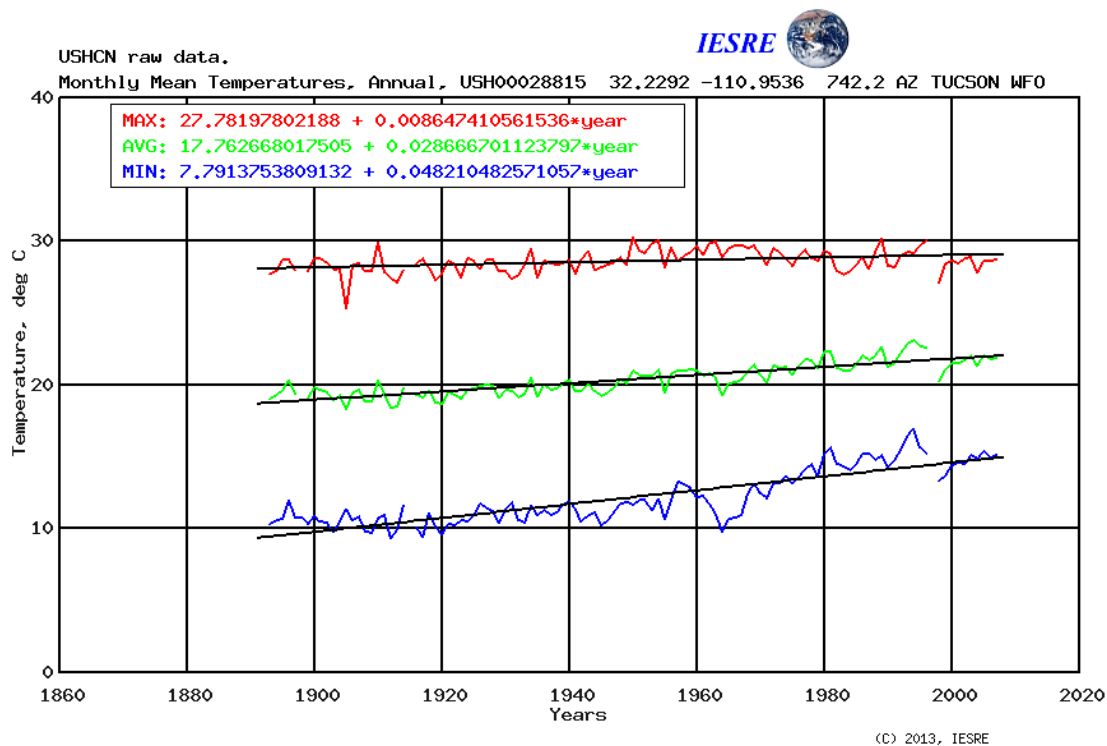


Figure 9.6(a). Raw USHCN yearly average maximum, mean, and minimum air temperatures for the site at the University of Arizona in Tucson, Tucson, Arizona.

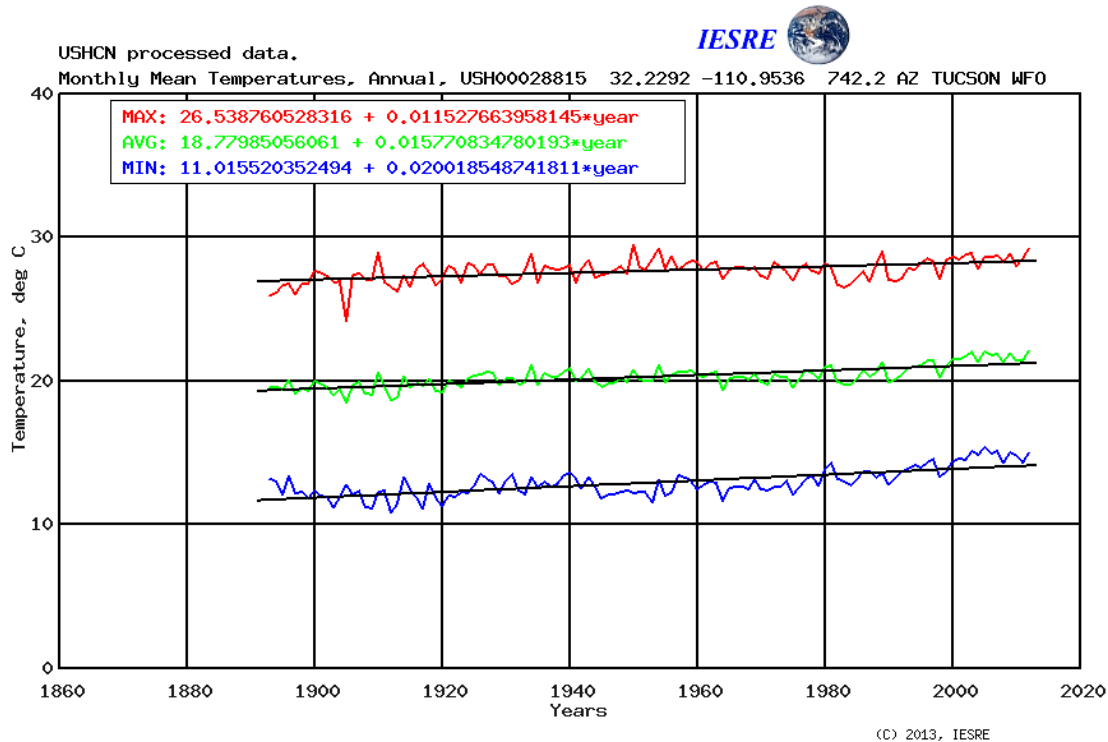


Figure 9.6(b). Processed USHCN yearly average maximum, mean, and minimum air temperatures for the site at the University of Arizona in Tucson, Tucson, Arizona.

The site in Figure 9.6(a) was not chosen at random! This site, which has the largest positive annual temperature trend in the U.S., has achieved considerable notoriety because of its location for many years on an asphalt parking lot at the University of Arizona in Tucson – it is the chain-link fenced area between parked vehicles in Figure 9.7. This is an incredibly poor choice, as weather stations are *supposed* to be located where they are representative of the local natural environment.



Figure 9.7. Former(?) USHCN site at University of Arizona at Tucson (between parked vehicles in asphalt lot).

As of fall 2007, the University was reported to be dismantling and moving this site. Indeed, there are no raw data after April 2008. The undated Google Earth image downloaded in August 2013, in Figure 9.7, showed that the fenced enclosure is still there. The instrumentation appears to be gone but the resolution is not quite high enough to know for sure. You can check this site yourself by going to coordinates 32.2294, -110.9543 in the Google Earth search window. Considering the length of the Tucson data record, it would be interesting to know more about the history of the site. Was it always here and the University just grew up around it?

Why was it allowed to remain in such an inappropriate location? What did this site (or previous different sites) look like 50 or 100 years ago? How do data from this site compare with other nearby (and more appropriate?) sites in Arizona? What does “nearby” mean?

What did NOAA do with these data, considering the very questionable location of the site? Figure 9.6(b) shows processed data from the same site. Note that the processed data include modeled values for data missing from the raw files and even modeled data extended through 2012. Presumably NOAA has compared this site with other nearby sites. The very suspicious increase in minimum (nighttime) temperatures in the raw data, which looks more like an exponential increase with time than a linear one, has been considerably reduced. This “correction” is consistent with the assumption that the asphalt parking lot absorbed a lot of heat during the day and released it during the night, causing the temperatures above the surface to be higher than they should be. There is still an upward trend in both the mean and maximum temperatures data. Are these trends now representative of real warming for this region of Arizona outside of metropolitan Tucson? Do they represent an urban heat island effect representative of Tucson? Or are they still influenced by the characteristics of this site in ways not addressed by NOAA’s algorithms? These are questions well worth addressing for this and other sites.

Problems with USHCN sites are so widespread that a “grass roots network of volunteers” has created a site devoted to assessing the quality of USHCN sites and identifying problematic sites [www.surfacestations.org]. Additionally, there is a contentious and ongoing battle between those who defend NOAA’s analysis of temperature records and those who believe that the warming trends derived from those records are flawed because they are based on the presumption that warming trends *will* be found, and therefore should not be believed.

One persistent complaint is that many of the USHCN sites which may have been sited appropriately in the past are now surrounded by urban development and therefore produce urban heat island effects that must be accounted for in some way. Are they to be “corrected” and/or discounted because they distort the actual climate change signal, or are they becoming so prevalent that they are helping to define (redefine?) climate and need to be included in any discussion of climate trends? The bubble charts for 30-year climate normals discussed in the previous section provide interesting insights to this question.

Another major complaint is that while the *results* of the NOAA corrections to the raw station data are readily available (as they are through the online USHCN application discussed here), the *process* which led to the corrections is not. Without commenting on the specifics of this particular situation, it is worth noting that a fundamental tenet of good research is that both results *and* methods must be made available for others to review. Without that access, fair and thorough peer review of results and conclusions is not possible.

In summary, to say that the treatment of USHCN data remains a subject of heated debate among climate scientists is a considerable understatement [Climate

Skeptic, undated; Skeptical Science a, undated]! See Inquiry and Research Topics at the end of this chapter for more information about urban heat island effects.

9.4 The U. S. Climate Reference Network

The acknowledged problems with collecting reliable long-term weather data from questionable sites led to NOAA's development of the Climate Reference Network (USCRN), starting with a pair of stations in Asheville, NC (home of the National Climatic Data Center) in 2000 [Diamond *et al.*, NOAA]. The USCRN has as its goal the establishment of high-quality monitoring sites in the U.S., away from urbanization effects in locations that are expected to remain environmentally stable for the foreseeable future – a very ambitious undertaking to isolate authentic climate signals from the confounding effects of civilization. There are currently about 125 such sites, distributed as shown in Figure 9.8.

Map of USCRN Stations

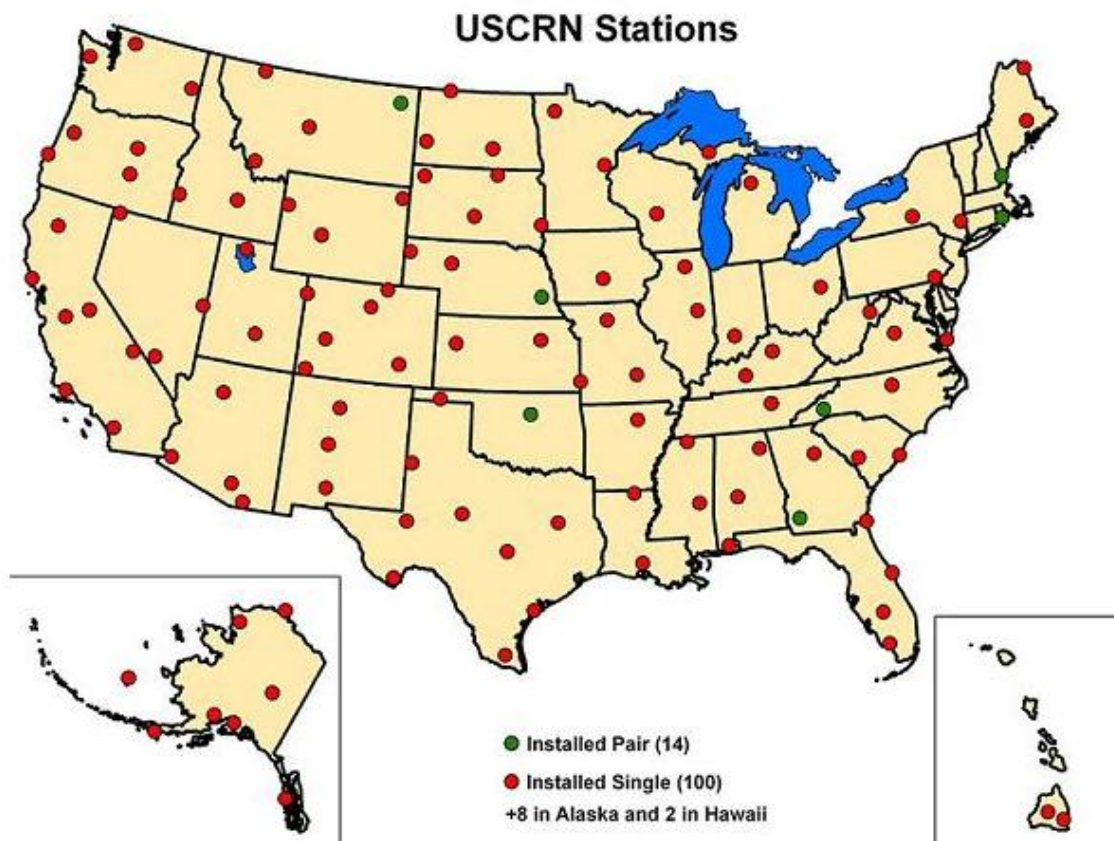


Figure 9.8. Map of NOAA Climate Reference Network sites (<http://www.ncdc.noaa.gov/crn/stationmap.html>).

The layout of and instrumentation at USCRN sites is standardized. Figure 9.9 shows a typical site at Avondale, (southeastern) Pennsylvania. The instrumentation tower, with its antenna for sending measurements to a satellite, is at the left. The

three identical white capped cylinders are redundant air temperature sensors. The solar panel for power is in the center. At the right is a structure consisting of two concentric rings of wood slats surrounding the precipitation gauge. The purpose of this structure is to minimize the effects of wind on precipitation measurements.

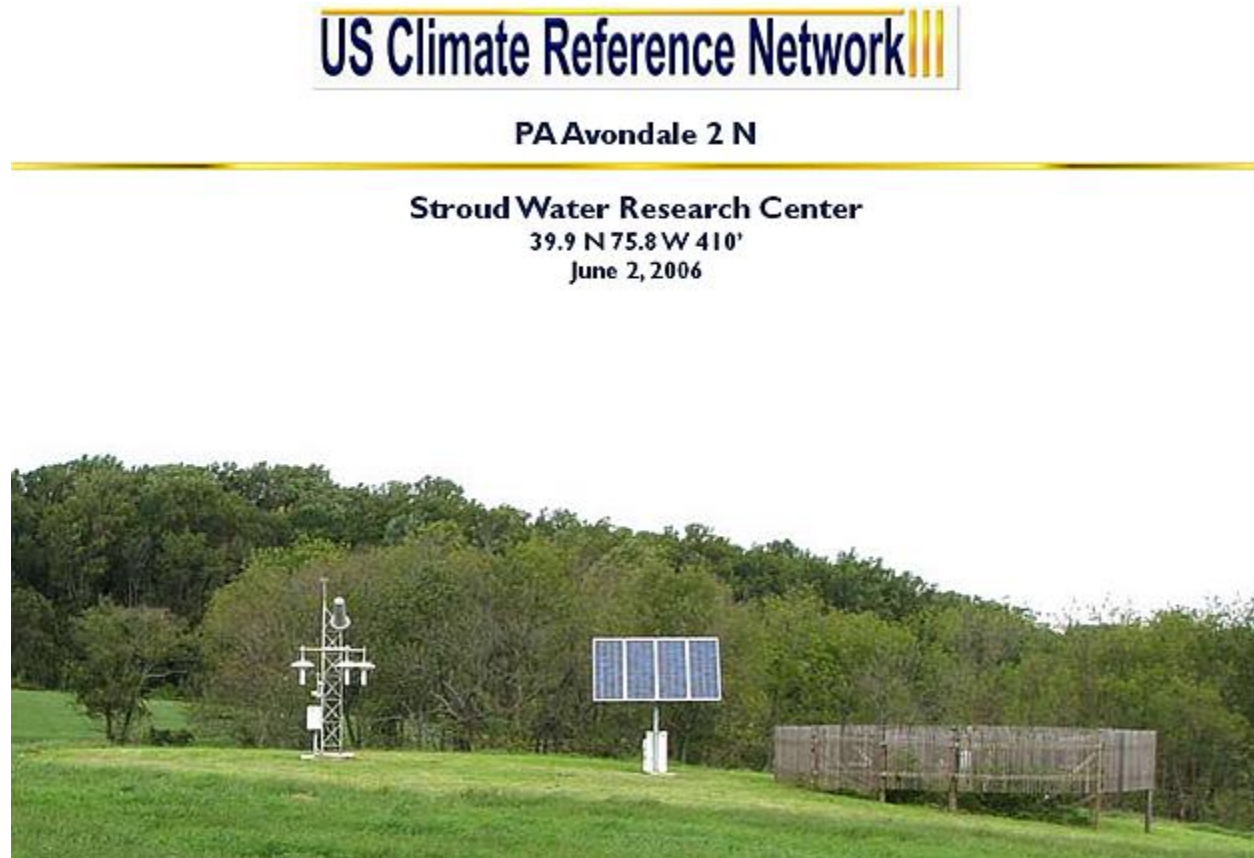


Figure 9.9. The USCRN site at Avondale, PA.

Understanding that climate needs to be defined over multiple decades, the USCRN is not yet a source of climate normals, but it *will* be in the future. By studying these data today, you can participate in the development of this critical project during the 21st century.

The input screen for accessing USCRN data is shown in Figure 9.10. There are many data options other than air temperature and precipitation. USCRN data also include surface and soil temperatures, precipitation, insolation, relative humidity, and soil moisture, although not all stations report all of these values. In particular, sites marked as “regional” (R) report only air temperature and precipitation.

By choosing the first option in this application, you can find the first reporting date for a selected site. You can generate tables of values in comma-delimited format for importing directly into Excel or some other spreadsheet program and you can graph data in 1, 2, 4, or 8-day segments.

This document last modified on 08/21/2013 08:37:56.



Retrieve and Display CRN Data

Use this application to investigate data from NOAA's Climate Reference Network (USCRN) at www.ncdc.noaa.gov/crn. The data are stored in space-delimited ASCII text files. See [this link](#) for a detailed description of the data format. See [this link](#) for a list of parameters in the file. Regional sites (USRCRN) are marked (R) and include only air temperature and precipitation data.

Select data here. (Sites marked (R) are regional sites (USRCRN).)

Year: 2000-2011 | Month: January-December | CRN Site: AK, Barrow, Fairbanks, Gustavus, Kenai, King Salmon, Metlakatla, Port Alsworth, Red Dog Mine, Sand Point, Sitka, St Paul, Tok

Select data sets for output option 2:

T_{avg} T_{max} T_{min} °C
 precipitation mm
 S_{avg} S_{max} S_{min} W/m²
 T_{surface}_{avg} T_{surface}_{max} T_{surface}_{min} °C
 T_{soil} (5, 10, 20, 50, 100 cm) °C
 soil moisture (5, 10, 20, 50, 100 cm) (water volume)/(sample volume)
 RH_{avg} %

Lower and upper values for graphing temperatures (air or soil), °C:
 Lower: -20 Upper: 40
 Lower and upper values for graphing soil moisture, 0.0 – 1.0:
 Lower: 0 Upper: 0.6
 Number of y-axis divisions: * 6
 *For temperatures, take range into account to create whole number y-axis labels. For soil moisture, y-axis division should be 0.05 or 0.1.

Select an output option here:

- 1. Display first and last data for specified site and year.
- 2. Retrieve all checked parameters for a specified year and location, in text format.
- 3. Graph air temperature.
- 4. Graph surface temperature (limited data available).
- 5. Graph insolation (earlier years may have only average value).
- 6. Graph relative humidity (limited data available) and precipitation.
- 7. Graph soil temperature, 5, 10, 20, 50, 100 cm (1st site, Lincoln, NE, August 2009).
- 8. Graph soil moisture, 5, 10, 20, 50, 100 cm (1st site, Lincoln, NE, August 2009).

Click here to generate specified output.

If you selected option 3-8:

Starting day (1-31, as appropriate): 1 How many days? 8

Figure 9.10. Input screen for accessing USCRN data

Figure 9.11 shows an 8-day graph of soil temperature data from Avondale, PA. These data show how soil temperature follows the diurnal cycle in air temperature close to the surface, but changes much more slowly (seasonally) farther below the surface. The “noise” in the values at 50 and 100 cm is a result of how data are averaged from redundant sensors which may not always agree with each other.

PAAvondale, starting 2012 June 1

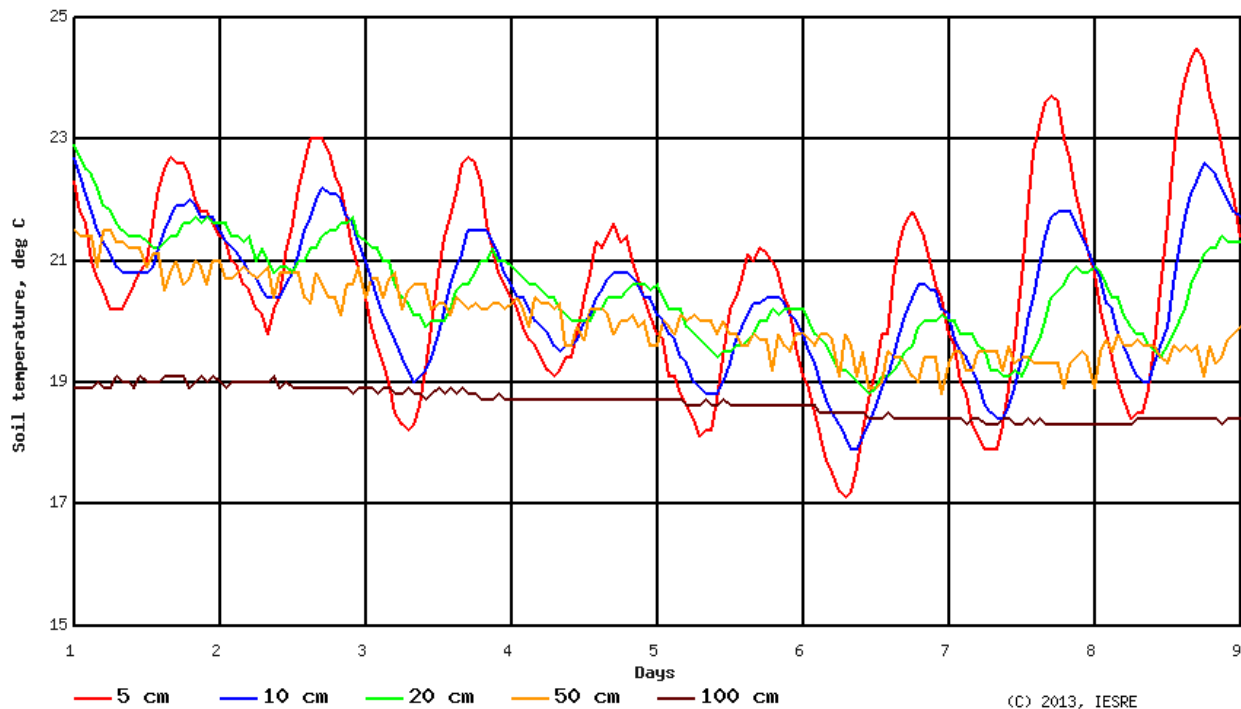


Figure 9.11. Soil temperature starting 01 June, 2012, at Avondale, PA.

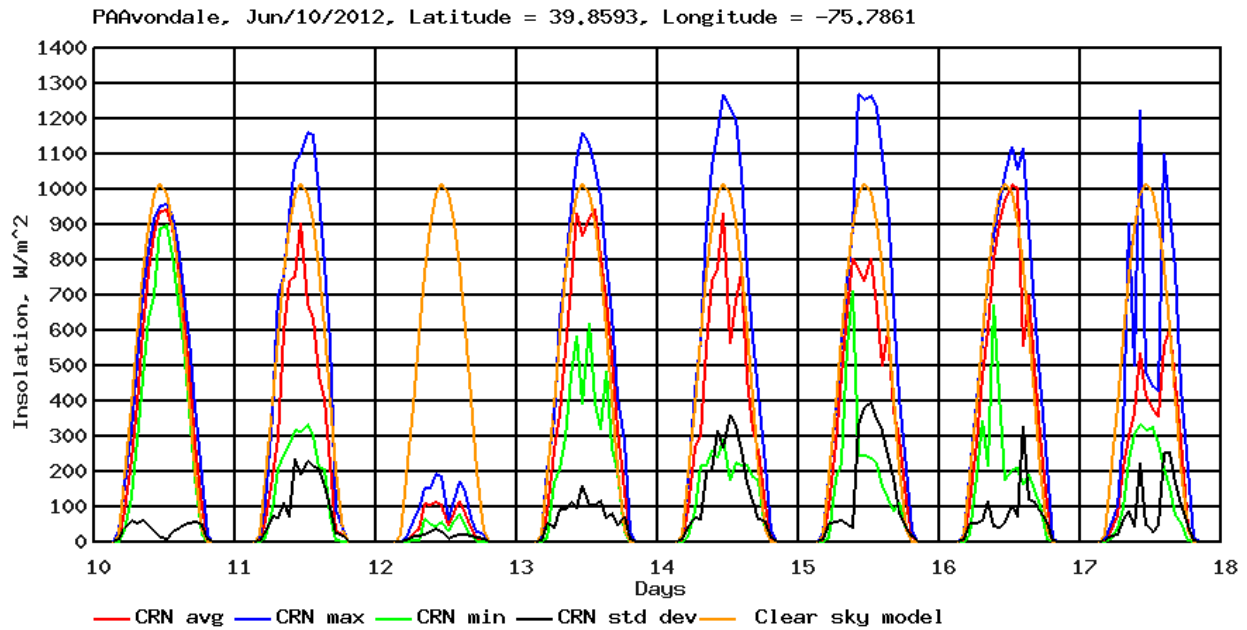
The publicly available online CRN data include maximum, average, and minimum insolation (for some time periods), but not a “standard deviation.” Data provided to IESRE by NOAA includes this value.²³ Standard deviation is in quote marks because it is calculated in the usual way from data collected during an hour, but it does not have the expected statistical meaning of describing the variability of data distributed normally about a mean value – see Chapter 4. Within each hour insolation changes continuously and, under clear skies, fairly predictably. For clear skies, the “standard deviation” will be minimum around noon and maximum during mid-morning and mid-afternoon when solar elevation is changing the fastest. As discussed in Chapter 4, this somewhat artificial value may be a more useful value than the range for generating cloud statistics.

The user interface for accessing these data is similar to that shown in Figure 9.10. Figure 9.12(a) shows data from June, 2012, at Avondale, PA, including the standard deviation calculations and a clear-sky model [IESRE, undated]. The data on June 10 is typical for a clear day – perhaps with some thin uniform cirrus because the values lie a little below the clear-sky model. The double-humped pattern for clear-sky standard deviation is consistent with the explanation given in the previous paragraph. On June 12, it was almost certainly raining all day under

²³IESRE thanks Michael Palecki, USCRN Science/Technology Contact, NOAA/NCDC, and his staff for providing these data.

heavily overcast skies. (The precipitation data for these days could be used to check this conclusion.)

This application also calculates total energy solar energy received per day (kWh) for clear-sky and observed insolation, as shown in Figure 9.12(b).



IESRE

(C) 2013, Institute for Earth Science Research and Education

Figure 9.12(a). Insolation data from Avondale, PA, including “standard deviations” and a clear-sky model.

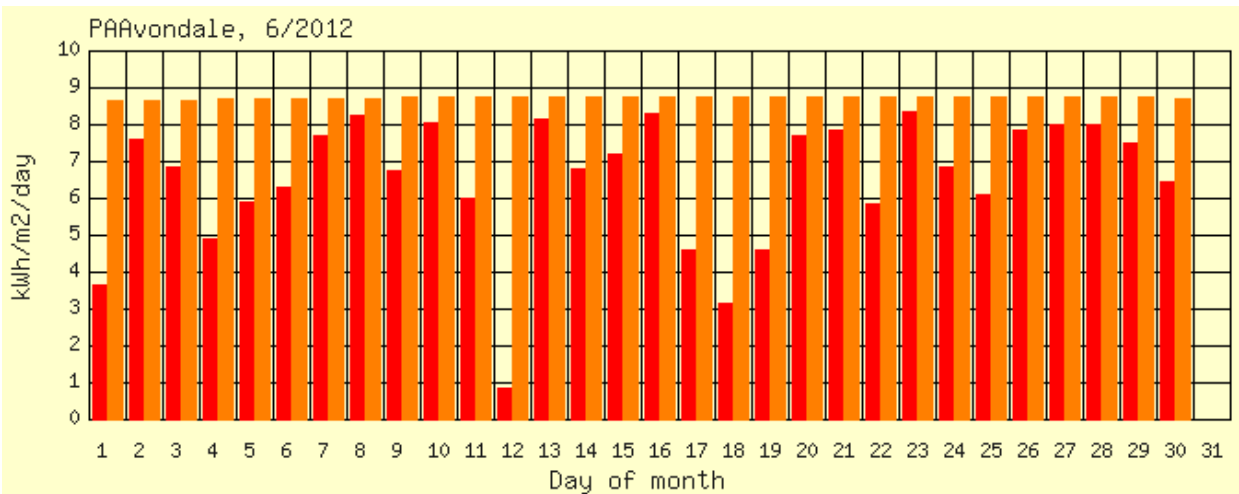


Figure 9.12(b). Daily solar energy received, observed and clear-sky.

9.5 Inquiry and Research Questions

(Inquiry)

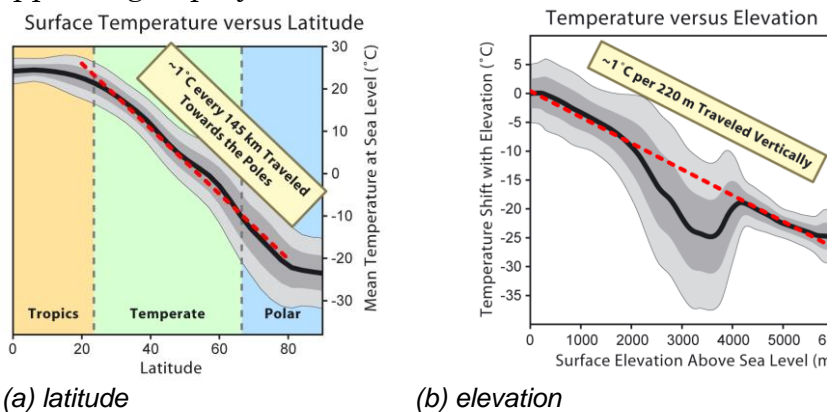
- Find a few nearby sites and explore the various databases. How do the data in these databases differ? How are they similar?

(Research)

- Climate normals are interesting for comparing sites within some defined area such as a state. Are there persistent differences among site normals for a selected state? If so, what are the possible causes of these differences?

The data shown in Figure 9.3 imply that latitude, elevation, and urbanization are three possibilities. The Colorado data are quite clearly influenced by elevation, which changes abruptly from the High Plains²⁴ in the eastern part of the state to the Rocky Mountains. In Pennsylvania, the picture is more complex, with elevation, latitude, and urbanization all appearing to play a role.

The climate normals are based on “raw” site data, rather than data that have been “adjusted” somehow, as has been done for the highly processed USHCN data product. It is tempting and most likely reasonable to associate warmer areas with urban heat island effects. For example, in the Pennsylvania data, there is a small “warm spot” at Williamsport, PA, 77°W and 41.25°N, population ~30,000, elevation ~175m).



(a) latitude

(b) elevation

Figure 9.13. Average temperature change as a function of latitude and elevation. (Images by Robert A. Rhode/Global Warming Art.)

The quantitative effects of other factors also need to be considered in any attempt to extract urban heat island data. Between roughly 20° and 80° north or south latitude, average temperatures decrease by about 1°C/degree of latitude, or about 1°C/145 km, as shown in Figure 9.13(a). In Figure 9.3, there is in fact some visual evidence of a south-to-north cooling. But, in Pennsylvania is this trend due to latitude or the fact that northern Pennsylvania is much more rural than southern Pennsylvania? Or both?

Land elevations in Pennsylvania vary from sea level in the southeast to a little over 3,000 feet (900 m) in the mountainous southwest. Temperature change with elevation, called the lapse rate, is about 10.0°C/km for clear skies and about 5.5°C/km under rainy conditions when the humidity is near 100%. (By convention, a positive lapse rate means that temperature decreases with altitude.) These lapse

²⁴ http://en.wikipedia.org/wiki/High_Plains_%28United_States%29

rates are larger than the value in Figure 9.12(b). The choice of which values to use is up to you.

With the understanding that latitude and elevation dependencies are only approximations, you could correct the annual mean temperature normals for elevation and latitude. This would be a justifiable approach to trying to separate urban heat island effects from geography-dependent effects. The online USHCN data access application described in this chapter does not support such modifications without changes to the code,²⁵ but a spreadsheet such as Excel will allow bubble charts to be made with these modifications (without the state boundary outlines).

- The history of the sites used for the long-term records contained in the USHCN dataset is of great interest.

If you are near one of these sites, it is worthwhile project to compile a history. This is especially important for sites with long records where it is likely that the site has been moved or conditions around the site have changed. Are there official or unofficial records of the site history? Are there photographs? Other documentation? You can contact the nearest National Weather Service office. Can you interview active and retired meteorologists who have worked with the site? Are unadjusted “raw” data from the site available? Can you find anomalies in unadjusted data that indicate possible changes in site location or environment?

This might not seem like a “real” science project, but is in excellent cross-disciplinary project, ideal for a group of students working together to make sense of climate data.

- It is sometimes the case that there are no USHCN sites in large cities even though there are weather records for those cities. But, it is at just those sites that one is particularly interested in urban heat island effects. The important early paper by Karl *et al.* [1988] discusses urban heat island effects; it includes an extensive list of references to previous work on this topic. See also these two Skeptical Science web pages [b, undated; c, undated].

There is no USHCN site in Philadelphia or Pittsburgh, the two largest cities in my state of Pennsylvania, for example. The Franklin Institute maintains historical weather data for Philadelphia at <http://www.fi.edu/weather/data/>, a record that extends back to 1872. All these data are available in a common format as a text file [IESREc]. Over the years these records have come from several different places including Philadelphia International Airport and the rooftop of the Franklin Institute building in downtown Philadelphia – both of which are *very* poor locations for collecting temperature data that is used to detect climate change!

Can you find ways of analyzing the Philadelphia records that will indicate where site-related problems might exist? Can you find ways of applying “NOAA-style” adjustments that will allow you fairly to compare these records with

²⁵ All the code for these applications is written in HTML/PHP, which can be run online or on a local server. The code is available on request from IESRE.

surrounding stations to determine the existence or extent of an urban heat island for Philadelphia?

It would be interesting to compare the situation in Philadelphia with New York City, where there is a very long USHCN data record from Central Park. This is certainly a better site than an airport or the roof of a building, but it is still in the middle of a huge urbanized area. It may be a reasonable site from which to investigate an urban heat island effect, relative to stations around New York City.

Here is one suggestion of a way to analyze historical term temperature records that are reported in integer Fahrenheit degrees (uniformly the case in original weather records from the U.S.), before the advent of automated data recording and reporting: look at the distribution of the digits in the “ones” position of the temperature. Over time, the digits 0 through 9 should be roughly equally likely. This might not be true if, for example, temperatures were manually read from a thermometer that marked only even degrees, in which case there might be a tendency for an observer to round readings to the nearest even degree. With an automated data reporting system, this “digit bias” should not exist.

Another possible indicator of site-related problems is the number of days with temperatures above or below a specified value. A sudden increase in the number of very high maximum temperatures (more likely) or a decrease in the number of very low minimum temperatures (less likely) may indicate that a weather station has been moved.

This is a problem that is more likely to occur in metropolitan areas where sites are moved or urbanization encroaches. Figure 9.14 shows the number of days per year with maximum temperatures above 95°F since the beginning of recordkeeping in Philadelphia, through 2012. Are these data

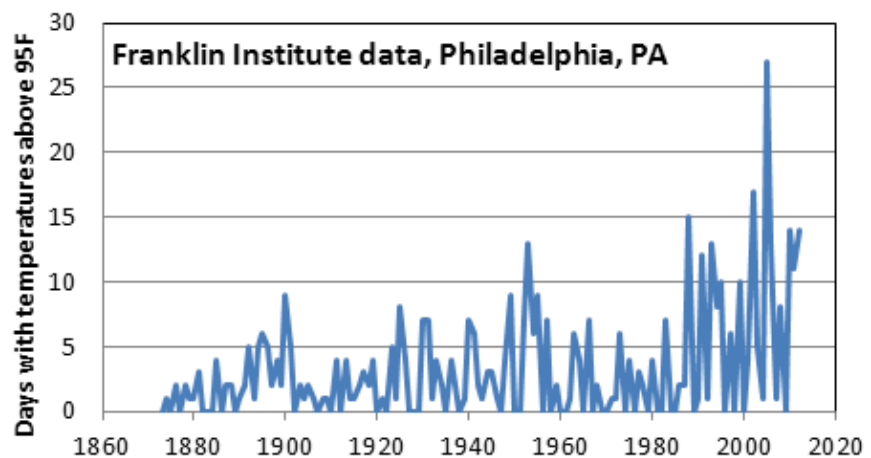


Figure 9.14. Days per year with temperatures above 95°F in Philadelphia, PA.

related to a real warming effect caused by urbanization? Or, are the increases in recent years related to siting or equipment problems? Would a graph of average air temperatures in Philadelphia indicate a warming trend that would consistent with these data? The increase in very hot days starting in 1988 is suspicious and the huge spike in 2005 is *very* suspicious. However, the only way to reach supportable conclusions about these data is by comparisons with other more stable sites around Philadelphia (which will most likely have shorter records).

- As noted above, the NOAA USHCN database includes raw station data and data that have been processed. The processed data are suggested for trend analysis, even though not all scientists agree with the “adjustments” NOAA has made, including their definition of “bias.”

Can you find sites where the adjusted data are significantly different from the raw data? (The data from Tucson, AZ, shown in Figure 9.6 show one rather extreme example.) If significant differences do exist, can you analyze the implications of “adjustments” to the trends present (or not present) in those sites?

USHCN data are subject to ongoing modifications. Data available online through IESRE are not necessarily the most recent versions. Hence, if you find interesting discrepancies between the raw and processed data for a particular site, you should download the latest version of files before you draw conclusions. NOAA provides several options for downloading and graphing data, including daily data, from USHCN sites.

- What do you see when you compare CRN data with nearby USHCN sites, or to a composite of nearby sites? Does this provide clues about how to interpret data from USHCN sites, some of which are of lower quality than the CRN data?

- The online CRN insolation data can provide input for a research project to study the relationship between insolation and cloud statistics, as discussed in Chapter 4, Section 5. Techniques for analyzing your own insolation data should be developed in a way consistent with CRN insolation data, based on clock-hour averages, including the special file that includes “standard deviation” calculations as shown in Figure 9.12(a).

9.6 Resources

Arguez, Anthony, Imke Durre, Scott Applequist, Russell S. Vose, Michael F. Squires, Xungang Yin, Richard R. Heim Jr., and Timothy W. Owen. NOAA’s 1981-2010 U.S. Climate Normals: An Overview. *Bulletin of the American Meteorological Society*, 1687-1697, November 2012.

Climate Skeptic. Global Warming Is Caused by Computers.
http://www.climate-skeptic.com/temperature_measurement/

Diamond, H. J., T. R. Karl, M. A. Palecki, C. B. Baker, J. E. Bell, R. D. Leeper, D. R. Easterling, J. H. Lawrimore, T. P. Meyers, M. R. Helfert, G. Goodge, P. W. Thorne. U. S. Climate Reference Network after One Decade of Operations: Status and Assessment. *Bulletin of the American Meteorological Society*, **94**, 485-498, 2013.

IESREa. 2013. <http://www.instesre.org/ClimateDataApplications.htm>

IESREb. <http://www.instesre.org/Solar/ClearSkyModelOnline.htm>

IESREc. Philadelphia weather data from Franklin Institute files.

<http://www.instesre.org/philtemp.txt>, undated.

Diamond, Howard J., Thomas R. Karl, Michael A. Palecki, C. Bruce Baker, Jesse E. Bell, Ronald D. Leeper, David R. Easterling, Jay H. Lawrimore, Tilden P. Meyers, Michael R. Helfert, Grand Goodge, Peter W. Thorne. U.S. Climate Reference Network after One Decade of Operations: Status and Assessment. *Bull. Amer. Meteor. Soc.*, **94**, 485-498, 2013.

<http://journals.ametsoc.org/doi/full/10.1175/BAMS-D-12-00170.1>

Karl, T. R., H. F. Diaz, G. Kukla. Urbanization: Its Detection and Effect in the United States Climate Record. *Journal of Climate*, **1**, 1099-1123, 1988.

NASA. Global Climate Change: Vital Signs of the Planet, 2013.

<http://climate.nasa.gov/scientific-consensus>

NOAA. Climate, 2013. <http://www.noaa.gov/climate.html>, updated March 20, 2013.

NOAAa.

<http://www.ncdc.noaa.gov/oa/climate/normal/usnormals.html#CLIMATECHANGE>

NOAAb.

<http://www.ncdc.noaa.gov/news/noaa%E2%80%99s-1981%E2%80%932010-us-climate-normal-overview>

NOAAc. <http://www.ncdc.noaa.gov/oa/climate/research/ushcn/>

NOAA d. <http://www.ncdc.noaa.gov/crn/>

NOAAe. <http://cdiac.ornl.gov/epubs/ndp/ushcn/access.html>

RealClimate: Climate science from climate scientists. Global Warming Since 1997 Underestimated by Half, November 2013.

<http://www.realclimate.org/index.php/archives/2013/11/global-warming-since-1997-underestimated-by-half/>

surfacestations.org (authors unknown)

http://www.surfacestations.org/USHCN_sites.htm

Skeptical Science a. Watts' New Paper – Analysis and Critique. 2012.

http://www.skepticalscience.com/watts_new_paper_critique.html

Skeptical Science b. Does Urban Heat Island effect exaggerate global warming trends? <http://www.skepticalscience.com/urban-heat-island-effect-intermediate.htm>

Skeptical Science c. Are surface temperature records reliable?

<http://www.skepticalscience.com/surface-temperature-measurements-advanced.htm>

Watts, Anthony. New study shows half of the global warming in the USA is artificial, 2012. www.wattsupwiththat.com

Appendix A: Student Research Project Template

As described in Chapter 1, the CSRES Program provides equipment and support for student research, but only in response to written research plans. These plans may be written by individual students, student teams, teacher/student teams, or just by teachers who wish to develop climate research opportunities at their schools.

These plans need to model even if in a very simple fashion what scientists do to support their research. They have to provide information about the purpose of the proposed research, how and by whom it will be done, and the kinds of support that are required. For student research, mentoring and equipment support are key requirements. For student research to be successful, teachers and schools need to develop partnerships that can help with research plans and provide ongoing support for that research. A good research plan will describe such collaborations.

Student research plans must include a plan for disseminating results. Participation in a science fair is one obvious path, although other paths are possible. Included here is a template for a simple student research plan that the CSRES Program has used.

Research Plan

NAME(s) _____ SCHOOL(s) _____

Project Title: _____

This project is (*check one*):

- an individual project
- a collaborative project with students at my school
- a collaborative project including students at other schools

This project will be conducted at:

- my school
- my home or some other site (specify) _____

I anticipate entering this project in a science fair:

- yes (if yes, which science fair?)

- no (if no, give an alternate plan for disseminating the results of your research.)

The purpose of this project is (provide a research question and a brief description of the project goals):

Provide an outline of your research plan, including an implementation timeline (Use an additional page if necessary):

For this project, I will need:

__ equipment (list hardware and/or software needed)

__ science support

__ other sources of data

__ "hands on" help (e.g., selecting and/or setting up a research site, using equipment, data collection and analysis)

__ other (please specify) _____

Have you developed partnerships with individuals or institutions that will help with your research? If so, please describe them here.

Appendix B: Sources for Figures

Except as noted here, all figures in this document represent the author's work.

- 2.1 <http://earthobservatory.nasa.gov/Features/EnergyBalance/page1.php>
- 2.2 <http://earthobservatory.nasa.gov/Features/EnergyBalance/page1.php>
- 2.3 (various)
- 2.5 <http://neo.sci.gsfc.nasa.gov/>
- 4.1(a) <http://www.apogeeinstruments.com/apogee-pyranometer-technical-information/>
- 4.2 <http://www.monarchinstrument.com/track-it.php>
- 4.3 http://www.fouriersystems.com/products/usb_logger/data_logger.php
- 5.6 <http://earthobservatory.nasa.gov/Features/MeasuringVegetation/>
- 6.1 <http://www.amazon.com/Kintrex-IRT0421-Non-Contact-Thermometer-Targeting/dp/B0017L9Q9C>
- 6.2
<http://www.excelitas.com/Downloads/TPS%201T%200134%20TPS%201T%200136%20L55%20TPS%201T%200136%20IRA%20Thermopile%20Sensor.pdf>
- 8.1 <http://www.weather.msfc.nasa.gov>
- 9.7 Google Earth image
- 9.9 <https://www.ncdc.noaa.gov/crn/photos.html>
- 9.13 <http://www.globalwarmingart.com/>